DRAG COEFFICIENT FOR TETHERED SPHERES IN A VERTICAL PIPELINE WITH AND WITHOUT POLYMER ADDITION

DRAG COEFFICIENT FOR TETHERED SPHERES IN A VERTICAL PIPELINE WITH AND WITHOUT POLYMER ADDITION

by

HANI A. R. ALNAKEEB, B.Sc. (Mech. Eng.)

A Thesis
Submitted to the Faculty of Graduate Studies
in Partial Fulfilment of the Requirements
for the Degree
Master of Engineering

McMaster University

September 1977

TO MY MOTHER

WITH LOVE

Master of Engineering (1977) McMaster University
Mechanical Engineering Hamilton, Ontario

TITLE: Drag Coefficient for Tethered Spheres In a Vertical Pipeline With and Without Polymer Addition

AUTHOR: HANI A. R. ALNAKEEB,
B.Sc. (Cairo University)(Mech. Eng.)

SUPERVISOR: Dr. B. Latto

NUMBER OF PAGES: x, 111.

ABSTRACT

This thesis is concerned with experimental study of the drag coefficient of tethered spheres in a vertical pipeline of approximately 0.05 m diameter using water and dilute polymer solutions.

Experiments were conducted using four different sphere-to-tube diameter ratios ranging from 0.439 to 0.87. The liquid velocities as well as the associated drag forces and pressure drops were measured, which enabled both the drag coefficients and pressure functions to be computed.

Semi-empirical correlations were obtained for the drag coefficient and the pressure function in the range of tube Reynolds number of 3.9×10^3 to 9.2×10^4.

In the experiments using Reten 423 for the diluted polymer solutions, it was observed that a maximized drag reduction would occur at concentration of about 24 wppm for spheres of $d/D > 0.74$. Drag reductions of up to 60% were obtained which are of a higher order of magnitude than that for non-tethered spheres which has been previously observed.

ACKNOWLEDGEMENTS

It is my pleasure to express my deepest gratitude to Dr. B. Latto for his kind guidance, valuable advise and continuous encouragement throughout the duration of the present investigation.

The author also expresses his appreciation to Ms. Lorraine A. Oneschuk for typing the manuscript.

This research was supported by the Defence Research Board and the National Research Council of Canada to whom grateful acknowledgement is made.

TABLE OF CONTENTS

LIST OF FIGURES

NOMENCLATURE

A_t	cross-sectional area of tank
A_{pipe}	cross-sectional area of pipe
C_D	drag coefficient in a bounded media
C	concentration of polymer solution (wppm)
D	pipe diameter
d	sphere diameter
f	Darcy-Weisbach friction factor
F_D	drag force in Newton
g	gravitational conversion factor, acceleration of gravity
Δh_m	manometer reading
ΔH	level difference of tank for calibration
K	constant
L	distance between the pressure taps
P	pressure
ΔP_f	pressure drop due to friction $\Delta P_f = (fL/D)(\rho V_{av}^2/2)$
ΔP_L	pressure drop due to liquid alone $\Delta P_L = \Delta P_f + L\gamma_w$
ΔP_S	pressure drop with the spheres present $\Delta P_s = \Delta h_m(\gamma_m - \gamma_w) + L\gamma_w$
PRF	pressure function (dimensionless) $PRF = \frac{\Delta P_S - \Delta P_L}{D\gamma_w}$

Q	volume flow rate
R_d	Reynolds number based on sphere diameter
R_D	Reynolds number based on pipe diameter
SG_m	specific gravity of the manometer fluid
V_{av}	average fluid velocity in the pipe $V_{av} = Q/(\pi D^2/4)$
wppm	weight parts per million
τ_o	shearing stress at the wall
ρ	density
μ	dynamic viscosity
ν	kinematic viscosity
γ_m	specific weight of manometer fluid
γ_w	specific weight of water

CHAPTER 1

INTRODUCTION

During the past decade there has been an increasing interest in the use of pipelines for the transportation of both solid and liquid materials. Over the past eight years research on the hydrodynamics of capsules in pipelines has been pursued at McMaster University. One aspect that has been investigated is that of drag coefficient of spheres and other symmetrical bodies. In the initial work the hydrodynamic suspension of spheres and cylinders in vertical pipelines was examined. The research was later extended to the effects of drag reducing additives on the transportation of these bodies. It was observed that the drag coefficient of untethered spheres was slightly increased by the use of dilute solutions of drag reducing additives as the d/D ratio was decreased. This at first sight, was surprising since other researchers have observed that the drag coefficient for freely falling bodies in semi-infinite media incurred a reduction. However, Latto suggested that there could be a two-fold effect for this phenomena for bodies in bounded media. Firstly, the polymer stabilizes the boundary layer keeping it laminar which in turn, gives rise to an earlier separation. Hence, the viscous drag is reduced whilst the form drag is increased, giving rise to virtually no change

or a slight increase in the drag. This is because the form drag would be a major component.

In order to verify this hypothesis flow, visualization experiments on untethered spheres in a pipeline were carried out which though limited in scope bore out the argument, Latto and Lai [24]. These experiments were limited to Reynold's numbers for hydrodynamically suspension and consequently, there needs to be more extensive research done on this aspect. The only way of achieving a high Reynolds number range would be to tether these spheres and unfortunately this restricts the natural movements of these bodies. The research with tethered bodies though not directly applicable to the transport of capsules would be the next logical step in investigating the phenomena involved.

CHAPTER 2

LITERATURE SURVEY

The flow around a sphere in an unbounded media was first studied by Stokes [1] in 1851. In his analytical solution, he neglected the inertia terms in Navier-Stokes equation, and obtained the velocity, shear stress and pressure distribution and thus established the following equation for the form and viscous drag as a function of the free stream velocity:

$$\text{Drag} = \text{Form drag} + \text{skin friction (viscous drag)}$$

$$= 6\pi\mu r_o U_\infty \quad \text{(Stokes' Law)} \qquad [2\text{-}1]$$

where

μ = The viscosity of the fluid

r_o = The radius of the sphere

U_∞ = The free stream velocity.

This law was found to be accurate up to a Reynolds number (based on sphere diameter) of 0.5, which is applied to very low velocities (creeping flow).

Sometime after Stokes, Oseen obtained a solution to the problem which in part included the inertial term in the equation of motion. Oseen assumed that the velocity components can be presented as the sum of a constant and perturbation term. He got the equation,

$$\text{Drag} = 6\pi\mu r_o U_\infty (1 + 3/8\ R_e) \qquad [2\text{-}2]$$

which was good up to Reynolds Number 5.0.

Other methods such as using a combination of the Stokes and Oseen approaches have been used to obtain better approximations for the flow, by using Stokes' solution near the wall and Oseen's solution distant from it.

Those works mentioned above were confined to creeping flow; however, when the Reynolds Number is much higher than the applicable upper limit for Stokes' or Oseen's laws, the inertial terms cannot be eliminated and an analytical solution of Navier-Stokes equation would be impossible, and either numerical solutions or experiments to obtain correlations between the drag and the other flow parameters are resorted to.

McNown and Newlin [ ] presented the earliest work and study for the drag coefficient variations of a sphere rigidly mounted in a tube, as a function of the sphere to tube diameter ratio, and for tube Reynolds Number for somewhat less than 10^4 to more than 10^5. They arrived at the following analytical relationship:

$$C_D = \left[\frac{d/D}{1-(d/D)^2} \right]^2 \qquad [2\text{-}3]$$

which neglects the effect of viscosity but still correlates the data for $d/D > 0.82$.

All the above mentioned works were done using either water or air as the fluid medium. However, this present study deals with the flow characteristics around a sphere in a con-

fined media in water and polymer solutions. The fluid mechanics of the polymer solutions has elicited much attention because they exhibit a variety of unusual behaviour characteristics, e.g. rod climbing and drag reduction. The latter is the main concern of this study, that is, using the polymer as a drag reducing agent. It has been found that amounts as small as 0.001% by weight or less, can in certain cases reduce the drag by as much as 80%.

Concerning the phenomenon of drag reduction, numerous papers have been published since the initial discovery of the phenomenon, sometimes attributed to Toms and consequently known as Toms' phenomenon.

Generally, the discovery is intriguing in two major aspects, as follows:

(1) on a fundamental basis, it focuses attention on how the turbulent skin friction is generated at the wall by a flow, and

(2) on an engineering basis, it provides a physical means of reducing the enormous energy losses due to turbulent skin friction.

Many investigations have been attempted to identify the major aspects of the phenomenon, such as the dependence of drag on pipe diameter, concentration, Reynolds Number and wall shear stress.

Gadd [3,4], Hoyt [5] and Palyvos [6] have presented

an extensive reviews of the experimental and theoretical work done on the majority of the aspects of polymer addition, including areas in which some progress toward applications has occurred. However, research directly pertinent to the present research is reviewed here.

The earliest known experiment with bluff bodies in drag-reducing polymers was carried out by Crawford and Pruitt [7] in 1963. They dropped 5/8-inch-diameter rubber and steel spheres in Guar Gum solutions and reported that at 2,500 wppm the drag on both the steel and rubber spheres was reduced. But at 5,000 wppm, only the drag on the steel sphere was less than it would be in water. Ruszczycky [8] carried out some measurements in 1965 on the fall velocity of steel spheres in polyethylene oxide "Polyox WSR-301", using spheres of diameters from 3/8" to 1.0" in concentrations up to 15,000 wppm. He found that for all spheres with a diameter less than 1/2", as the concentration was increased, the drag at first decreased, reaching a minimum between 2,500 and 7,500 wppm. The largest drag reduction observed was 26%, obtained with the 1.0" sphere in 7,500 wppm solution. These results, although inconclusive because of their limitations and confinement to polymer solutions of very high concentrations, appear to point out that a mechanism different from that observed for turbulent flow in pipes may be in operation.

White [9] carried out a series of pipe flow experiments over a wide range of flow Reynolds number with pipes

of different diameters, using various concentrations of the guar gum solutions. He found that the pipe diameter has a considerable effect on the drag reduction, the reduction being greater with the smaller pipe sizes, for the same polymer concentration and Reynolds number.

White [10] described a simple experiment which demonstrated that in some circumstances the use of polymer additives can increase drag of submerged bodies owing to a change in the position of boundary layer separation which results in a change of wake size and thus form drag. It was seen that although polymer addition can significantly reduce skin friction, the effect can in certain circumstances be more than offset by an increase in form drag caused by a change in the separation point and wake size. He conducted his experiments through dropping a sphere into a tank (almost unbounded media). Also he [11] used the same technique of dropping spheres into a tank, and he found the terminal velocity using a photographic technique. The results seem to show that:

(1) at R_e = 7000 there seems to be no change in C_D,

(2) maximum reduction of C_D occurred in 75 wppm,

(3) the percent reduction of C_D increases with R_e,

(4) the maximum reduction in C_D noted was 45%.

He suggested to consider the reduction in friction factor of "polyox" solutions as a gradual motion of the point of

separation back towards the trailing edge as R_e increases. If this is so, then the actual process of transition has been changed by the addition of polymer.

Lang and Patrick [12] observed the flow about freely falling spheres, cylinders, discs, and cones in polyox solutions, 200 to 1,000 wppm. They noted that there was drag reduction for only those bluff bodies which had a movable separation point. However, they also reported that there was no significant drag reduction for circular cylinders for $R_e < 2 \times 10^4$. They further suggested that the mechanism which causes the polymer molecules to shift the separation point is not apparent and merits further investigation. In Lang and Patrick's experiments, the fall of the objects was not always steady and at times there were sudden shifts in the direction of fall. For reasons yet unknown, the drag in polyox solutions did not follow the typical trend of sphere drag in plain water as a function of Reynolds number as far as the characteristic sharp decrease, which is due to sudden transition to turbulent separation is concerned.

Extensive studies on freely falling spheres have been conducted by Hayes [13] and Chenard [14] with WSR-301, in a Reynolds number range of approximately 10^4 to 10^5. Hayes observed that there was no drag reduction at Reynolds number below 10^4, drag reduction increased with the Reynolds number,

and the maximum drag reduction occurred in a concentration of 100 wppm for Reynolds numbers between 10^4 and 10^5.

White [15], in 1967, showed that the drag on spheres in water, at Reynolds numbers exceeding the critical value (Vd/ν > about 2×10^5), could be increased by dissolving a very small quantity of polyethylene oxide in water, and suggested that this effect resulted from suppression of turbulence in the boundary layer by the additive, which caused earlier separation and a corresponding increase in the wake size. Experiments carried out below the critical Reynolds number, where the boundary layer is laminar, have shown that the drag on a sphere is considerably reduced by adding "polyox", although drag reduction in the pipe flow occurs only in the turbulent regime. Flow visualization studies showed delayed layer separation and a smaller wake size with the polymer solutions, which is consistent with the reduction of drag. White carried out his experiments by dropping steel spheres down through cylinders containing the test liquid. The maximum sphere to tube diameter ratio used was 0.25, such that for the majority of cases the fluid media could be considered to be semi-infinite, i.e. non-bounded media.

Stow et al [16] conducted experiments which were concerned with the drag on an aluminum ball tethered in a vertical pipe with fully developed turbulent flow. The

results they obtained indicated that the drag coefficient is not altered by the addition of polymer to the solvent. This disagrees with the results of the present study which indicates that the drag coefficient decreases.

An examination of their experimental method suggests a possible explanation. The polymer used was polyox (WSR301, a polymer that is highly susceptible to shear degradation, and rather than using an open circuit system they used a closed circuit in which the polymer was continually recirculated using a centrifugal pump. To obtain results at different concentrations the original polymer was then diluted. Because of the sensitivity of polyox to shear degradation, it is probable that over the period of experimenting, the actual concentration was not accurately known and the polymer was totally degraded.

Barenblatt et al [17] measured the drag force on a rough cylinder from which highly concentrated solutions of long-chain polymers were injected. Drag reductions of 20% to 34% were achieved. Tests with glycerin injection, which did not reduce drag, showed that contraction of the wake was independent of the type of fluid injected. He therefore, concluded that the contraction of wake and the displacement of the separation point further downstream cannot conclusively explain the drag reduction phenomenon.

There have been a few studies on the effects of

injected polymer additives on the drag of bodies in semi-infinite media, but these are not really applicable to the present study. This is because the polymers were not homogeneously dispersed, the bodies were usually torpedo shaped, and the media was semi-infinite.

Recently, an investigation was made by Latto, Round, and Anzenavs [19, 24] using single spheres and sphere trains hydrodynamically suspended in a 2" diameter vertical glass tube. Diameter ratios ranging from 0.2 to 0.97 were used and measurements were made using polymer solutions of different concentrations and results were compared to those obtained using water. It was found that the drag coefficient was not affected for diameter ratios greater than 0.7 but there was an obvious increase (which does not agree with the present research) for diameter ratios less than this value.

Another related work to that of Anzenavs, is that of Aly [21] in which he used an open circuit to prevent the polymer from getting degraded, while samples were taken during the experiments and tested in a turbulent flow capillary tube rheometer to make sure that the polymer did not suffer any mechanical degradation. His results tended to uphold Elliot's and Stow's data [11] and do not agree with Whites data, (as well as the present work). Furthermore, Latto et al [22] substantiated previous observations, that polymer has little effect on the pressure drop and drag

coefficient for cylinders and sphere trains, and that a sphere is a more efficient geometry than that of a cylinder. It was also observed that polymer addition appreciably affects the location of the point of separation of the flow over a spherical capsule, which would certainly account for the observations on the drag coefficient.

It is apparent from the foregoing, that the mechanisms proposed for the reduction of the drag of bodies moving through polymer solutions are less coherent and loosely related to the mechanisms for the drag reduction in pipes. This is partly because the drag reduction has been studied more extensively in conduits and additional data provided ways and means of refusing or substantiating the mechanisms proposed. Secondly, in pipe flows, the motion was essentially steady, uniform, had a uniform wall-shear distribution (somewhat affected by the polymer degradation along the length of the pipe), had no separation, no stagnation point, no curvatures and the motion was often beyond the transition point.

In external flows, however, the motion is unsteady due to the vortex shedding in the aft region of the body, has variable shear and is accompanied by separation, stagnation, and "drag crisis" at or near the transition of the laminar boundary layer to a turbulent state. Obviously, the flow about bodies introduces many complex factors which

are not encountered in the experiments conducted with pipes. It, therefore, seemed appropriate that a comprehensive investigation be initiated to study the characteristics of the flow of dilute polymer solutions about bluff bodies through the measurement of the pressure distribution, drag, and separation angle.

CHAPTER 3

APPARATUS AND EXPERIMENTAL PROCEDURE

3.1 The Apparatus:

The apparatus used was basically the same as that used in reference [21] with some modifications. A general schematic diagram of the arrangement of the apparatus is shown in Figure (3.1) (see also photograph page 16).

Since the system can be used as either an open or closed circuit, two sources of water have been used, the city mains for open circuit flow, and a reservoir of approximately 0.3 m^3 capacity for closed system.

The water was drawn from the water main (or from the reservoir). A 0.01 m^3 capacity surge chamber attached to the 0.0508 m pipeline reduced the pressure fluctuations in the system. The water then passed through a precalibrated "Brooks" rotameter (see apparatus) which measured the flow rate and hence, the fluid velocity of approach in the test section. After leaving the rotameter, the water flowed down a vertical steel pipe, 0.0508 m diameter, then via a 1.3 m diameter bent vertically up to the level of the reservoir to the test section. The water then was discharged to the main drainage line (or into the reservoir if a closed circuit system was to be used.)

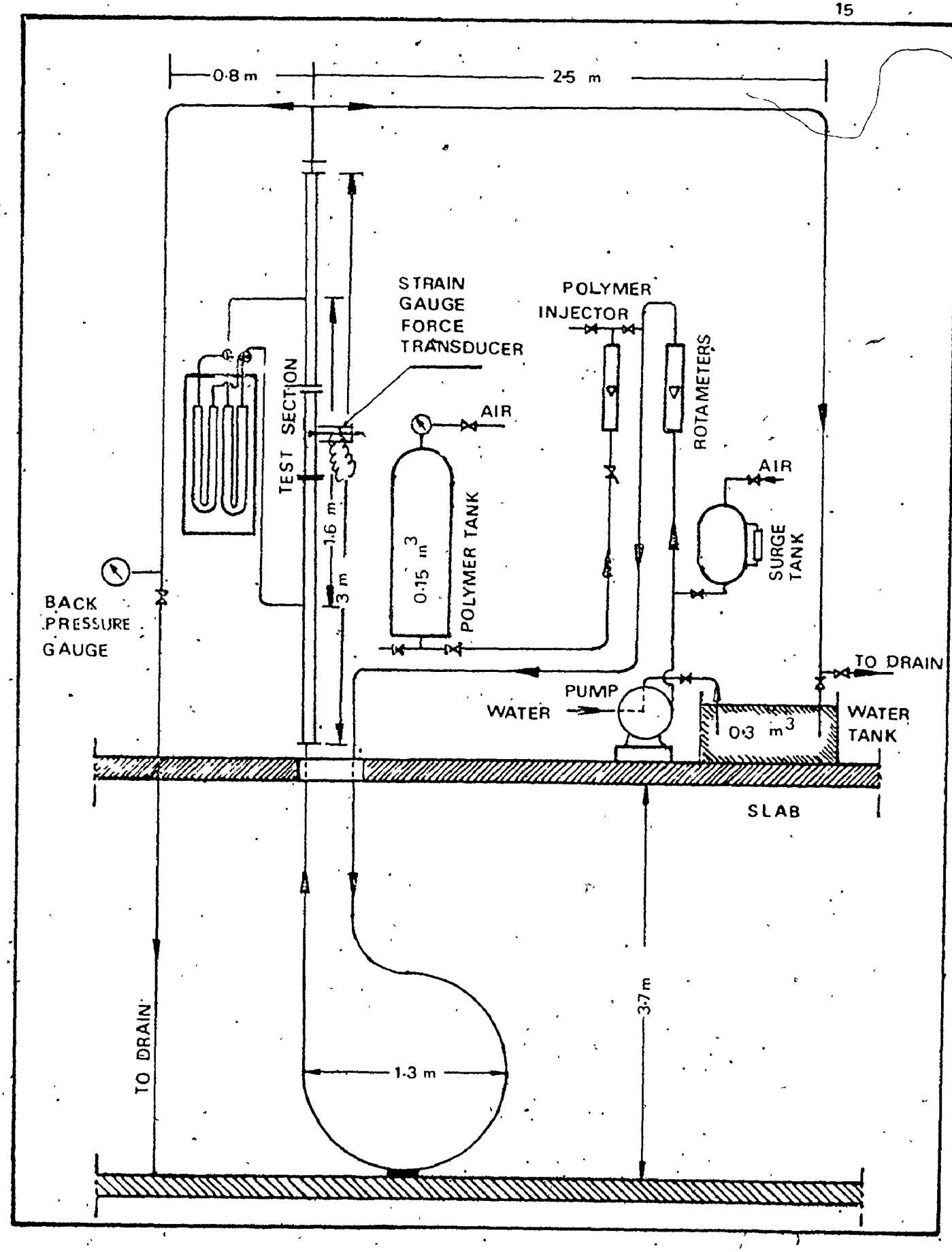

Figure (3-1) General schematic diagram of the apparatus.

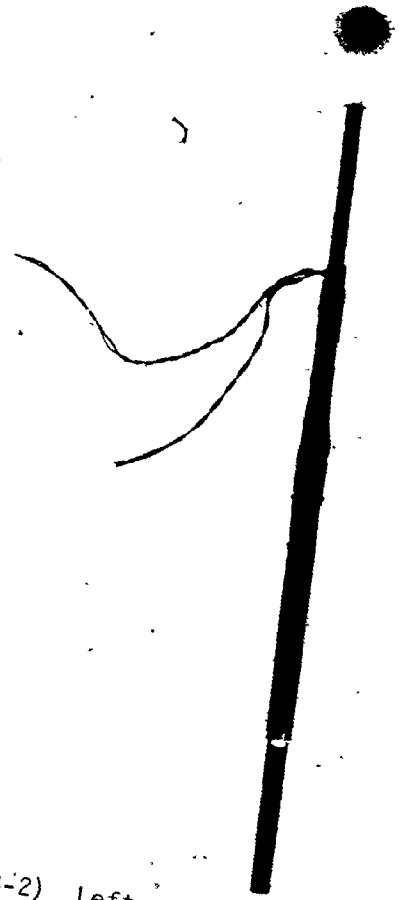

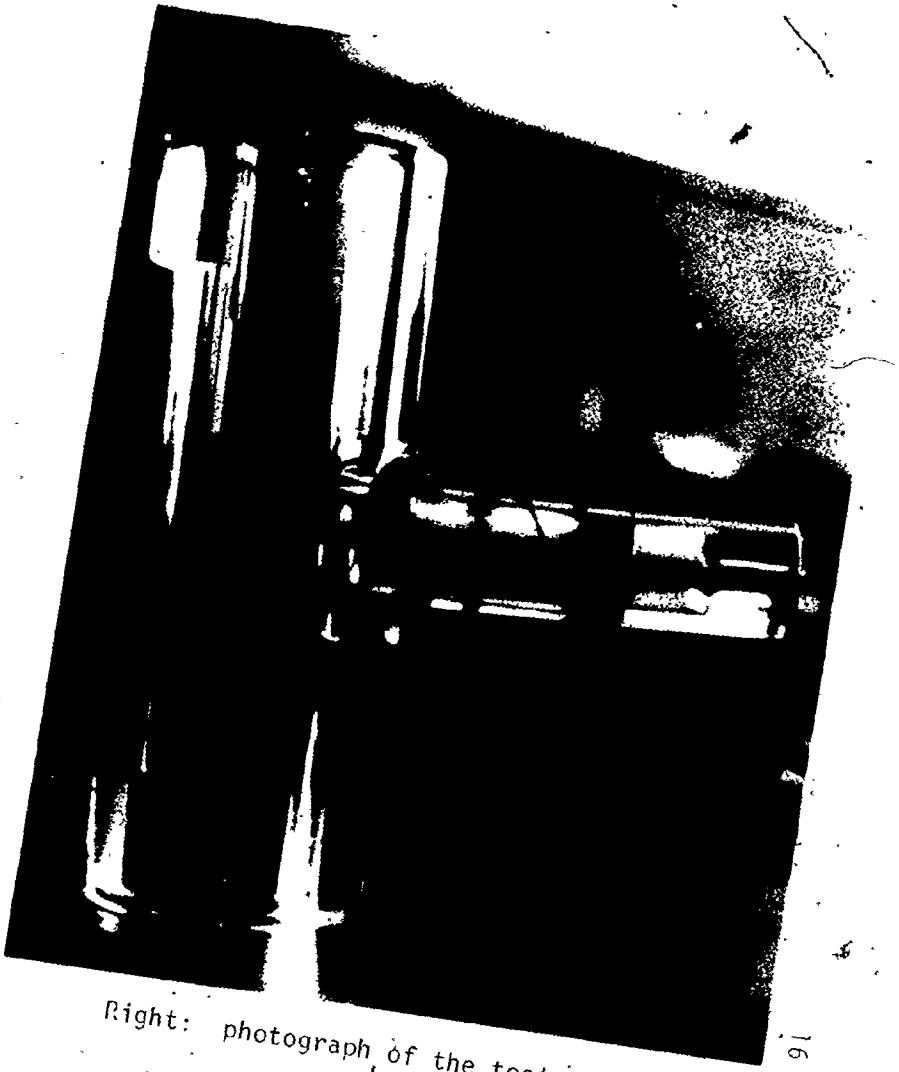

Figure (3-2) Left: photograph of the suspension rod with the sphere, showing strain gauges

Right: photograph of the test section

Two gate valves at appropriate locations controlled the open or closed circuit flow, while a third valve on the drain section of the pipeline regulated the back pressure.

The test section which was a vertical plexiglass tube of 0.0508 m I.D. and about 3 m long was braced by rubber lined clamps. To achieve homogeneous turbulence in the test section, a honeycomb was placed at the entrance of the tube. Two pressure tapes located 1.6 m apart in the plexiglass tube were used to measure the pressure gradient. It should be noted that the flow in the test section had previously checked using multiple pressure taps and was fully developed.

The spheres were mounted concentrically in the test section on a cantilever rod (force transducer) through which the drag force was measured directly using strain gauges (number EA-09-125BT-120) calibrated before and after each test to measure the force, (see apparatus). The strain gauges were moisture and water-proof, see Appendix (B).

Plastic spheres were used, rather than steel spheres, to increase the natural frequency of the system and to elevate the velocity at which vibration commences.

Four sphere to tube diameter ratios of 0.868, 0.74, .6181, and 0.439 were used. Two stainless steel rods were used to cover the range of drag forces caused by such dia-

meter ratios and the Reynolds numbers achieved in the experiments (see Appendix B).

The pressure drop between the two pressure taps was measured using either a mercury or a carbon tetrachloride-in-glass U-tube manometer which were connected in parallel. Due to the difference between the room and water temperature, a temperature gradient in the connecting lines arose, which caused a zero reading. To avoid this problem, they were continually bled before taking any manometer readings, thus, maintaining a uniform temperature in the manometer lines. Also, the bled lines were used to take samples from the tube during a run which were used to check the dispersion and also the degradation of the polymer within the liquid in the test section.

Two different systems were considered for the polymer additive experiments:

a) To inject high concentration aqueous polymer solution directly into the pipeline upstream of the test section;

b) To use the reservoir and utilize recirculating homogeneous polymer flows.

The results obtained from the injection method (open system) were not reliable enough, since it was difficult to adjust the two rotameter readings to achieve the required pre-determined concentrations. This difficulty arose because of the

pressure fluctuations in the main water supply, which affected the discharge rate of the injected polymer. To overcome this problem, it was decided to work with the polymer as a closed system for short periods of time.

The water reservoir was filled with water and the required polymer concentration was controlled through mixing the proper weight of pre-made polymer solution of 10,000 wppm in the water reservoir. Rheometer tests showed no signs of degradation before and after each test (for a running period of about 20 minutes) with closed circuit flow and therefore, this method was employed for all the polymer tests.

3.2 The Rheometer System:

It is essential that the homogenuity of dispersion of the concentrated aqueous polymer solution as well as the degree of degradation be known throughout the experiment. A simple but extremely reliable method is to use a vertical tube (turbulent flow) rheometer.

Figure (E-1) shows the construction of such an apparatus which works on the principle that the same volume of fluid of different concentration of polymer additive takes dissimilar times to pass through a narrow cross section pipe under identical pressure head provided in this case by a 6 m height of water, (see Appendix E). The volume of fluid is

contained in a funnel and drainage of this fluid through the narrow 1.5 mm capillary tubing is initiated by the opening of a 1/2" "ascoelectric" solenoid valve at the exit end on the lower floor level.

3.3 Procedure:

Prior to the actual testing, the water was circulated through the system for an hour or so, to ensure isothermal conditions. The flow was then stopped and the manometer zero reading was adjusted.

For each rotameter setting, both readings of the strain gauge and manometer were recorded. From such readings, drag coefficient, the Reynolds number and the pressure function could be computed, (see Appendix A).

During the runs with the polymer solutions, samples were taken at random time intervals from the tube, and were tested in the turbulent rheometer (see Appendix E) to check the level of concentration and mixing in the test section. The temperature of the water tank was recorded before and after each test, and it was found that the maximum temperature rise was $2^{o}C$.

The above procedures were repeated for four diameter ratios of spheres both in water and dilute polymer solution concentration of 20, 40 and 60 wppm.

CHAPTER 4

THEORITICAL AND EXPERIMENTAL ANALYSIS

4.1. THEORY

A simplified theoritical model can be used to describe some of the macroscopic phenomena involved. The theory is well documented in detail in References [2], [19] and [21], however a review of the pertinent equations is presented here. The theoritical analysis is divided into two sections; first part is concerned with the relationship between the drag coefficient and the other flow parameters, whilst the second part with a pressure drop analysis.

1. Drag coefficient analysis:

McNown and Newlin [2] made an analysis of the flow past a sphere for a diameter ratio approaching unity. If the ratio of the sphere diameter to the tube diameter (d/D) and the Reynolds number are both comparatively high, the momentum equation can be used to obtain an approximate expression for F_D, the drag on the sphere.

This is conventionally expressed in terms of the coefficient of drag, the cross-sectional area of the body, and the relative velocity between the body and the undisturbed fluid, as follows:

$$F_D = \frac{C_D A \rho V_o^2}{2} \qquad (4\text{-}1)$$

The converging flow upstream from the sphere's equator is essentially irrotational, so that (see illustrating figure below).

$$P_o + \frac{\rho V_o^2}{2} = P_1 + \frac{\rho V_1^2}{2} \qquad (4\text{-}2)$$

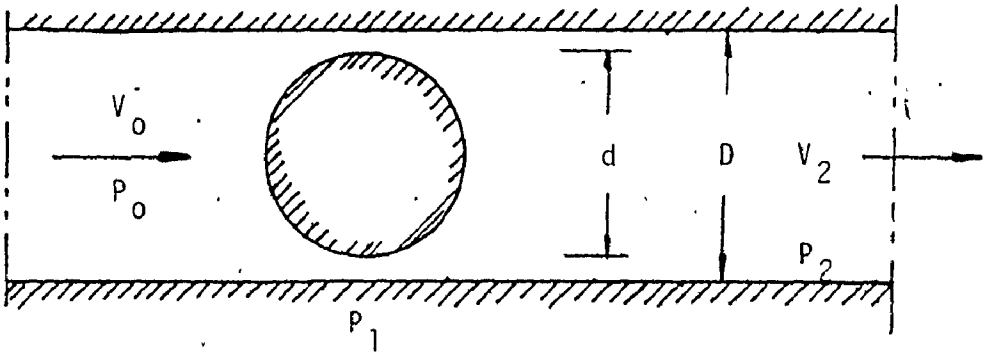

DEFINITION SKETCH

and the equation of continuity can be written:

$$V_1(D^2 - d^2) = V_o D^2 \qquad (4\text{-}3)$$

If, in addition, the pressure over the downstream face of the sphere is assumed to be equal to P_1, as in the analysis of an abrupt expansion, the equation of momentum can be applied between points 1 and 2:

$$(P_2 - P_1)(\pi D^2/4) = \rho Q(V_1 - V_o) \qquad (4\text{-}4)$$

since $V_2 = V_1$

The momentum equation can again be applied for points 0 and 2, whereby a relationship between the total pressure drop and the drag force is obtained

$$(P_o - P_2)(\pi D^2/4) = F_D \qquad (4\text{-}5)$$

Finally, the preceding equations can be combined so as to relate the coefficient of drag and the pressure difference to the diameter ratio

$$C_D = \frac{D^2}{d^2} \frac{P_o - P_2}{\rho V_o^2/2}$$

$$= \frac{D^2}{d^2} \frac{(P_1 + \rho V_1^2/2 - \rho V_o^2/2) - \frac{\rho Q}{A}(V_1 - V_o)}{\rho V_o^2/2}$$

Since $\frac{\rho Q}{A} = V_o$

where $A = \pi D^2/4$

$$\therefore \quad C_D = \frac{D^2}{d^2} \frac{(V_1 - V_o)[\rho/2(V_1 + V_o) - \rho V_o]}{\rho V_o^2/2}$$

$$= \frac{D^2}{d^2} \frac{(V_1 - V_o)[\rho V_1/2 - \rho V_o/2]}{\rho V_o^2/2}$$

$$= \frac{D^2}{d^2} \frac{(V_1 - V_o)^2/2}{V_o^2/2} = \frac{D^2}{d^2} \frac{(\frac{D^2}{D^2 - d^2} - 1)^2 V_o^2}{V_o^2}$$

$$= \frac{D^2}{d^2}\left[\frac{d^2}{D^2 - d^2}\right]^2 = \left[\frac{d/D}{1 - (d/D)^2}\right]^2 \qquad (4\text{-}6)$$

It is evident that the assumptions made in the derivation of the previous equation are justifiable only if d/D is nearly equal to unity and if the viscous shear is small. Since real viscouse fluids were used, a semi-empirical form of McNown and the equation can be written in the form of:

$$C_D = \left(\frac{(d/D)^m}{1 - (d/D)^n}\right)^{\ell} \qquad (4\text{-}7)$$

The constants m, n and ℓ will be evaluated experimentally as will be seen from results analysis.

2. Pressure drop analysis:

Considering macroscopic momentum balance in the direction of the tube center line for the control volume shown in Figure (4-1), in a tube (pipe) inclined at an angle θ degrees to the horizontal, we get:

$$P_1A_1 + (\rho A_1V_1)V_1 = P_2A_2 + \tau_o\pi DL + (\frac{\pi}{4}D^2L - \frac{\pi}{6}d^3)\gamma_\omega \sin\theta + (\rho A_2V_2)V_2 \qquad (4\text{-}8)$$

Since $A_1 = A_2$ and $V_1 = V_2$ by continuity

$$\therefore (\rho A_1V_1)V_1 = (\rho A_2V_2)V_2 \qquad (4\text{-}9)$$

$$\therefore \Delta P_s \frac{\pi}{4}D^2 = \tau_o\pi DL + (\frac{\pi}{4}D^2L - \frac{\pi}{6}d^3)\gamma\omega\sin\theta \qquad (4\text{-}10)$$

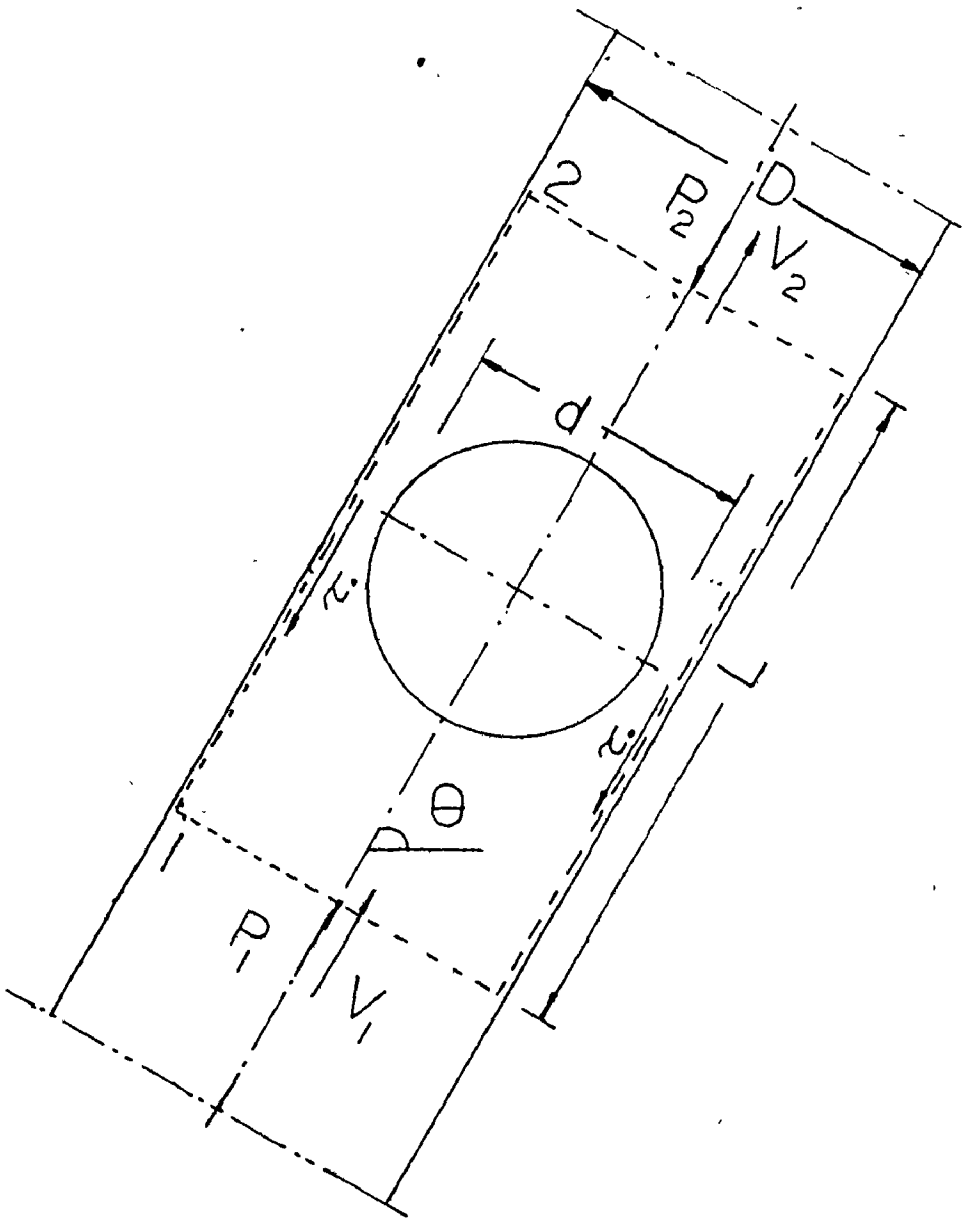

Fig.4.1
"Flow through a Control Volume containing a tethered sphere"

If we consider the same control volume without the object present and apply the momentum balance in the direction of the tube center line, we get:

$$\Delta P_L \frac{\pi}{4} D^2 = \tau_o \pi D L + \frac{\pi}{4} D^2 L \gamma_\omega \sin\theta \qquad (4\text{-}11)$$

It should be noted that τ_o in equation (4-11) is not necessarily equal to the average τ_o in equation (4-8). Substituting in equation (4-10) for the value of $\tau_o \pi D L$, we we obtain:

$$\Delta P_s \frac{\pi}{4} D^2 = \Delta P_L \frac{\pi}{4} D^2 - \frac{\pi}{4} D^2 L \gamma_\omega \sin\theta + (\frac{\pi}{4} D^2 L - \frac{\pi}{6} d^3)\gamma_\omega \sin\theta$$

$$\therefore \quad (\Delta P_s - \Delta P_L) \frac{\pi}{4} D^2 = -\frac{\pi}{6} d^3 \gamma_\omega \sin\theta \qquad (4\text{-}12)$$

By further manipulation we can arrive at:

$$\frac{\Delta P_s - \Delta P_L}{\gamma_\omega D} = -\frac{2}{3}(\frac{d}{D})^3 \sin\theta \qquad (4\text{-}13)$$

which is explicit function between the pressure drop, $\frac{d}{D}$ and the angle of tube inclination to the horizontal θ.

For a vertical tube, which is the case encountered in the present study, $\theta = 90$ and equation (4-13) becomes:

$$\frac{\Delta P_s - \Delta P_L}{\gamma_\omega D} = -\frac{2}{3}(\frac{d}{D})^3 \qquad (4\text{-}14)$$

This last equation is the expression used to

express the pressure drop in a nondimensional form, which is called the pressure function (PRF_1). However, due to the complexity of the flow system, the above rather simplified analysis is not sufficient to accurately describe the situation. Consequently, it was anticipated that an empirical equation of the form:

$$PRF = \frac{\Delta P_s - \Delta P_L}{\gamma_\omega D} = f(R_D, \frac{d}{D}) \qquad (4\text{-}15)$$

would more accurately correlate the data.

4.2. EXPERIMENTAL ANALYSIS

The following discussion is presented in two sections; the first deals with the work using water, and the second with the work using dilute polymer solutions. An error analysis related to the measurements and data reduction is given in Appendix C. Also the numerical values of the actual experimental data and the calculated functions are displayed in Appendix G.

i) The research using water.

The basic objective of studying the flow around bodies is to observe how the drag is related to the other flow parameters in a confined boundary media.

Figure (4-2) of C_D vs. R_d shows the effect of R_d on the drag coefficient for various d/D ratios. It is apparent, for the R_d range investigated, that at higher d/D ratios C_D is a function of R_d, which is not apparent for the mid d/D ranges. The most noticable effect is the inflection in the d/D = 0.44 curve, which might be due to the shift to turbulent boundary layer (before separation). It occurs spontaneously at a certain Reynolds number which depends upon the smoothness of sphere and the turbulence in the fluid stream. This sudden drop in drag coefficient could possibly occur at higher R_d for the larger d/D ratios and further investigation at

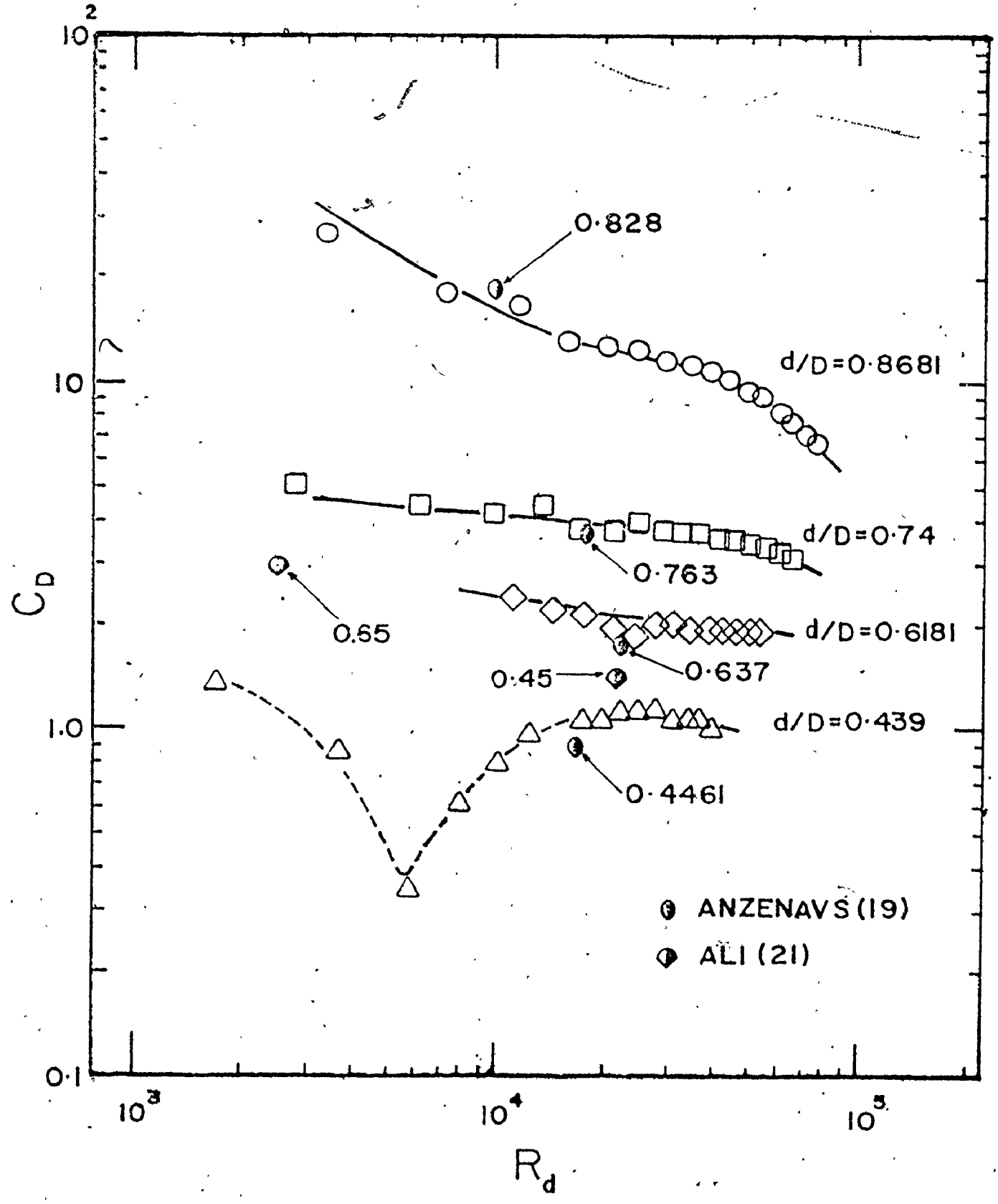

Figure (4-2) Drag coefficient C_D versus Reynolds number.

higher Reynolds numbers is required to confirm this phenomena (which was beyond the limit of the apparatus used). Attempts at obtaining visual observations of the flow behaviour were unsuccessful due to minor body oscillations which caused localized flow instability.

It is noticable that the limited hydrodynamic suspension data of Anzenavs et al (19) and Ali et al (21) agree very favourably with the present data, though unfortunately since their experiments involved hydrodynamic suspension, only one point on the C_D - R_d plot was observed for each d/D ratio.

Figure (4-3) shows the relation of C_D vs. d/D ratio for various Reynolds numbers. It appears that within the range of Reynolds numbers used, C_D can be considered as a function of d/D alone (except at the higher d/D ratios). The data were correlated using the following semi-empirical form of Equation (2.3):

$$C_D = \left(\frac{(d/D)^m}{1 - (d/D)^n}\right)^{\ell} \qquad (4\text{-}7)$$

which satisfies the boundary conditions of $C_D = 0$ when $d/D = 0$, $C_D = \infty$, when $d/D = 1$

By curve fitting, the constants m, n, and ℓ were found to be:

$m = 0.1828$ $n = 2.1475$ $\ell = 1.9357$

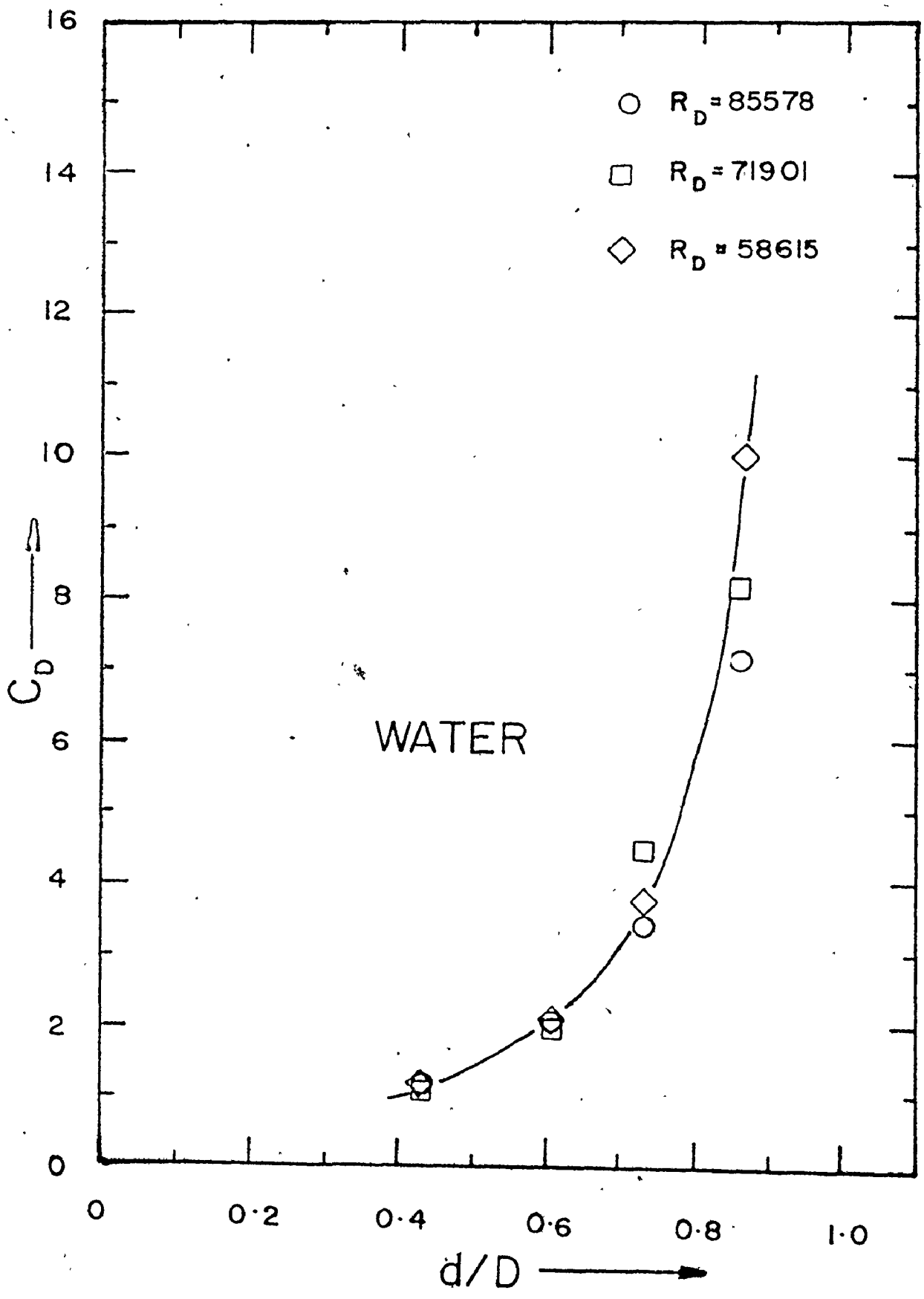

Figure (4-3) Drag coefficient C_D versus diameter ratio d/D.

Figure (4-4) shows the deviation of the mean experimental drag coefficient with the one obtained from the previous Equation (4.7) as a function of d/D ratio. This gives reasonable agreement of the data with the equation over the Reynolds number range.

When the pressure function, PRF, data were plotted against d/D for different Reynolds numbers, Figure (4-5), it was noticed that there were a family of curves asymptotic to d/D = 1, pointing out that PRF is a function of both Reynolds number R_D and the d/D ratio.

Since the curves took the same trend as that for C_D vs. d/D, it is suggested that the same function of d/D which was previously used to represent the diameter ratio function term in the PRF function be used. When a logarithmic plot of PRF is plotted against Equation (4-7) as seen in Fig.(4-6) an exponential relationship with a power of 1.19 gave a reasonable fit of the data, producing a family of straight lines for the different Reynolds numbers. A logarithmic plot of PRF vs. R_D for different d/D ratios as seen in Fig.(4-7) shows that PRF is proportional to the square of R_D. In actual fact using an equation in the form:

$$PRF = K R_D^2 \left(\left(\frac{(d/D)^{0.182}}{1 - (d/D)^{2.15}}\right)^{1.9357}\right)^{1.19} \qquad (4\text{-}16)$$

or

$$PRF = K R_D^2 \left(\frac{(d/D)^{0.182}}{1 - (d/D)^{2.15}}\right)^{2.3} \qquad (4\text{-}17)$$

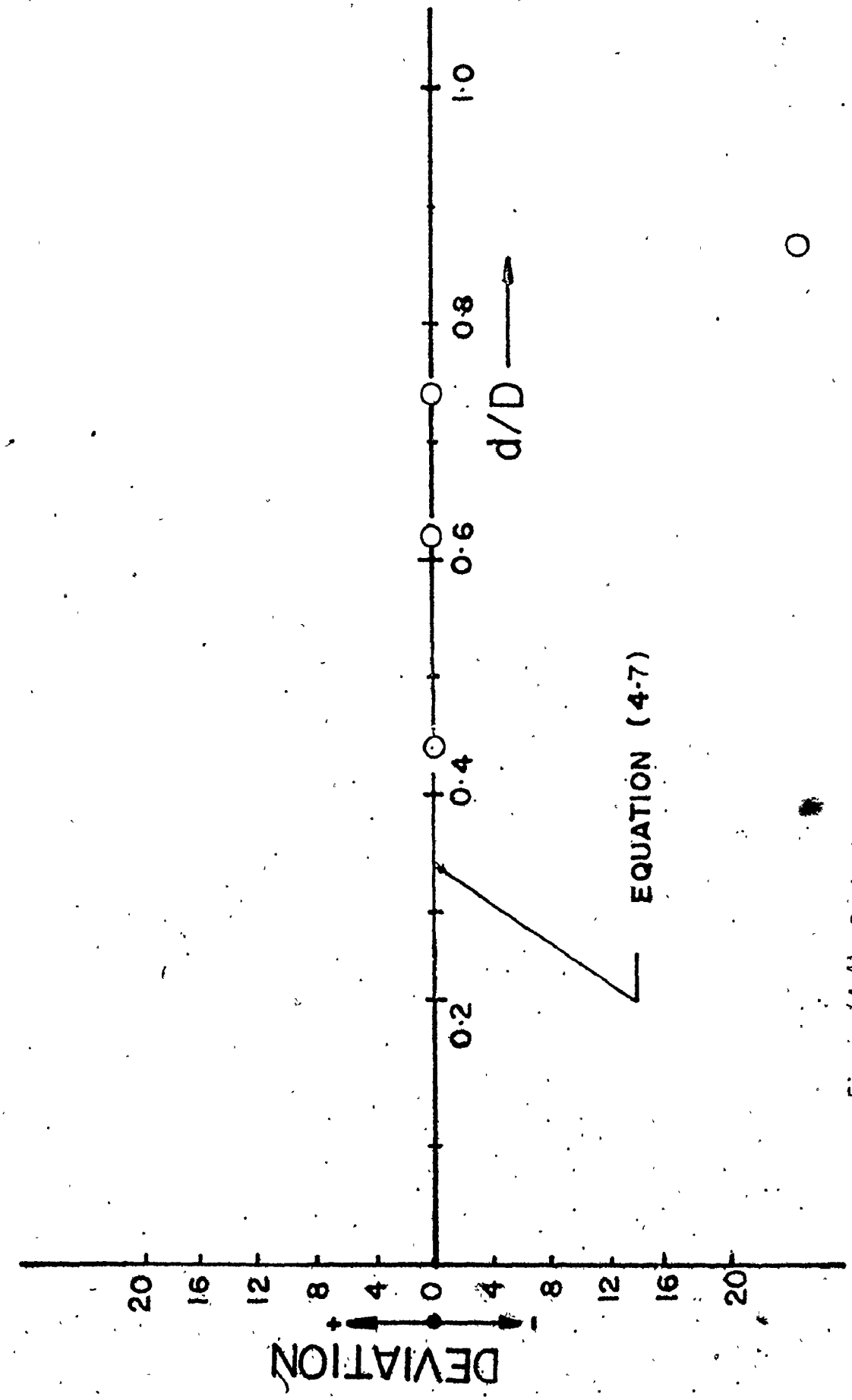

Figure (4-4) Deviation of the fitted C_D curve from the correlated equation.

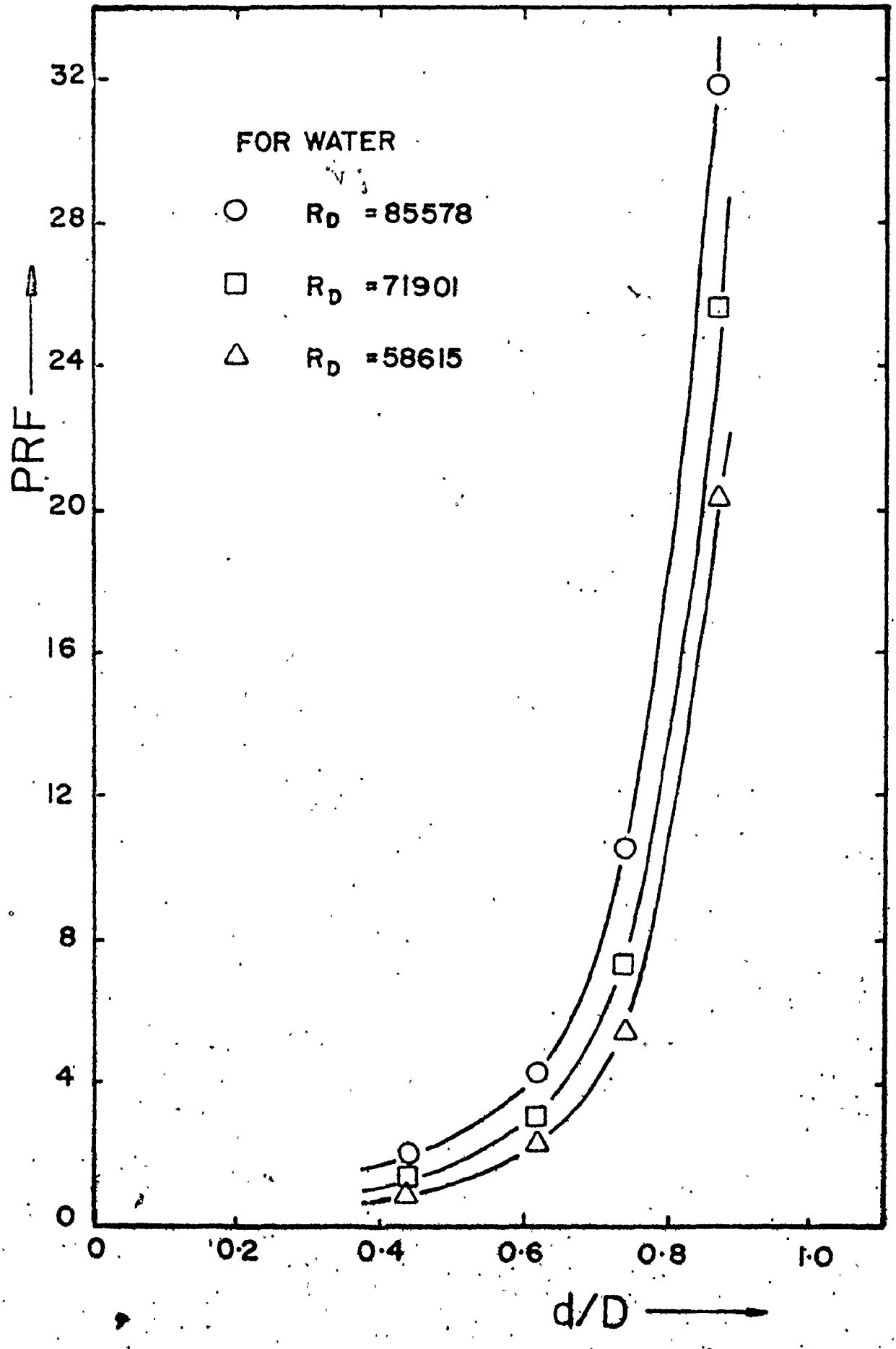
FOR WATER
R_D = 85578
R_D = 71901
R_D = 58615
PRF
32
28
24
20
16
12
8
4
0
0
0·2
0·4
0·6
0·8
1·0
d/D

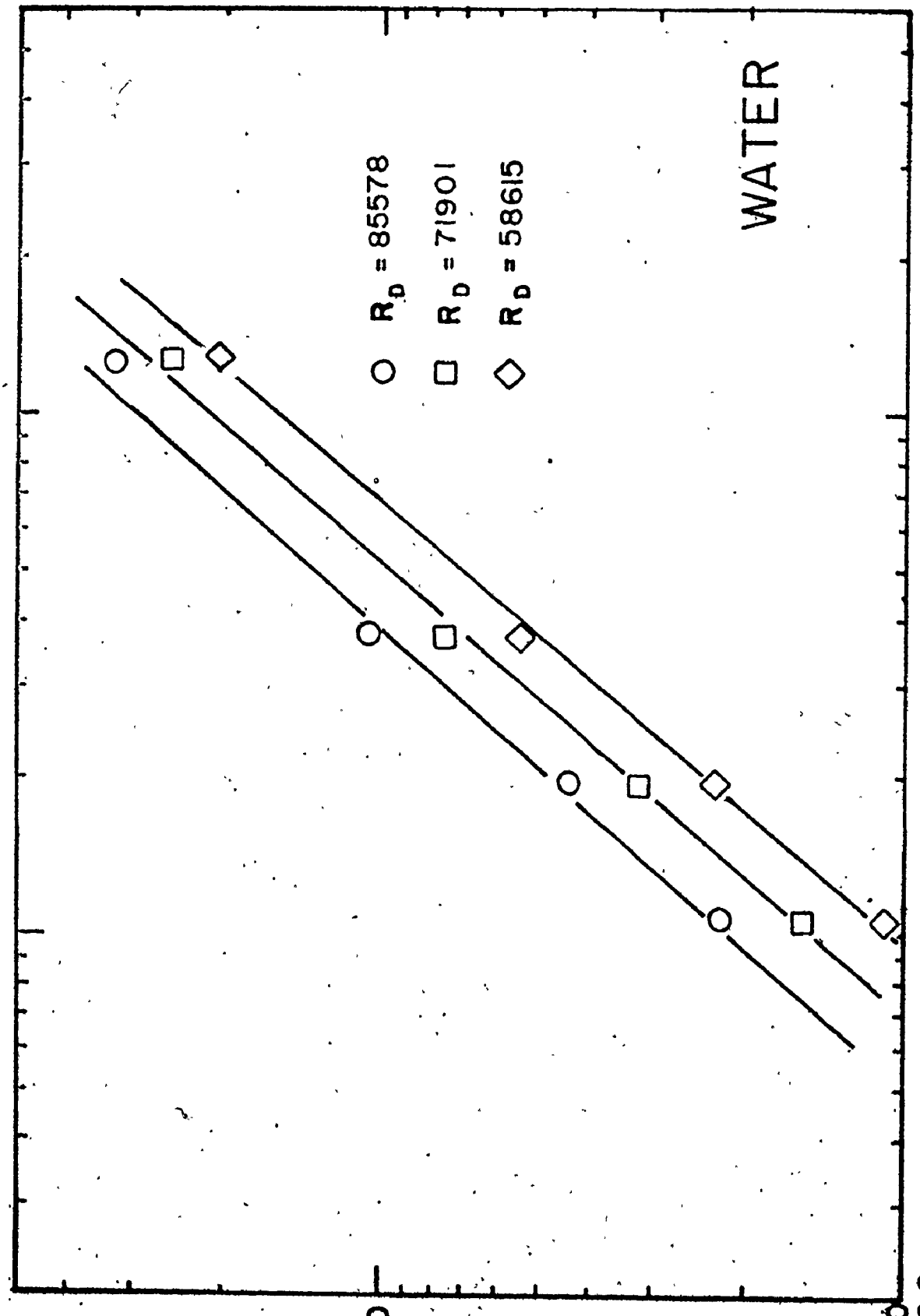

Figure (4-6) Pressure function versus the diameter ratio function.

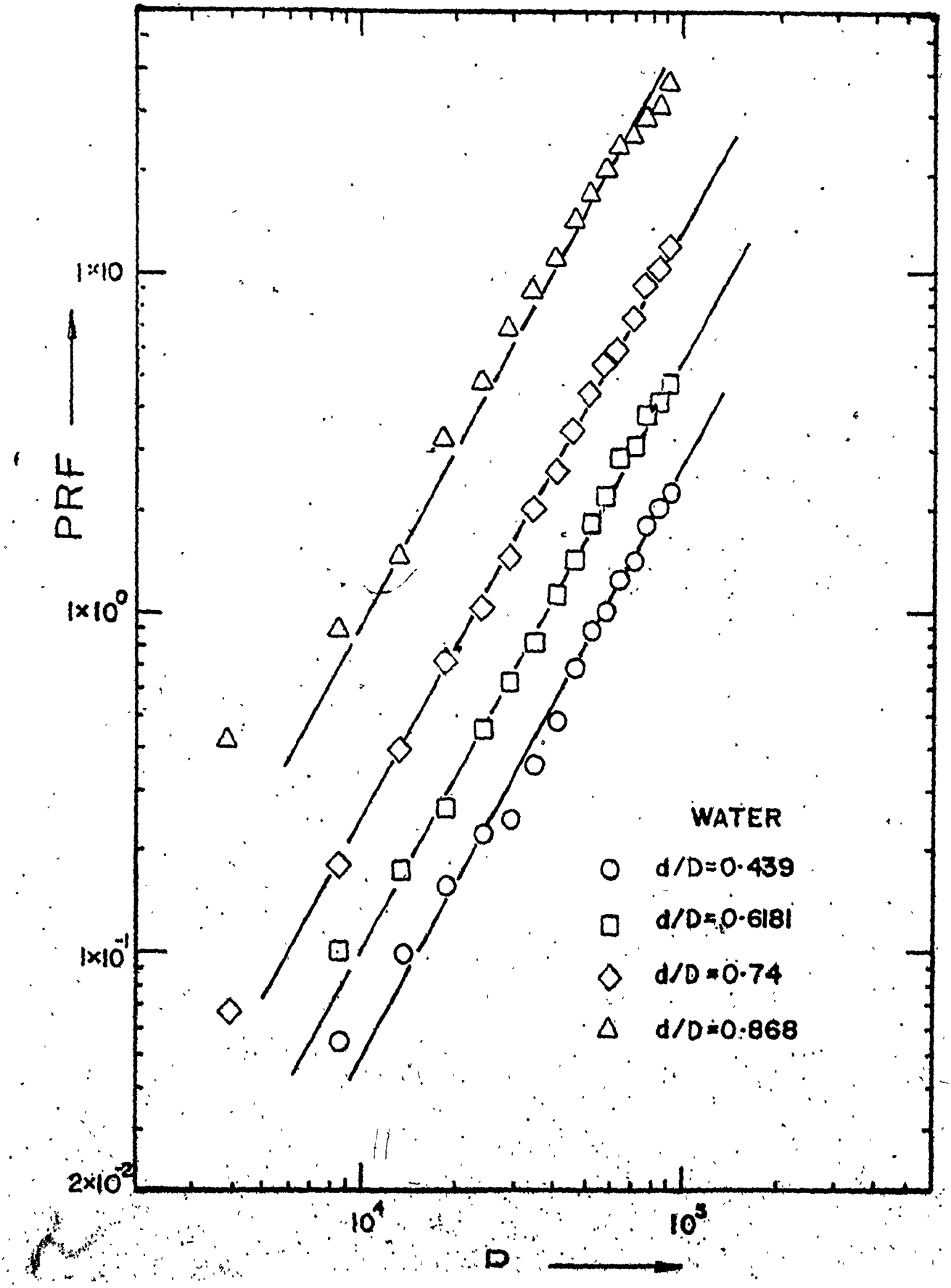
PRF
1×10
1×10⁰
1×10⁻¹
2×10⁻²
10⁴
10⁵
D
WATER
d/D=0·439
d/D=0·6181
d/D=0·74
d/D=0·868

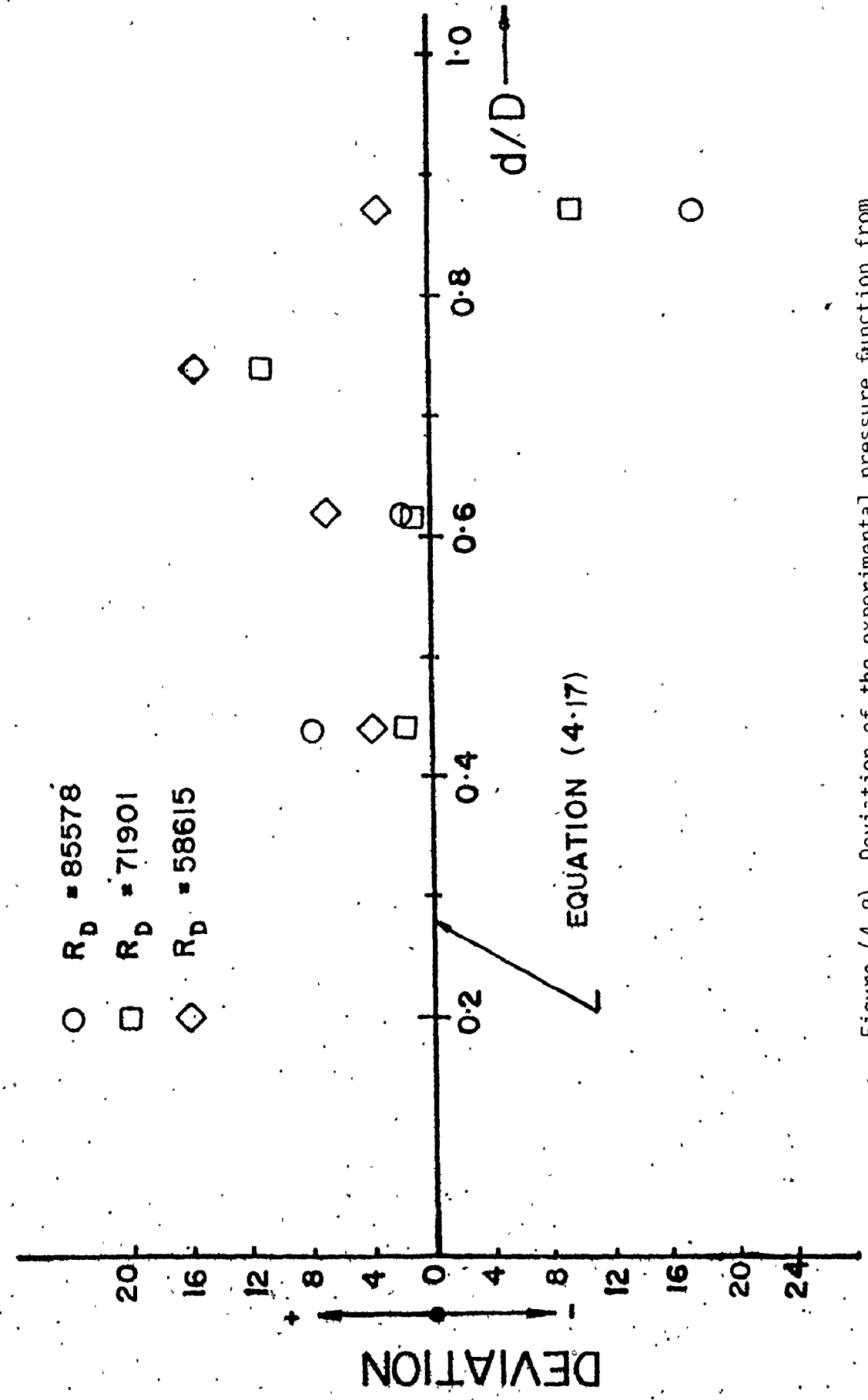

Figure (4-8) Deviation of the experimental pressure function from the correlated equation.

was found to best represent the data.

Since a value of $K = 2.6 \times 10^{-10}$ was found to best fit the data, therefore equation (4-3) can be rewritten as:

$$PRF = 2.6 \times 10^{-10} R_D^2 \left(\frac{(d/D)^{0.182}}{1 - (d/D)^{2.15}}\right)^{2.3} \qquad (4\text{-}17\text{-A})$$

Furthermore, the function for d/D in this equation can be replaced by $C_D^{1.19}$, thus giving

$$PRF = 2.6 \times 10^{-10} R_D^2 C_D^{1.19} \qquad (4\text{-}18)$$

The significance of the above equation is that by measuring the pressure drop, and hence obtaining PRF, the drag coefficient can be directly calculated without the need of measuring the drag force. Figure (4-8) shows the deviation of the experimental results from those of Equation (4-17) for several values of R_D and d/D ratios.

ii) The research using polymer solutions.

In the range of R_d investigated, the effect of R_d is small and in all cases C_D was reduced by additional polymer and at the first sight there was no apparent effect of concentration level, Figures (4-9) to (4-19). However, on referring to Figures (4-20) to (4-23), the effect of concentration is dependent upon the diameter ratio, there being little effect below a d/D of 0.74. For a d/D of 0.87, over the Reynolds number range investigated, there was an

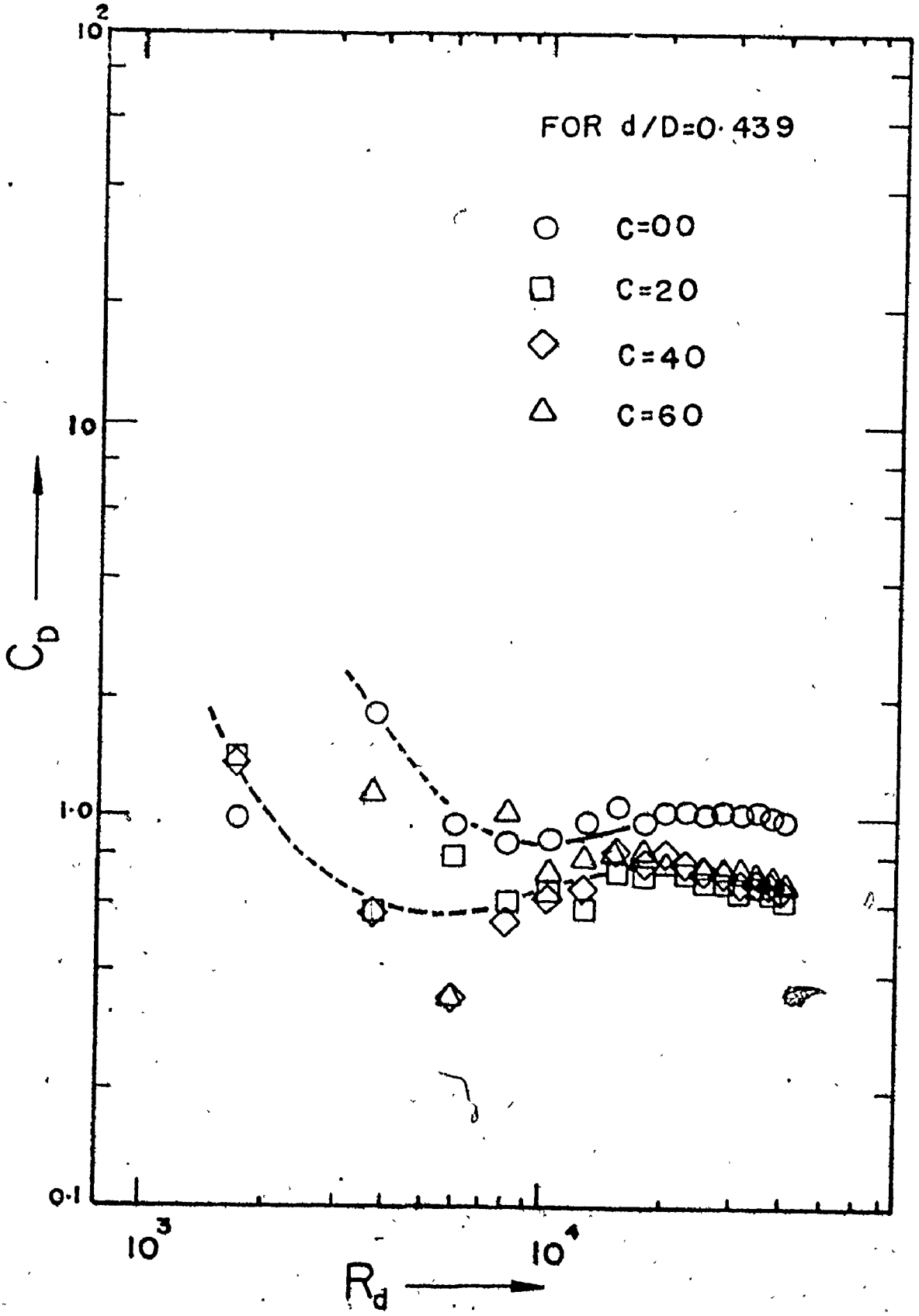

Figure (4-9) Drag coefficient versus Reynolds number for d/D = 0.439.

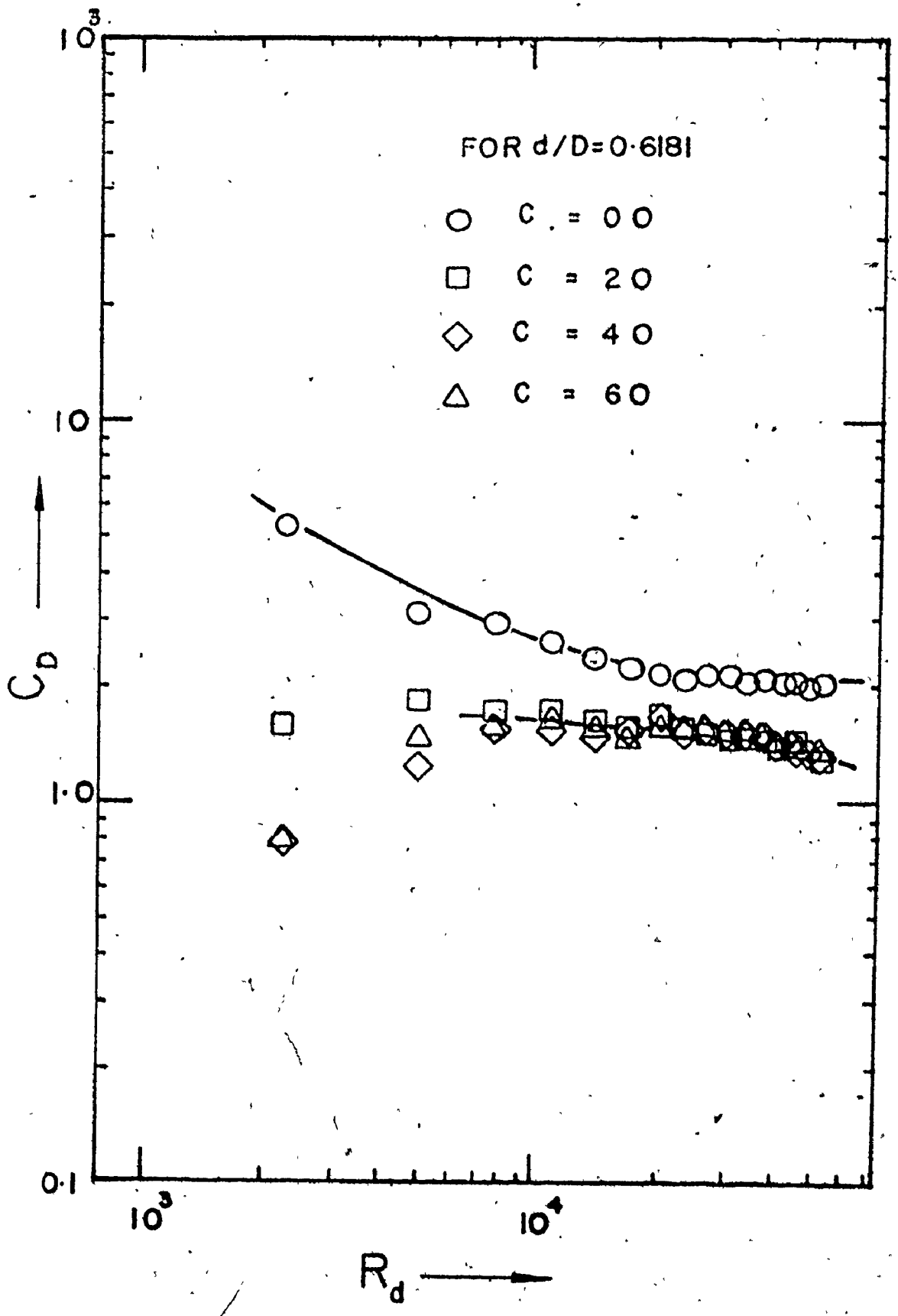

F[illegible] (4-10) Drag coeff[illegible]

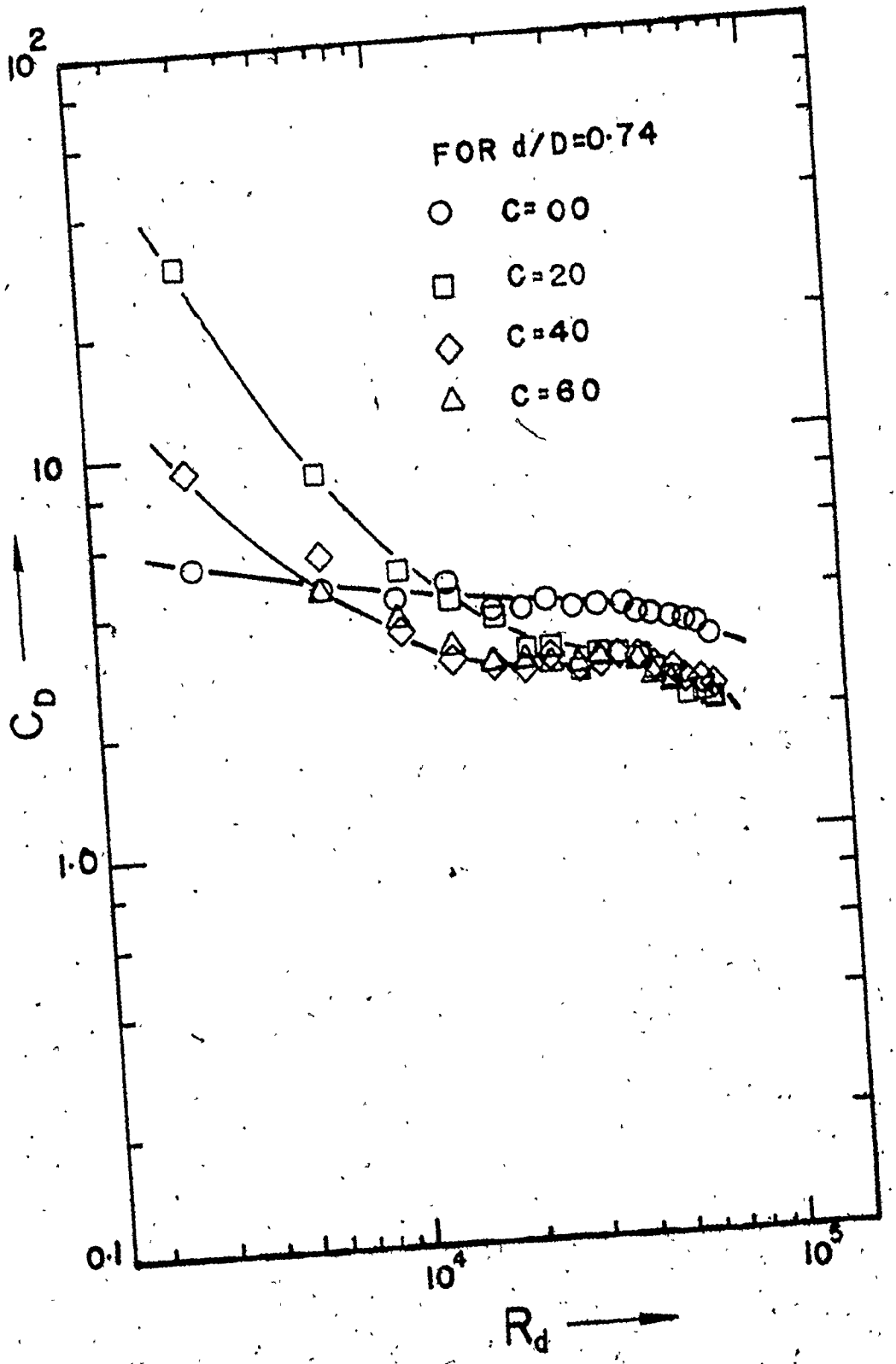

Figure (4-11) Drag coefficient versus Reynolds number for d/D = 0.74.

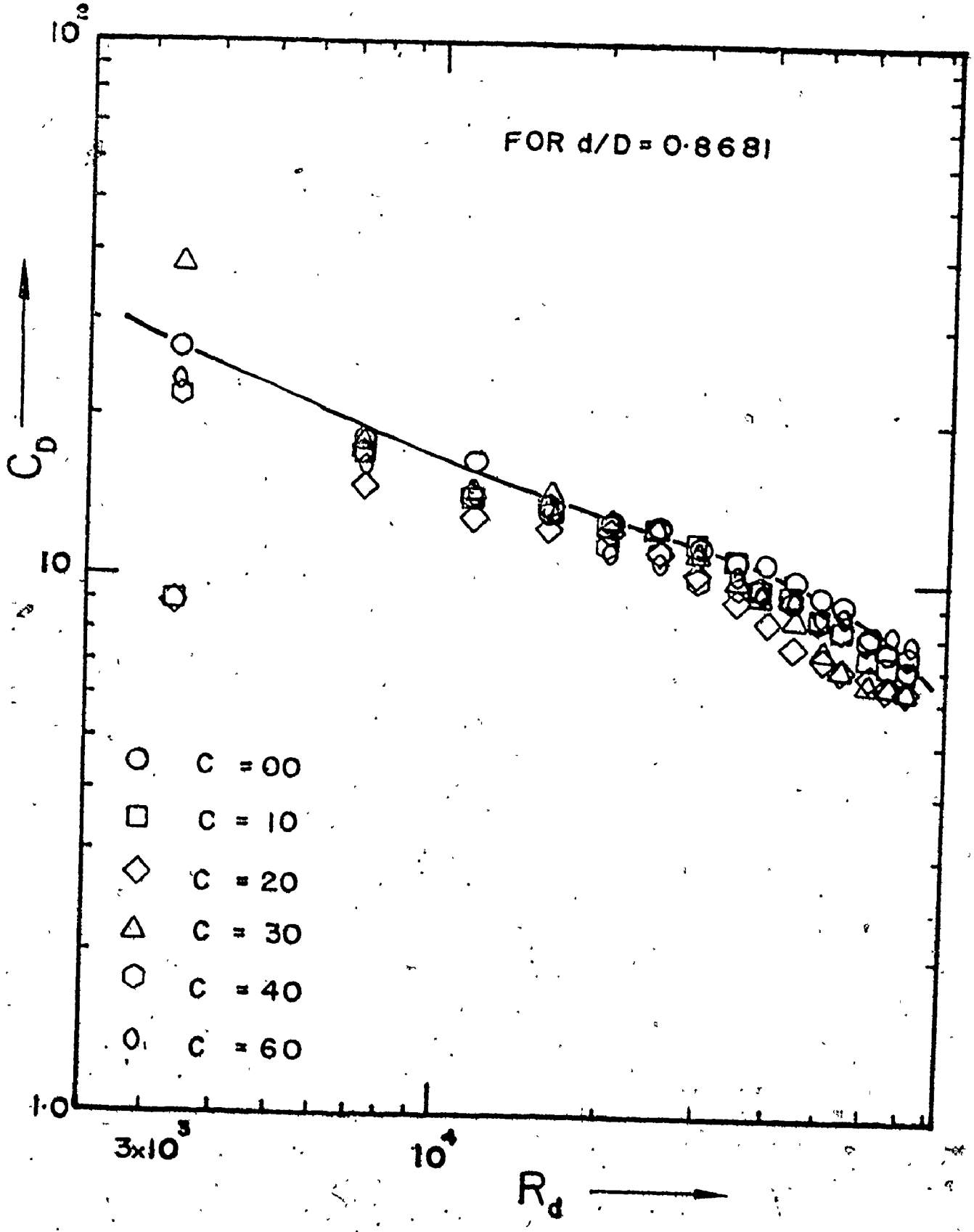

Figure (4-12) Drag coefficient versus Reynolds number for d/D = (

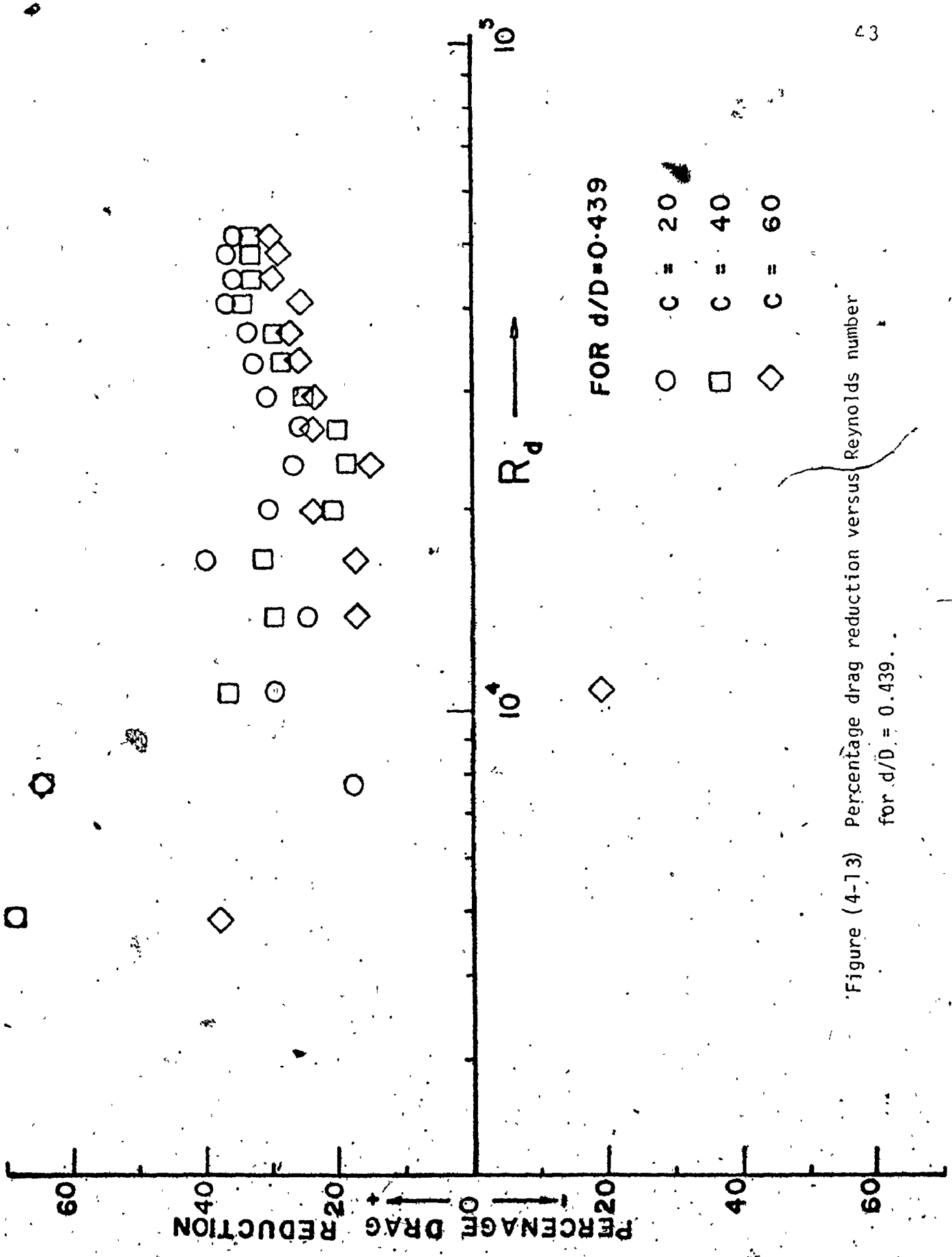

Figure (4-13) Percentage drag reduction versus Reynolds number for d/D = 0.439.

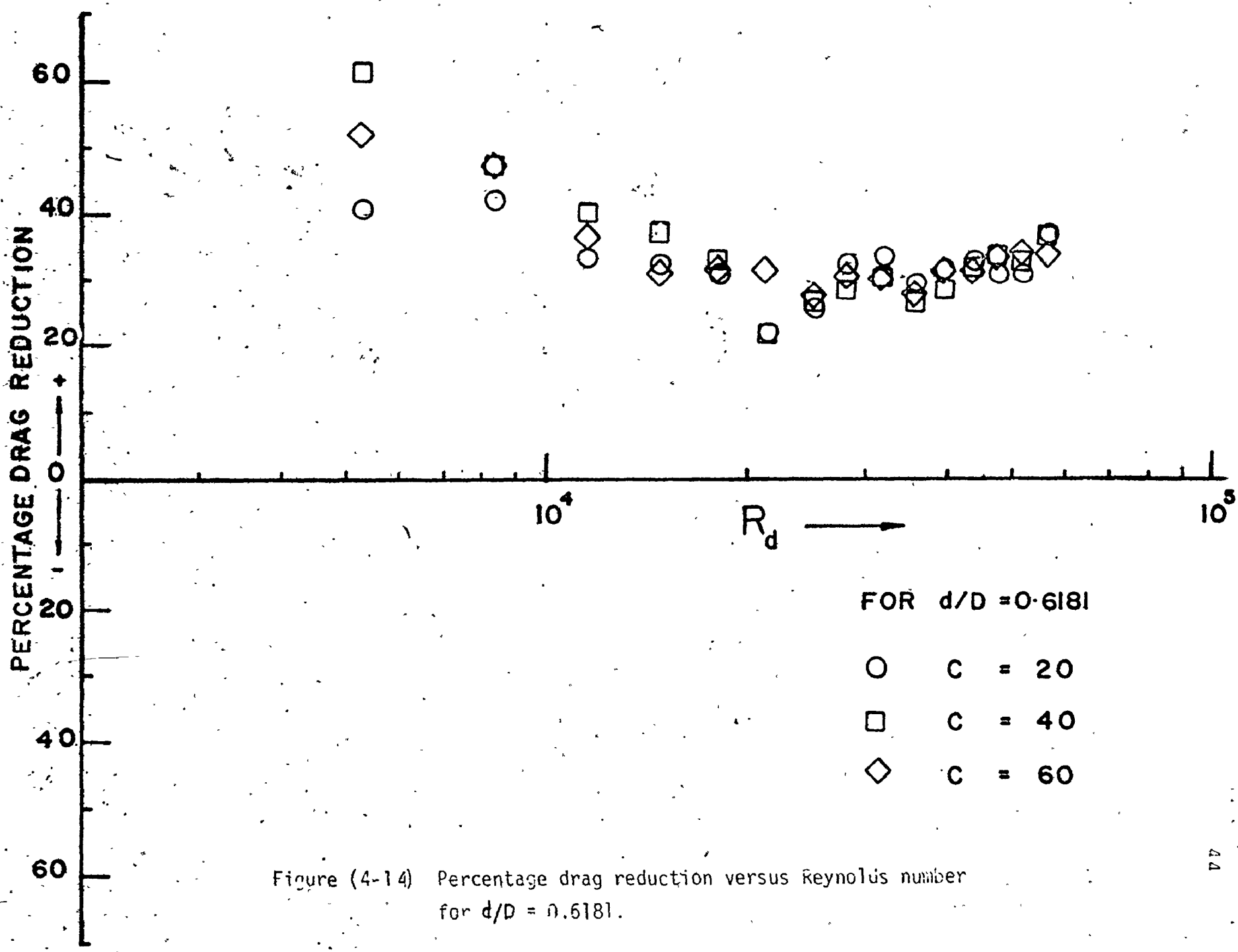

Figure (4-14) Percentage drag reduction versus Reynolds number for d/D = 0.6181.

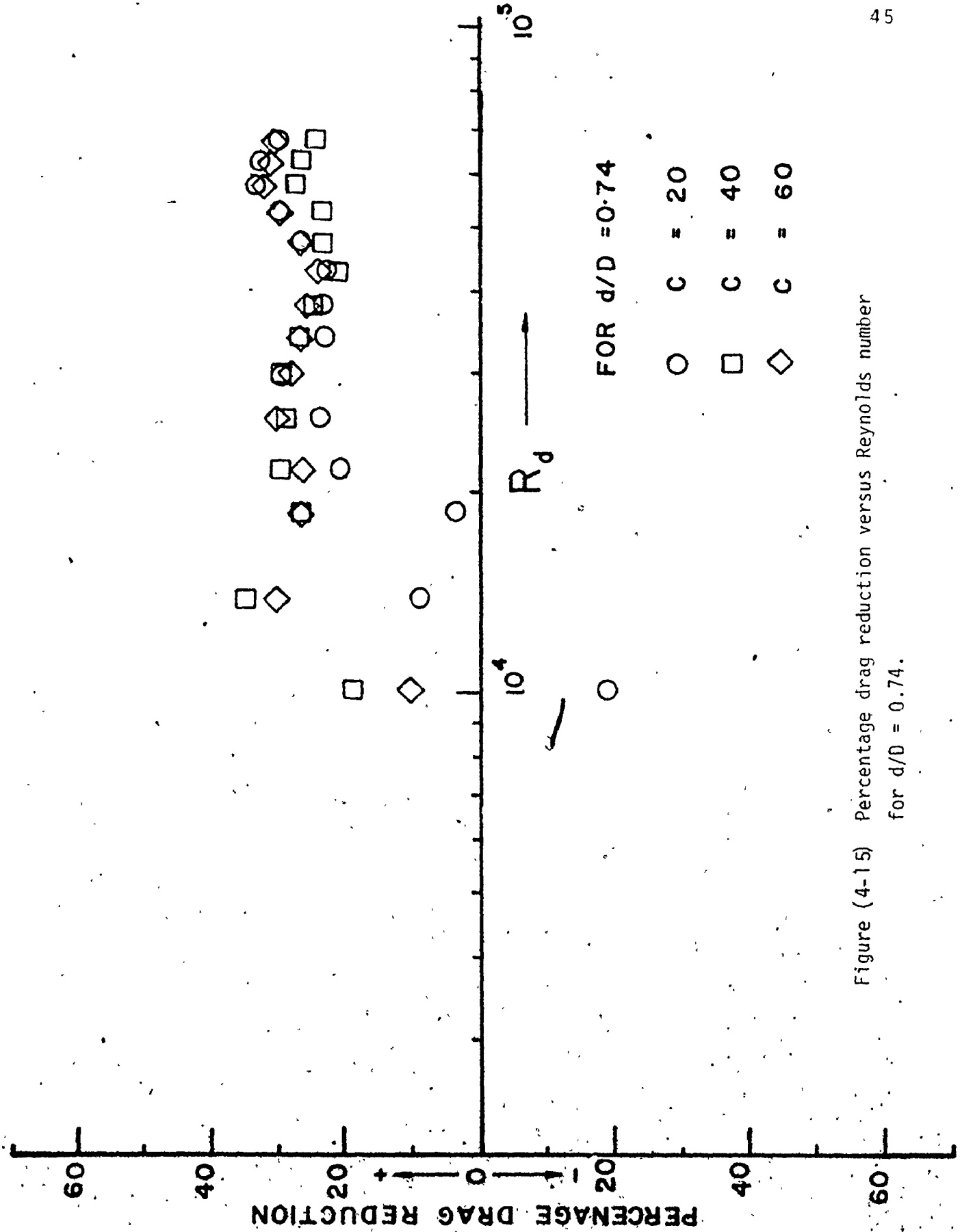

Figure (4-15) Percentage drag reduction versus Reynolds number for d/D = 0.74.

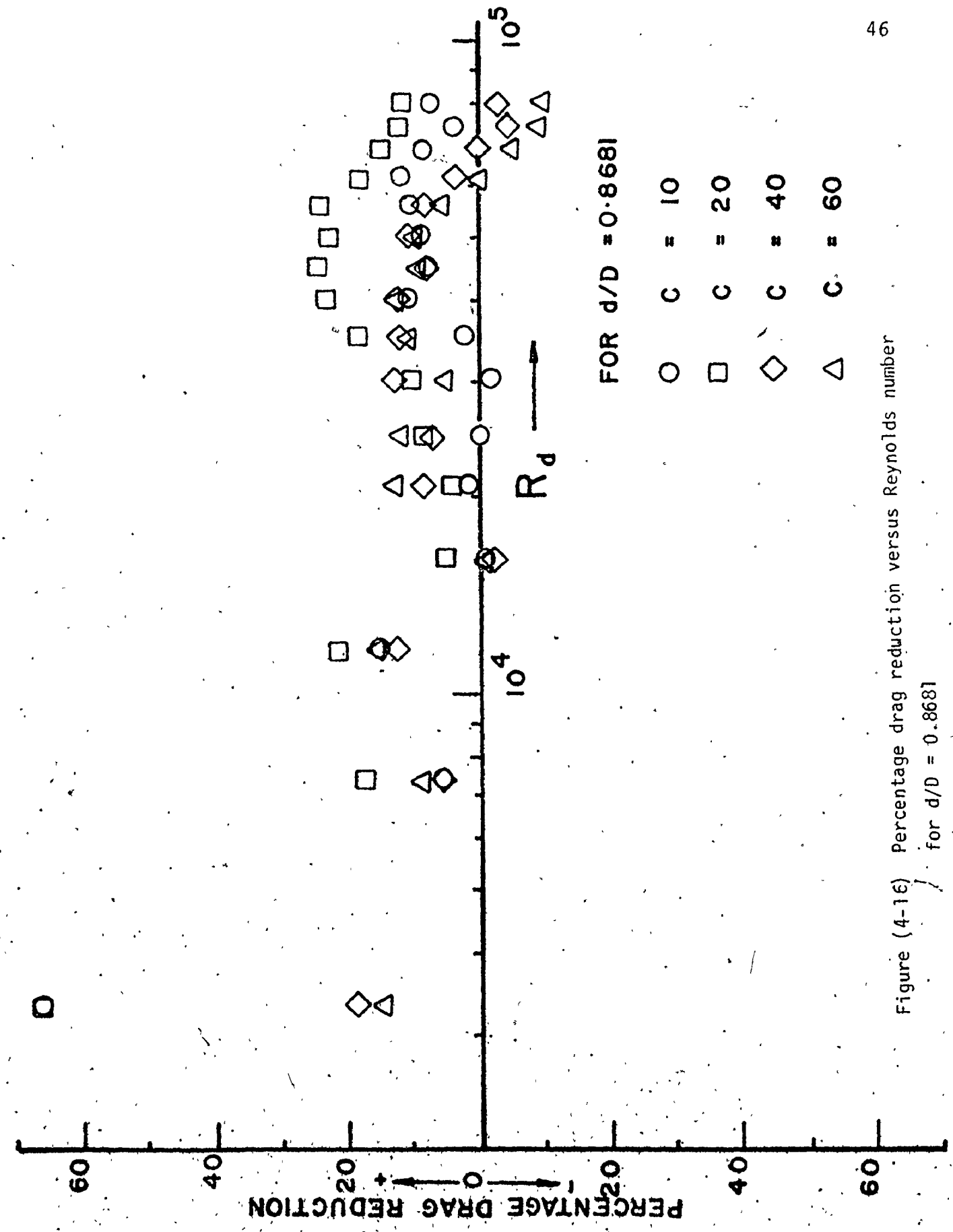

Figure (4-16) Percentage drag reduction versus Reynolds number for d/D = 0.8681

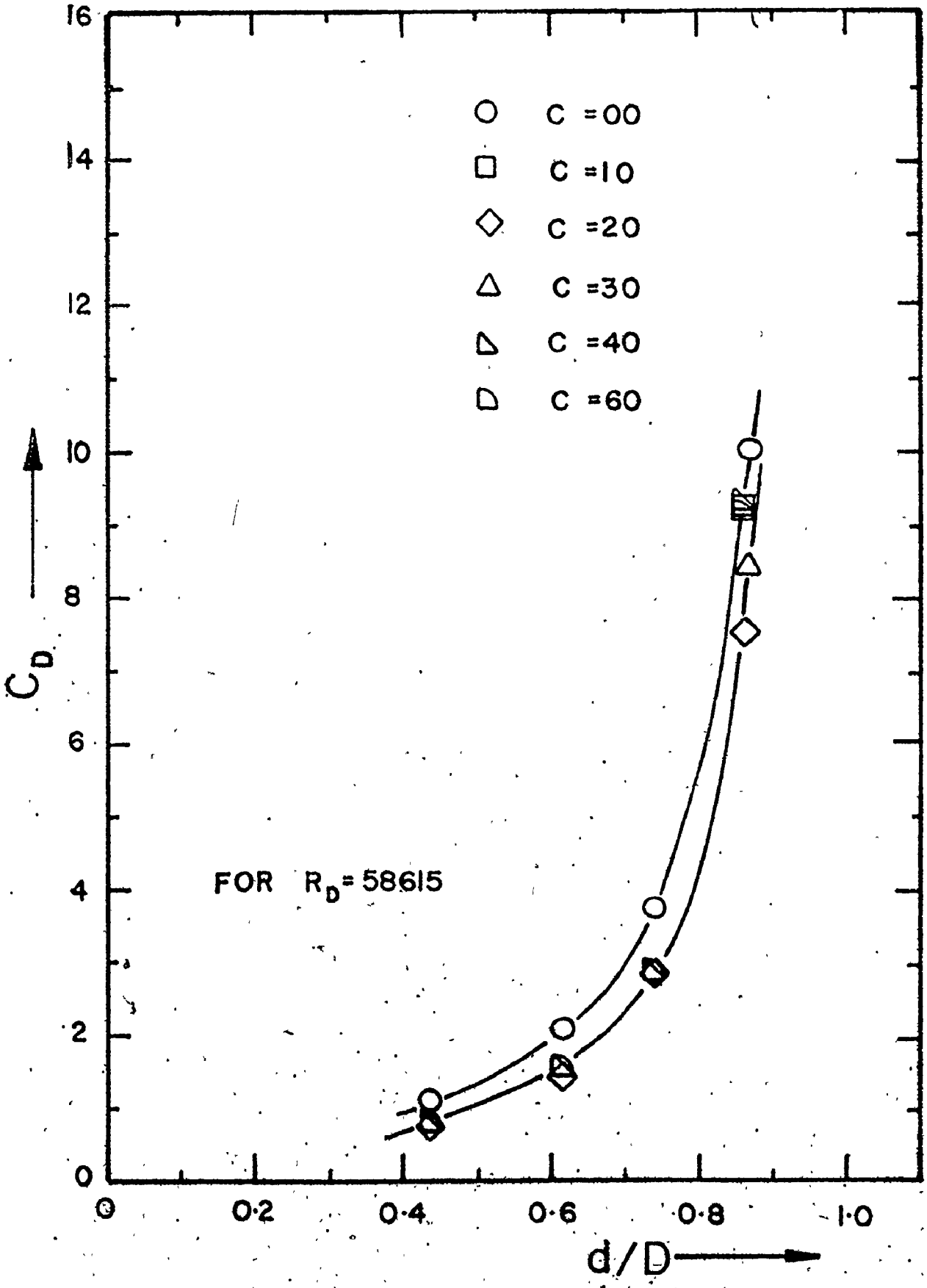

Figure (4-17) Drag coefficient versus diameter ratio for R_D = 58615.

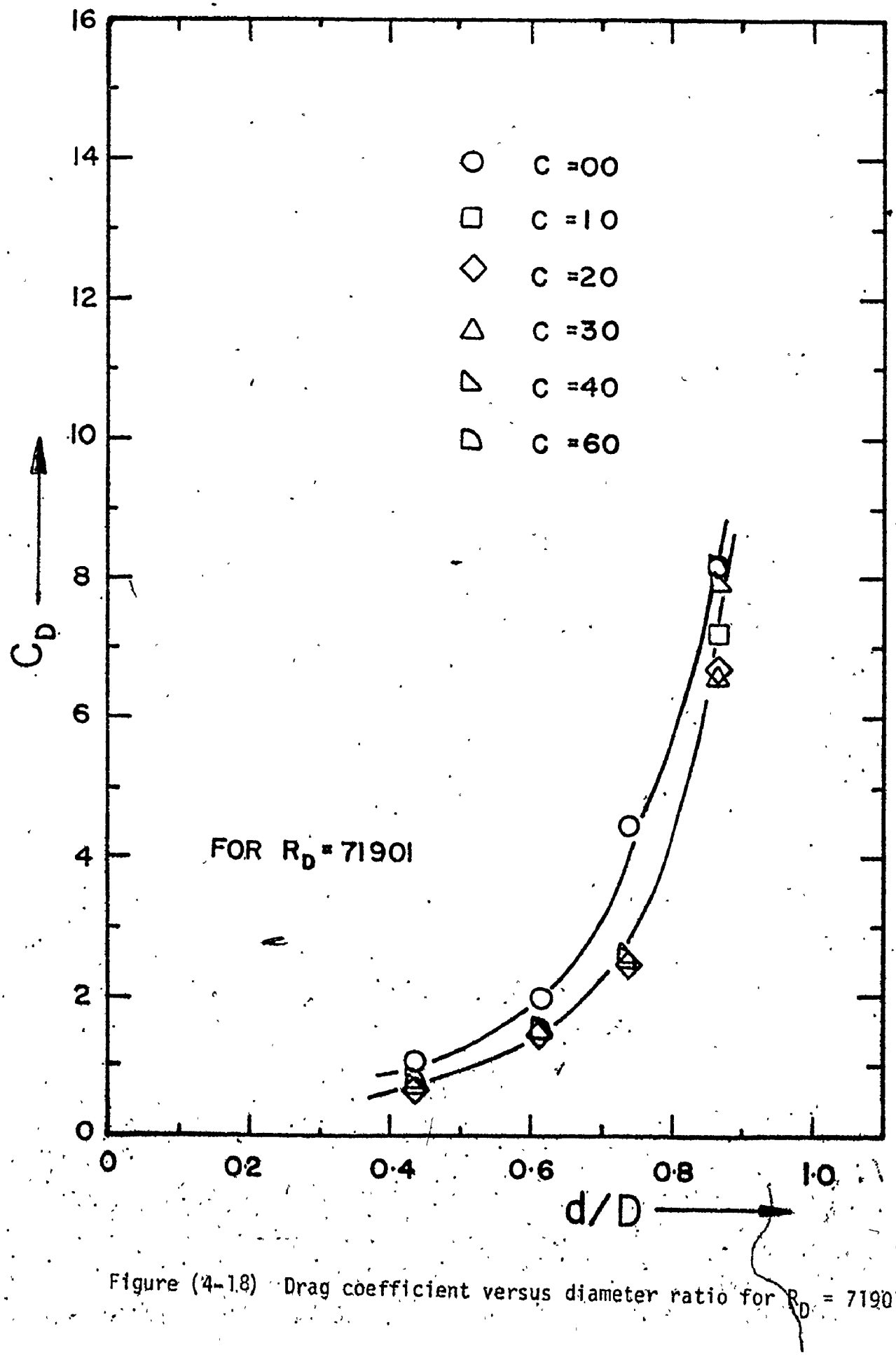

Figure (4-1.8) Drag coefficient versus diameter ratio for R_D = 71901.

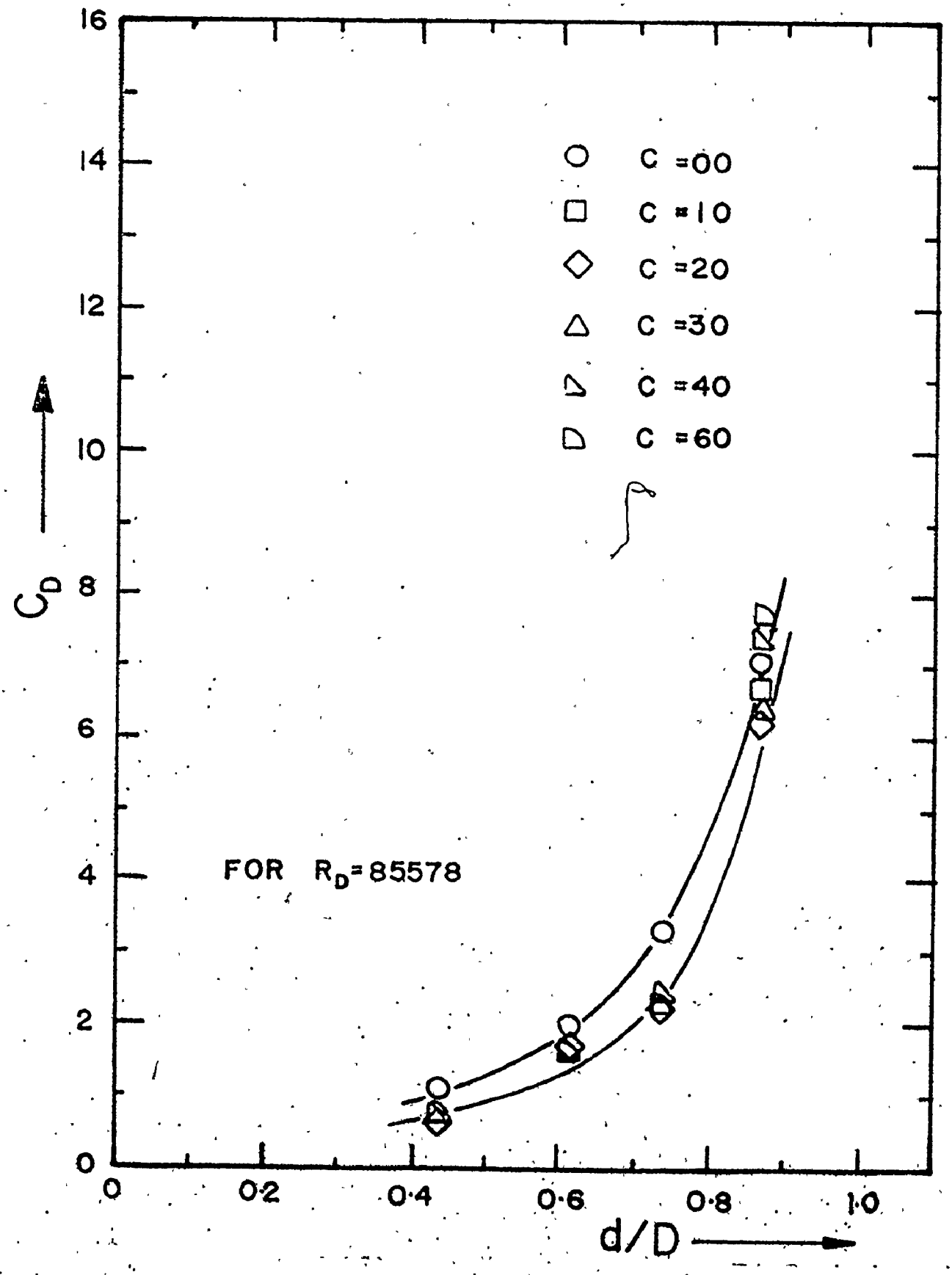

Figure (4-19) Drag coefficient versus diameter ratio for R_D = 85578.

obvious maximized drag reduction where the concentration C was about 24 wppm. This is more apparent from Figure (4-12), and graphically illustrated in Figures (4-13) to (4-16), which show that drag reductions of up to 60% are observable which is certainly a high order of magnitude than that for non-tethered spheres. This may be due to the fact that for non-tethered spheres the motion of the body is substantially different to that of tethered speheres and consequently the polymer has an effect on the separation phenomena.

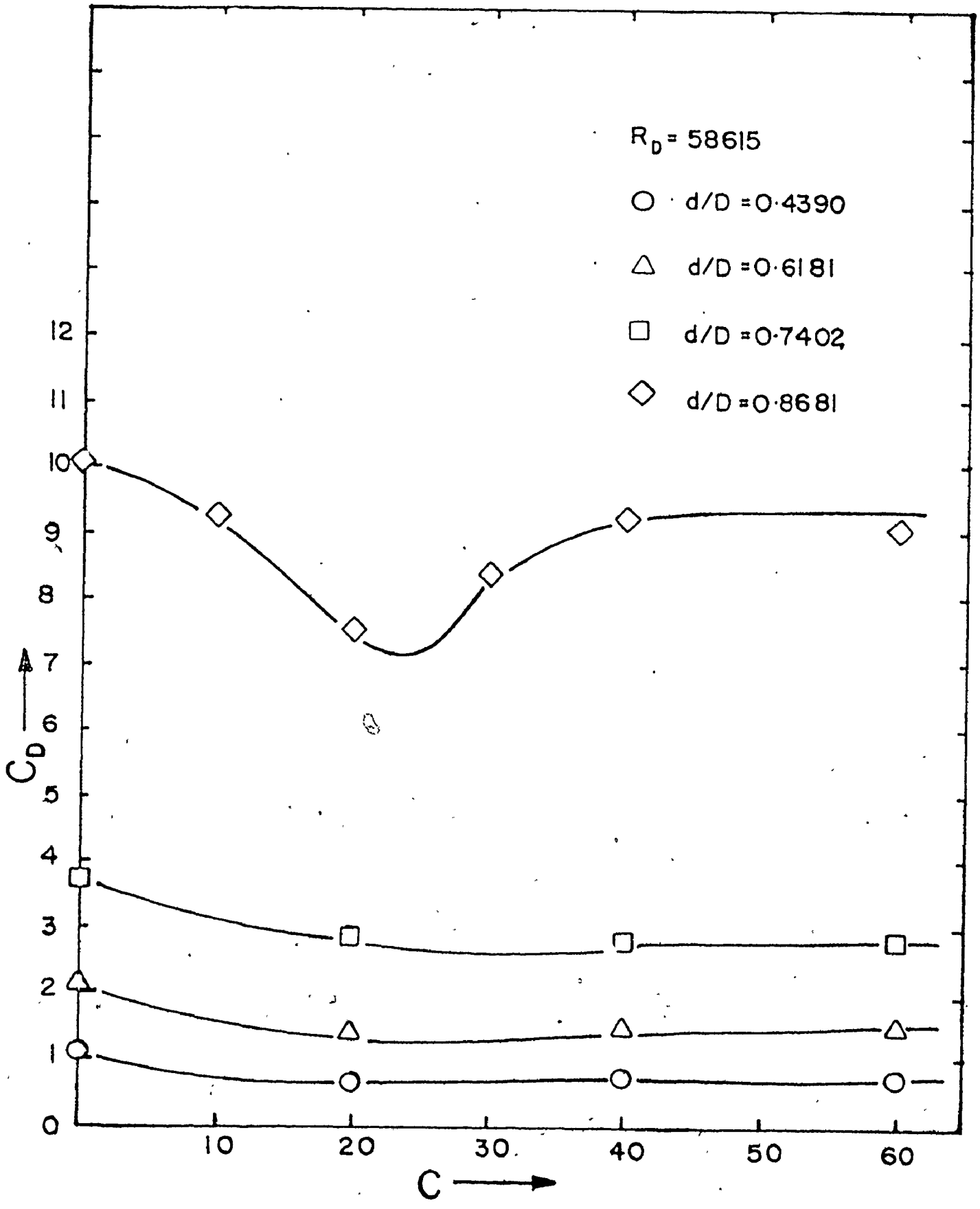

Figure (4-20) Drag coefficient versus concentration level for R_D = 58615.

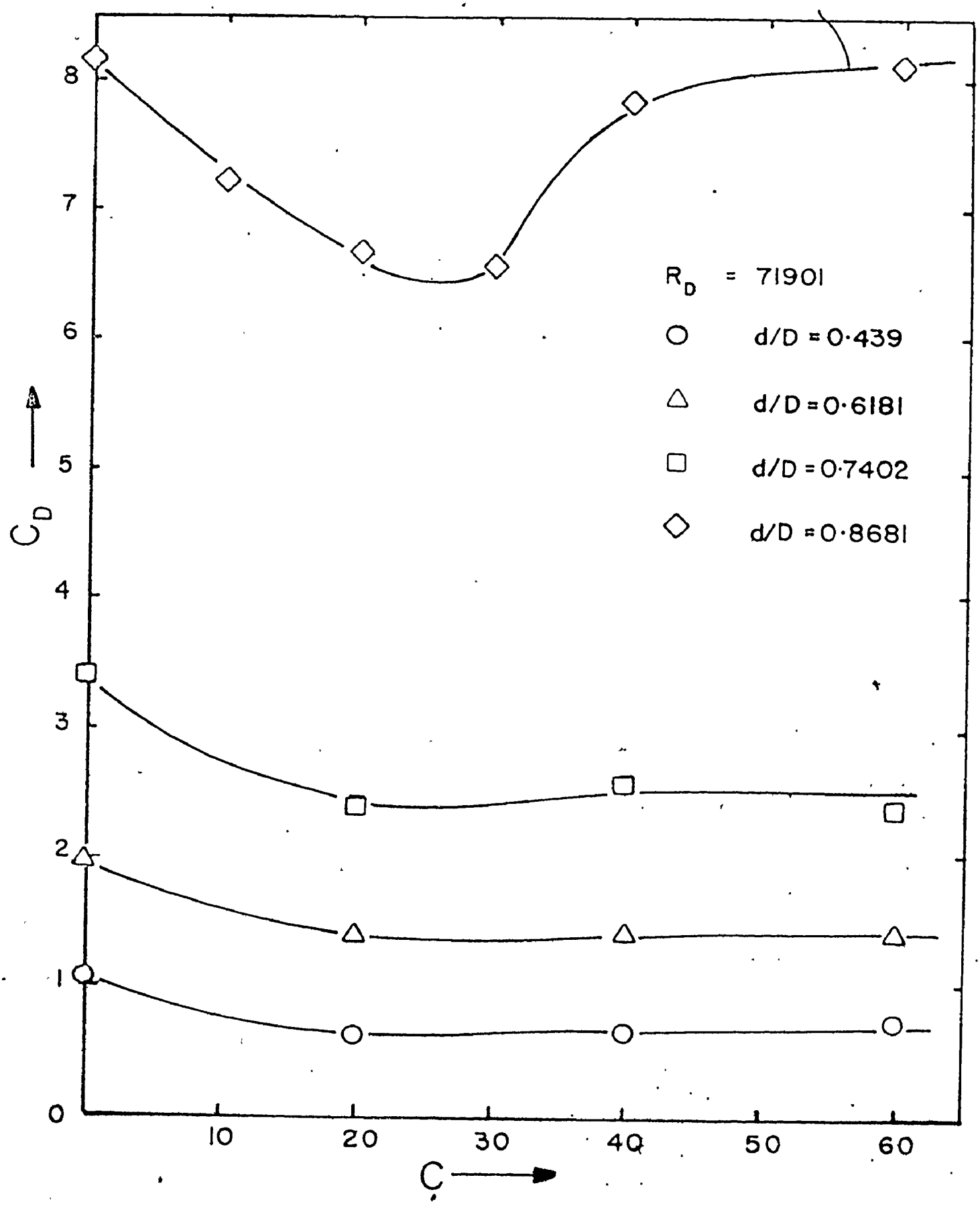

Figure (4-21) Drag coefficient versus concentration level for R_D = 71901.

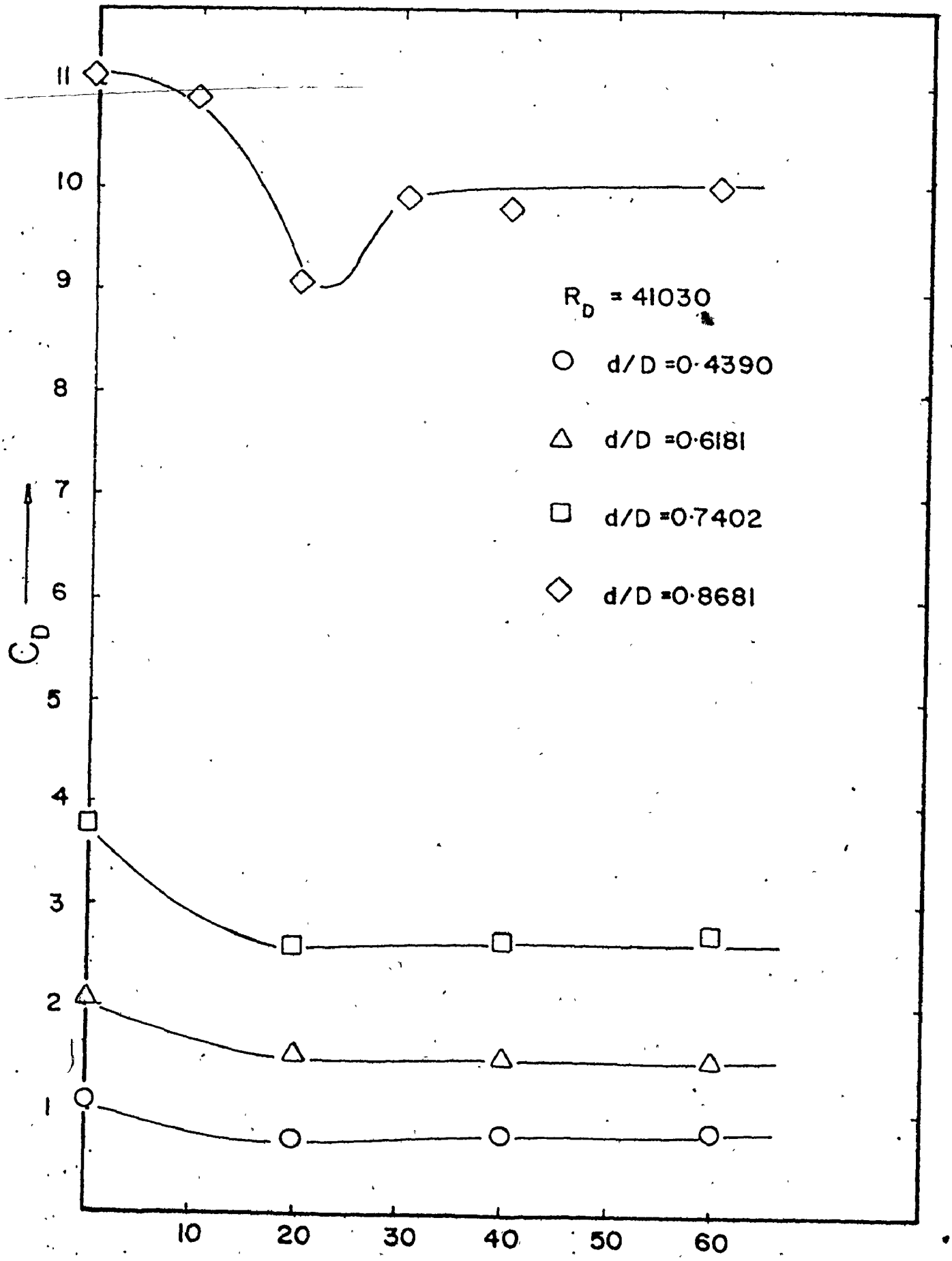

Figure (4-22) Drag coefficient for R_D

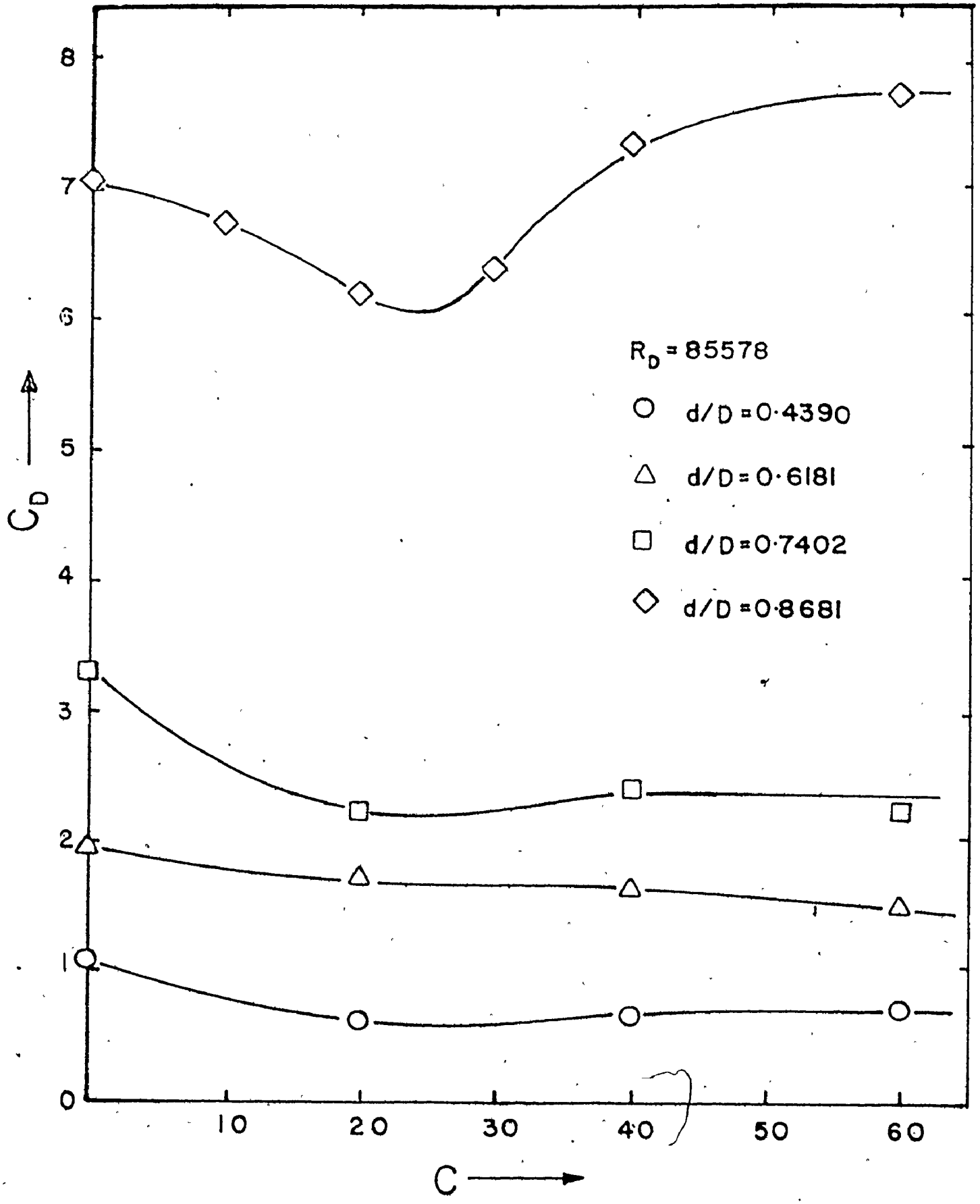

Figure (4-23) Drag coefficient versus concentration level for R_D = 85578.

CHAPTER 5

CONCLUSIONS

On the basis of the foregoing study, the following conclusions can be drawn:

i) For the study of the flow, using water:

1) As $d/D \to 1.0$, C_D was found to be a function of both Reynolds number and diameter ratio (for the range of R_d investigated), while it was apparent that it is a function of d/D alone for $0.4 < d/D < 0.74$. It can be represented by the semi-empirical equation:

$$C_D = \left(\frac{(d/D)^{0.1828}}{1 - (d/D)^{2.1475}}\right)^{1.9357}$$

which is similar in form to that equation of McNown and Newlin.

2) The pressure function, PRF, was found to be proportional to the square of Reynolds number and to the previous diameter function of C_D to the power 1.19, as follows:

$$PRF = 2.6 \times 10^{-10} R_D^2 \left(\frac{(d/D)^{0.1828}}{1 - (d/D)^{2.1475}}\right)^{2.3}$$

or can be written as:

$$PRF = 2.6 \times 10^{-10} R_D^2 C_D^{1.19}$$

which is relating the pressure drop to the drag coefficient.

ii) For the study of the flow, using dilute polymer solutions:

1) In all cases C_D was reduced by the addition of polymer.

2) The effect of concentration is dependent upon the diameter ratio, which has little effect below d/D of 0.74.

3) For a d/D of 0.87, there was an obvious maximized drag reduction at a concentration of about 24 wppm.

4) Drag reduction of up to 60% are observed, which is certainly a higher order of magnitude than that which has been previously observed for non-tethered spheres.

REFERENCES

1. Stokes, G. G., "On the effect of the internal friction of fluids on the motion of pendulums", Cambridge Phil. Soc. 9, No. 8 (1851).

2. McNown, J. S. and Newlin, J. T., "Drag of spheres within cylinderical boundaries", Proc. 1st., U.S. Nath. Congr. Appl. Mech. Chicago, 1951, pp. 801 - 806.

3. Gadd, G. E., "Reduction of turbulent friction in liquids by dissolved additives", Nature, Vol. 212, 1966, p. 874.

4. Gadd, G. E., "Turbulence damping and drag reduction produced by certain additives in water" of Hydronautics, Vol. 2, 1968, p. 108.

5. Hoyt, J. W. "The effect of additives on fluid friction", Transactions of the ASME, p. 258, June 1972.

6. Palyvos, J. A., "Drag reduction and associated phenomena in internal and external liquid flows", National Tech. Univ., School of Mech. Eng., Athens 147, Greece.

7. Crawford, H. R. and Pruitt, G. T., "Symposium Non-Newtonian Fluid Mechanics", 56th Annual Meeting Inst. Chem. Eng., Houston, Texas, Dec. 1963.

8. Ruszczycky, M. A., "Sphere Drop Tests in High-polymer Solutions", Nature, V. 206, pp. 614 - 615, May, 1965.

9. White, A. "Turbulent drag reduction with polymer additives", J. Mech. Eng. Science, Vol. 8, No. 4, 1966.

10. White, A. "Effect of polymer additives on boundary layer separation and drag of submerged bodies", Nature, V. 211, p. 1390.

11. White, A. "Drag Coefficients for Sphere in high Reynolds Number Flow of Dilute Solutions high Polymers", Nature, V. 212, Oct. 1968.

12. Lang, T. G. and Patrick, H. V. L., "Drag of blunt bodies in polymer solutions", Naval Ordnance Test Station Tech. Report 4379, July, 1967.

13. Hayes, M. F., "Drag Coefficients of Spheres Falling in Dilute Aqueous Solutions of Long-chain Macromolecules", M.S. thesis, Naval Post-graduate School, Monterey, 1966.

14. Chenard, J. H., "Drag of Spheres in Dilute Aqueous Solutions of Poly ethylene oxide within the Region of Critical Reynolds", M.S. thesis, Naval Postgraduate Sch., Monterey, 1967.

15. White, A., "Drag of Spheres in Dilute High Polymer Solutions", Nature, Vol. 216, Dec. 9, 1967.

16. Stow, F. S. and Elliot, J. H., "Drag on tethered ball in solutions of drag-reducing polymers", Polymer Letters, Vol. 8, pp. 611 - 615, 1970.

17. Barenblatt, G. I., Bulina, I. G. and Myasnikov, V. P., "Drag Reducing effect of solutions of some high-Molecular Compounds in Turbulent flow past bodies", Zhurnal Prikladnoi Mekh. i Tekhn Fiziki, No. 3, pp. 95 - 96, 1965.

18. Sarpkaya, T. and Rainey, P. G., "Flow of dilute polymer Solutions about Circular Cylinders", Naval Postgraduate School - 59SLIOZIA; Feb. 26, 1971.

19. Anzenavs, R. A., "An experimental study of the hydro-dynamic suspension of spheres and sphere trains in a vertical pipe using water and polymer solutions", M.S. thesis, McMaster University, 1972.

20. Latto, B., Round, G. F. and Anzenavs, R. "Drag Coefficients and pressure drops for hydrodynamically suspended spheres in vertical tube with and without polymer", Can. J. Chem. Eng. V. 51, Oct. 1973.

21. Ali, S., "The hydrodynamic suspension of sphere and cylinder trains in a vertical tube using water and polymer solutions", M.S. thesis, McMaster University, 1974.

22. Latto, B., Round, G. F., and Ali, S., "The hydrodynamic suspension of sohere and cylinder trains in a vertical tube with and without polymer addition", Fourth International Conference on Hydraulic Transport of Solids in pipe, May, 1976.

23. Streeter, V.; Wylie, E., "Fluid Mechanics", textbook, McGraw Hill, Sixth Edition.

24. Latto, B., and Lai, A., "The Separation Angle for Spheres in a Pipeline", Proc. of the 4th Biennial Symposium on Turbulence in Liquids, Paper B1, Organized by the University of Missouri, Rolla, September, 1975.

APPENDIX (A)

METHOD OF ANALYSIS OF RESULTS

The analysis of results was carried out, using a computer program, as follows:

Drag force F_D = K x strain gauge reading (A.1)

where K = Force transducer constant N/mV

defining; $F_D = C_D (\pi d^2/4)(\rho v^2/2)$ (A.2)

we get $C_D = F_D/((\pi d^2/4)(\rho v^2/2))$ (A.3)

also $R_d = V_{av} d\rho/\mu$ (A.4)

where V_{av} is obtained from the calibration curves. The pressure drop due to flow and without spheres is;

$$\Delta P_f = f \frac{L}{D} \rho \frac{V_{av}^2}{2} \quad (A.5)$$

where f is obtained from Colebrook equation for a smooth pipe which is:

$$\frac{1}{\sqrt{f}} = -0.86 \ln \frac{2.51}{R_D \sqrt{f}} \quad \text{(Ref. 23, pp.293)} \quad (A.6)$$

∴ total pressure drop without the sphere is

$$\Delta P_L = f \frac{L}{D} \rho \frac{V_{av}^2}{2} + L \gamma_\omega \quad (A.7)$$

The pressure drop with the sphere based on the manometer readings is:

$$\Delta P_s = \Delta h_m (\gamma_m - \gamma_\omega) + L\gamma_\omega \quad (A.8)$$

Also, the pressure function is defined by;

$$PRF = \frac{\Delta P_s - \Delta P_L}{D\gamma_\omega} \quad (A.9)$$

Sample of Calculation Procedure:

For sphere of d/D = 0.6181 in pure water at the following conditions:

Rotameter reading = 11 cm

The strain gauge reading = 16.2 mv

The manometer reading = 12.2 cm of CCl_4

The corresponding velocity = 0.90 m/s

The water kinematic viscosity = 1.3×10^{-6} m^2/s (at $10^{o}C$)

The water density = 1000 kg/m^3

Force transducer constant = 0.04155 N/mv

we have

$$F_D = 16.2 \times 0.04155 = 0.673142 \text{ N}$$

and $$R_d = \frac{V_{av} d}{\upsilon} = \frac{0.9 \times .0508 \times .6181}{1.3 \times 10^{-6}} = 21738$$

and $$R_D = \frac{V_{av} D}{\upsilon} = 35169$$

Hence, from equation (A.3)

$$C_D = F_D/(\pi/4\ d^2)(1/2\rho v^2)$$

$$= \frac{0.673142 \times 4 \times 2}{\pi(.0508 \times .6181)^2 \times 1000(0.9)^2} = 2.14$$

To obtain the pressure function, f must be calculated from equation (A.6).

$$\frac{1}{\sqrt{f}} = -.86 \ln \frac{2.51}{R_D\sqrt{f}}$$

By iteration we get, f = 0.0231

thus, $$\Delta P_L = \frac{0.0231 \times 1.524 \times 1000 \times (.9)^2}{.0508 \times 2} + 1.524 \times 9.8 \times 1000$$

$= 1.52158 \times 10^4 \quad N/m^2$

and, $\Delta P_s = 9.8 \times 1000 \ (0.122 \times (1.583-1) + 1.524 \times 1)$

$= 1.5632 \times 10^4 \quad N/m^2$

$PRF = 0.837$

Sample of Calculations With Polymer Solutions:

Considering the condition of polymer solution of concentration 20 wppm and flowing at the same rate as in the previous case of pure water, we have;

The strain gauge reading = 17 mv

Strain gauge constant = 0.03 N/mv

then

$$F_D = 17 \times 0.03 = 0.52 \text{ N}$$

and

$$C_D = \frac{0.52 \times 4 \times 2}{\pi(.0508 \times .6181)^2 \times 1000(.9)^2}$$

$$= 1.6727$$

hence, percentage drag reduction $= \frac{2.1464 - 1.6727}{2.1464} \times 100$

$= 22.03\%$

APPENDIX (B)

FORCE TRANSDUCER DESIGN

B.1. ROD DESIGN

The rod design was based on the estimated maximum drag force on the spheres. The force was calculated using the approximate equation of McNown and Newlin for inviscid flow. Two different rod sizes were used to cover d/D range of 0.87, 0.74, 0.62 and .44. This was done because a single rod for all sphere sizes would have had a too large diameter, hence it would not be sensitive in measuring tne drag for the small sphere sizes. Calculations were done for the design condition of maximum flow velocity which was 2.2 m/s.

1. Design of the large rod:

Force Calculation:

Sphere to tube diameter ratio d/D = 0.868.

Drag coefficient calculated using the McNown and Newlin equation is:

$$C_D = \left[\frac{d/D}{1-(d/D)^2}\right]^2 = 12.494$$

$$\text{Drag force } F_D = \frac{C_D A \rho V_{av}^2}{2}$$

where A is the sphere cross section area $= \frac{\pi}{4}(.0508 \times .868)^2$

$= 0.00153\ m^2$

$$F_D = \frac{12.494 \times 0.00153 \times 1000 \times 2:2 \times 2.2}{2} = 46.2 \text{ N}$$

For convenience in design the drag force is taken as 50N.

The rod material is stainless steel 304.

$\therefore \sigma_{elastic} = 400 \times 10^6 \text{ N/m}^2$

and $E = 21 \times 10^{10} \text{ N/m}^2$

assuming a factor of safety F.S. = 1.5

then $\sigma_{working} = \frac{400 \times 10^6}{1.5} = 260 \times 10^6 \text{ N/m}^2$

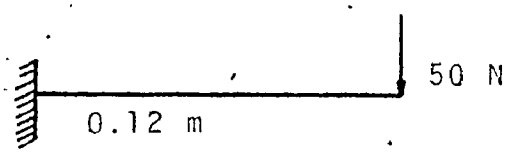

$M = 50 \times 0.12$

$= 6 \text{ N.m}$

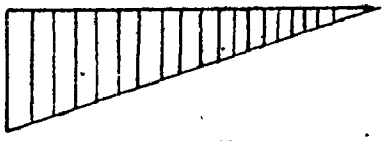

B.M.D.

The maximum bending stress $S = \frac{M_b Y}{I}$

then the circular cross section;

$$S = \frac{32 M_b}{\pi d^3}$$

$$260 \times 10^6 = \frac{32 \times 6}{\pi d^3}$$

$$d^3 = \frac{32 \times 6}{\pi \times 260 \times 10^6} = 0.23506 \times 10^{-6}$$

$\therefore d = 0.00617 \text{ m}$

hence the maximum deflection (δ) $= \frac{FL^3}{3EI}$

$$= \frac{50 \times (.12)^3 \times 64}{3 \times 21 \times 10^{10} \times \pi\ (.00617)^4}$$

$$= .00193 \text{ m}$$

2. Design of the small rod: (similar to that for the large rod):

Force Calculations:

Sphere to tube diameter ratio d/D = 0.74

Drag coefficient C_D = 2.7

Area of Sphere cross section A $= \frac{\pi}{4}(.0508 \times .74)^2$

$= 0.00111 \text{ m}^2$

$$\therefore F_D = \frac{2.7 \times 0.00111 \times 1000 \times 2.2 \times 2.2}{2} = 7.25 \text{ N}$$

Since the McNown and Newlin equation is not accurate enough for small diameter ratios, a maximum design load of 20 N was used. A rectangular cross section was selected for the ease of applying the strain gauges. It was designed to give a maximum deflection of 0.0025 m to give a higher sensitivity for the smaller spheres.

Deflection $\delta = \frac{FL^3}{3EI}$

where $I = 1/12\ bh^3$

taking $b = 0.005$ m.

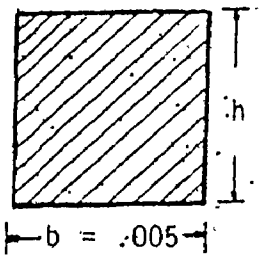

$$\therefore 0.0025 = \frac{20 \times (.12)^3 \times 12}{3 \times 21 \times 10^{10} \times .005 \times h^3}$$

i.e. $h = 0.00375$ m

Check for strength:

$$S = \frac{M_b Y}{I} = \frac{M_b X h/2}{bh^3/12} = \frac{6M_b}{bh^2} = \frac{6 \times 20 \times 0.12}{.005 \times (.00375)^2}$$

$$= 204 \times 10^6 \text{ N/m}^2 < \sigma_\omega$$

The working drawing and dimensions of both rods are shown in Figure (B-1) and (B-2).

B.2. THE STRAIN GAUGES*

Two strain gauges (EA-09-125 BT-120) were glued to the top and bottom surfaces of each rod using contact cement (VISHAY M-BOND 200) and were water and moisture proofed by coating them with nitrile rubber (VISHAY GW2). The gauges were wired up in a half bridge arrangement in order to double the sensitivity.

The deflection of the rod was sensed using a strain gauge indicator (VISHAY 1011).

The signal of the indicator was introduced to a digital multimeter (HONEYWELL, 630S) from which the final reading in villivolts was recorded.

* Fixing the strain gauges was carried out with the grateful assistance of Dr. D.S. Weaver in the Mechanical Engineering Department, McMaster University.

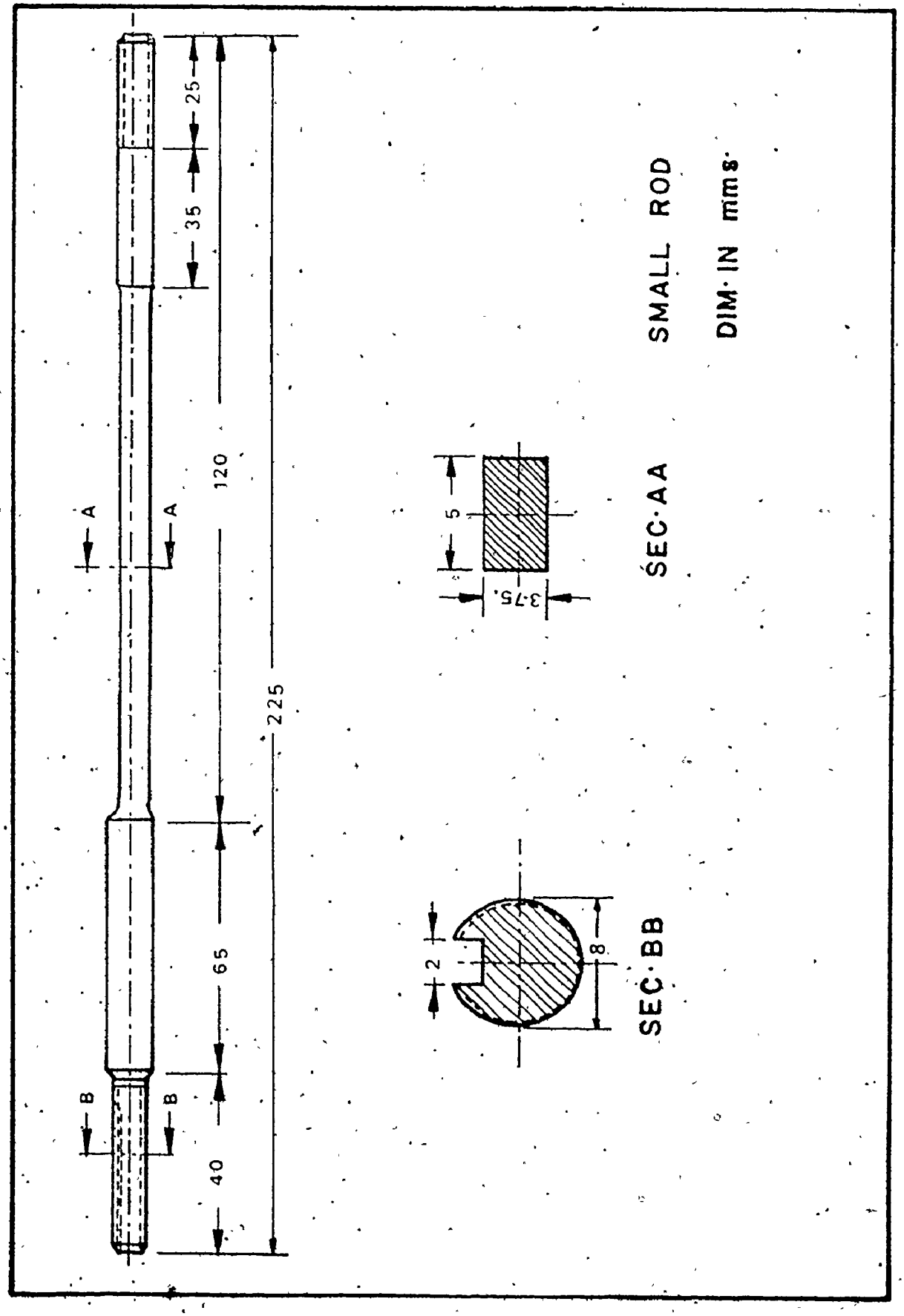

Figure (B-1) Small Rod.

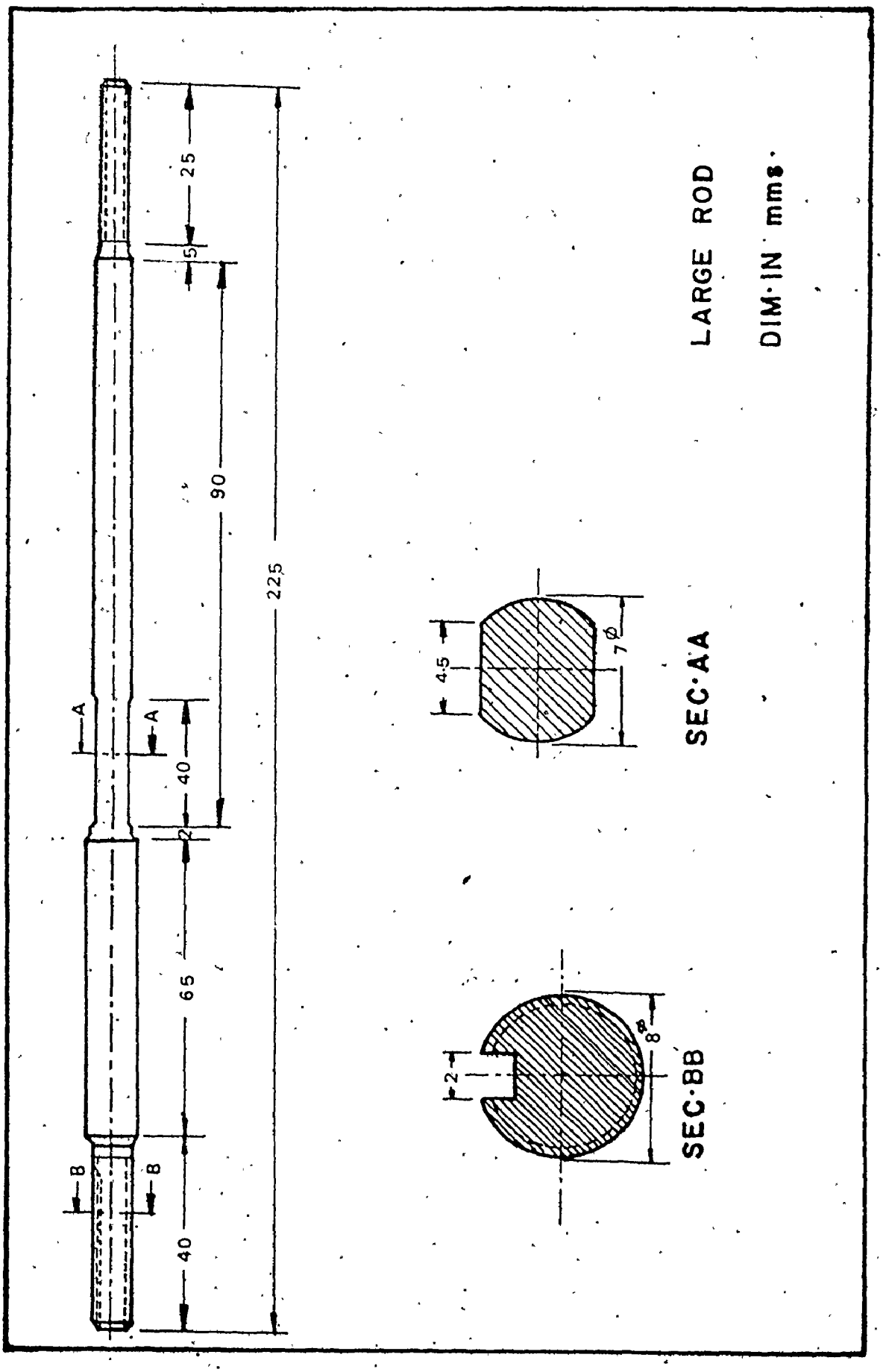

Figure (B-2) Large Rod.

APPENDIX (C)

ERROR ANALYSIS

There was no convenient general method to measure the error in the individual measurements. However, informed estimates based on the type of instruments used and the experience gained in using them, can be attempted.

Estimates of the error of the primary measurements made in the present research are listed in table (C-1). For some quantities, a range of error has been given depending on the range in which these quantities were measured. For example, the relative error in measuring small flow rates is larger than in the case of large flow rates.

1. Error in V_{av}

The average velocity in the test section was computed using the formula:

$$V_{av} = \frac{Q}{\pi D^2/4}$$

$$= k' \frac{Q}{D^2}$$

where Q = flow rate

and k' = constant

$$\therefore \quad dV_{av} = \frac{\partial V_{av}}{\partial Q} dQ + \frac{\partial V_{av}}{\partial D} dD$$

$$= \frac{k'}{D^2} dQ - \frac{2k'Q}{D^3} dD$$

Table (C-1)

Error estimates in the measured primary quantities

Description	Symbol	% Error
Tube diameter	D	± 1.0
Rotameter reading	Q	± 6.0 ⟶ ± 1.0
Distance between pressure taps	L_t	± 0.5
Manometer reading	h_m	± 7.0 ⟶ ± 1.0
Specific weight of manometer fluid	γ_m	± 0.1
Strain gauge force transducer	F_D	± 5.0 ⟶ 2.0
Kinematic viscosity (due to increase of 2°C)	ν	-7

The variation in V_{av}, which is dV_{av}, may be considered as the V_{av} error produced by error in Q, which is dQ, and D, which is dD.

Normally, the major interest is the relative error in V_{av}, which is given by:

$$\frac{dV_{av}}{V_{av}} = \frac{dQ}{Q} + \left(-2\frac{dD}{D}\right)$$

The above equation will give a rather unrealistically high estimation of error. In that, it assumes that all the errors are maximised because the signs of the individual components are taken into account. A more realistic method is to obtain the R. M. S. value of the errors.

$$\therefore \left(\frac{dV_{av}}{V_{av}}\right)^2 = \left(\frac{dQ}{Q}\right)^2 + 4\left(\frac{dD}{D}\right)^2 + 2\frac{dQ}{Q}\left(-2\frac{dD}{D}\right)$$

If the relative error components $\frac{dQ}{Q}$ and $\frac{dD}{D}$ are independent and symmetrical in regard to positive and negative values, then the cross-product terms will tend, on the average, to disappear, hence:

$$\frac{dV_{av}}{V_{av}} = \sqrt{\left(\frac{dQ}{Q}\right)^2 + 4\left(\frac{dD}{D}\right)^2}$$

$$\therefore \frac{dV_{av}}{V_{av}} = \sqrt{36 + 4 \times 1} = \pm 6.32\% \text{ at low flow rates}$$

and $$\frac{dV_{av}}{V_{av}} = \sqrt{1 + 4} = \pm 2.2\% \text{ at high flow rates.}$$

The amounts of polymer added to the water to form the required concentrations were very small, such that any slight error in the mixing process would hardly affect the error in the total discharge; hence the error in the average velocity.

2. Error in evaluating Reynolds number:

$$R_D = \frac{V_{av} D}{\nu}$$

$$dR_D = \frac{\partial R_D}{\partial V_{av}} dV_{av} + \frac{\partial R_D}{\partial D} dD + \frac{\partial R_D}{\partial \nu} d\nu$$

$$= \frac{D}{\nu} dV_{av} + \frac{V_{av}}{\nu} dD + \left(-\frac{V_{av} D}{\nu^2}\right) d\nu$$

$$\frac{dR_D}{R_D} = \frac{dV_{av}}{V_{av}} + \frac{dD}{D} - \frac{d\nu}{\nu}$$

Squaring and taking the square root for the relative error in Reynolds number:

$$\frac{dR_D}{R_D} = \sqrt{\left(\frac{dV_{av}}{V_{av}}\right)^2 + \left(\frac{dD}{D}\right)^2 + \left(\frac{d\nu}{\nu}\right)^2 + \ldots \text{(negligible terms)}}$$

$$= \sqrt{(6.32)^2 + (1)^2 + (7)^2} = 9.5\% \text{ for low flow rates}$$

$$= \sqrt{5 + 1 + 49} = 7.42\% \text{ for high flow rates.}$$

3. Error in the drag coefficient:

The drag coefficient was calculated from the equation:

$$F_D = C_D A_S \frac{\rho V_{av}^2}{2g}$$

$$C_D = \frac{F_D}{(\pi D^2/4)(\rho V_{av}^2/2g)}$$

$$= k' \frac{F_D}{D^2 V_{av}^2}$$

where k' = constant

Differentiating

$$dC_D = \frac{k'}{D^2 V_{av}^2} dF_D + \left(\frac{-2}{V_{av}^3}\right) \frac{k' F_D}{D^2} dV_{av} + \left(\frac{-2}{D^3}\right) \frac{F_D}{V_{av}^2} dD$$

$$\frac{dC_D}{C_D} = \frac{dF_D}{F_D} - 2\frac{dV_{av}}{V_{av}} - 2\frac{dD}{D}$$

Squaring and taking the square root for the relative error in drag coefficient:

$$\frac{dC_D}{C_D} = \sqrt{\left(\frac{dF_D}{F_D}\right)^2 + 4\left(\frac{dV_{av}}{V_{av}}\right)^2 + 4\left(\frac{dD}{D}\right)^2 + \ldots}$$

for low flow rates (small drag force):

$$\frac{dC_D}{C_D} = \sqrt{25 + 4 \times 40 + 4 \times 1} = 13.75\%$$

for high flow rates (large drag force):

$$\frac{dC_D}{C_D} = \sqrt{4 + 20 + 4} = \sqrt{28} = 5.3\%$$

4. Error in pressure drop ΔP_m:

The pressure drop between the provided pressure taps was calculated from the formula:

$$\Delta P_m = h_m \gamma_\omega (1 - SG_m) + L_t \gamma_\omega$$

Generally, from the equation:

$$d(\Delta P_m) = \sqrt{\Sigma \left(\frac{(\delta P_m)}{\delta x_i} dx_i\right)^2}$$

which determines the error in ΔP_m in terms of the errors in x_i, it can be seen that if one step has a much smaller error than some of the others, it may be ignored. For the case under study, the errors in L_t and SG_m could be ignored as they are small when compared to that of h_m. Consequently, one can arrive directly at the following percentage error in pressure:

$$\frac{d(\Delta P_m)}{\Delta P_m} = \frac{dh_m}{h_m} = \pm 7\% \text{ in the small pressure drop regions.}$$

$$= \pm 1\% \text{ in the high pressure drop regions.}$$

APPENDIX (D)

CALIBRATIONS

1. Calibration of the water rotameter:

The calibration of the water rotameter was carried out by measuring the time, using a stop watch, required to collect a certain volume of water in the main tank of the rig.

Table (D-1) gives the results of the calibration, and Figures (D-1), and (D-2) show the volumetric discharge and velocity calibration curves.

2. Calibration of the strain gauge force transducer:

Calibration of the force reducing system was carried out using dead loads gradually applied to the spheres. For each load, the corresponding strain gauge reading was recorded. An average value of the force transducer constant in N/mV was obtained for each sphere diameter. Before each reading, the strain gauge recorder was set to zero under zero loading conditions, which would compensate for the weight and the buoyancy forces acting on the sphere. Tables (D-2), (D-3) give the calibrations for the small rod and the large rod force transducers respectively.

Table (D-1)

A_t = cross sectional area of tank = 60 X 120 = 7200 cm^2

ΔH = 20 cm

ΔV = 7200 X 20 = 0.144000 m^3

A pipe = 0.0020 27 m^2

Rotameter Reading cm	time to discharge ΔV in sec.	$Q = \frac{\Delta V}{t}$ m^3/sec	$V_{average} = \frac{Q}{Ap}$ (m/S)
3.5	0	0	0
5	656	0.00021951	0.1083
7	204	0.00070588	0.3482
8.6	122	0.00118033	0.5823
10	91	0.00158242	0.7807
11	79	0.00182278	0.8993
12	65.8	0.00218845	1.0796
13	59.7	0.00241206	1.190
14	51	0.00282353	1.393
15	46.3	0.00311015	1.5344
16	44.1	0.00326531	1.6109
17	38.7	0.00372093	1.8357
18	35.75	0.00402797	1.9872
19.5	31.1	0.00463023	2.2843

TABLE (D-3)

CALIBRATION OF THE LARGE ROD FORCE TRANSDUCER

DEAD WEIGHT (g)	MULTIMETER READING (mV)	FORCE TRANSDUCER CONSTANT (g/mV)
500	23.5	21.276
1000	46.6	21.459
1500	70.4	21.3

Average force transducer constant = 21.345 g/mV

= .2092 N/mV

TABLE (D-2)

CALIBRATION OF THE SMALL ROD FORCE TRANSDUCER

DEAD WEIGHT (g)	MULTIMETER READING (mV)	FORCE TRANSDUCER CONSTANT (g/mV)
200	46.7	4.282
300	69.8	4.2979
500	118.3	4.2265
1000	241.6	4.1390

Average force transducer constant = 4.236 g/mV

= .04155 N/mV

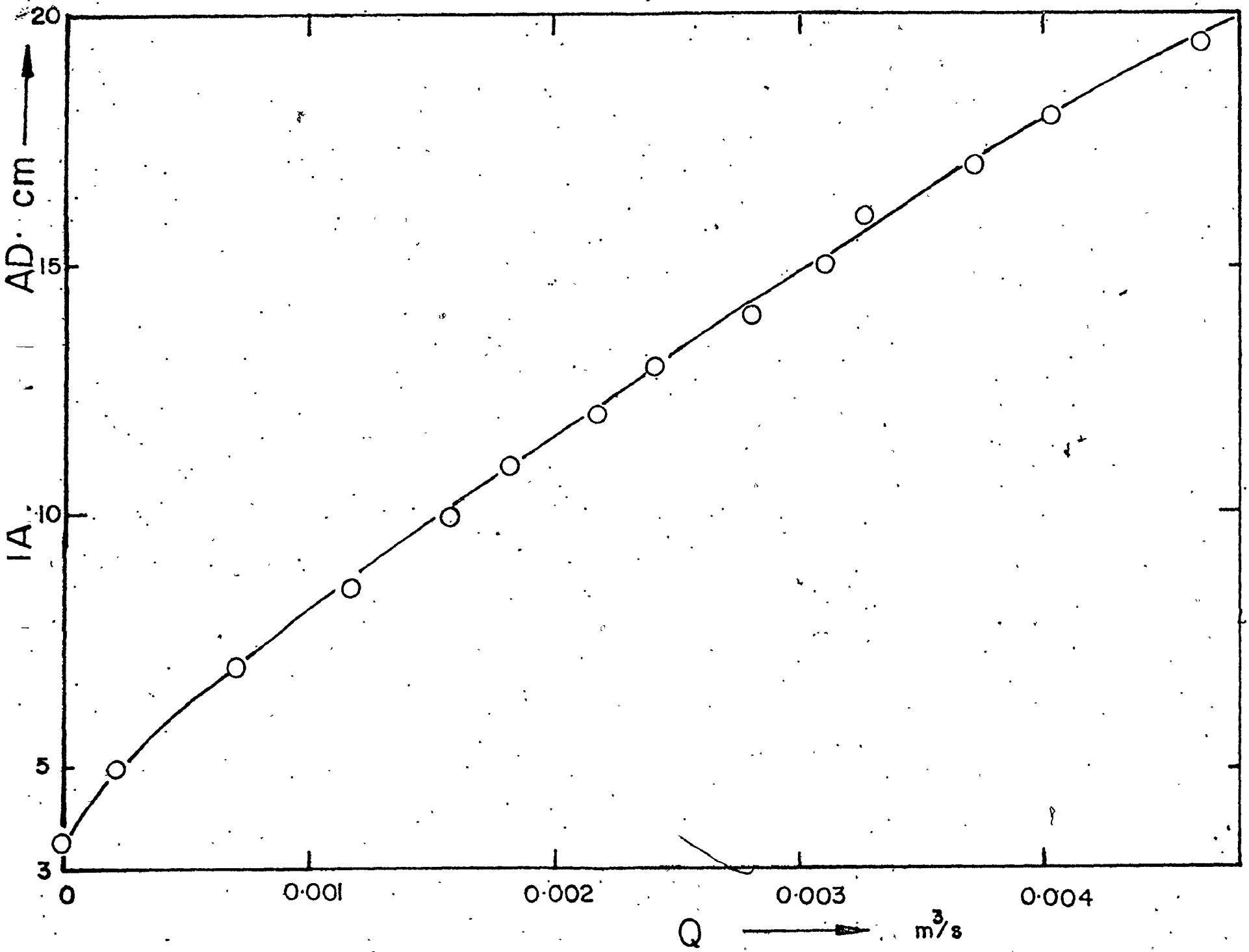

Figure (F-1) Rotameter Reading versus discharge

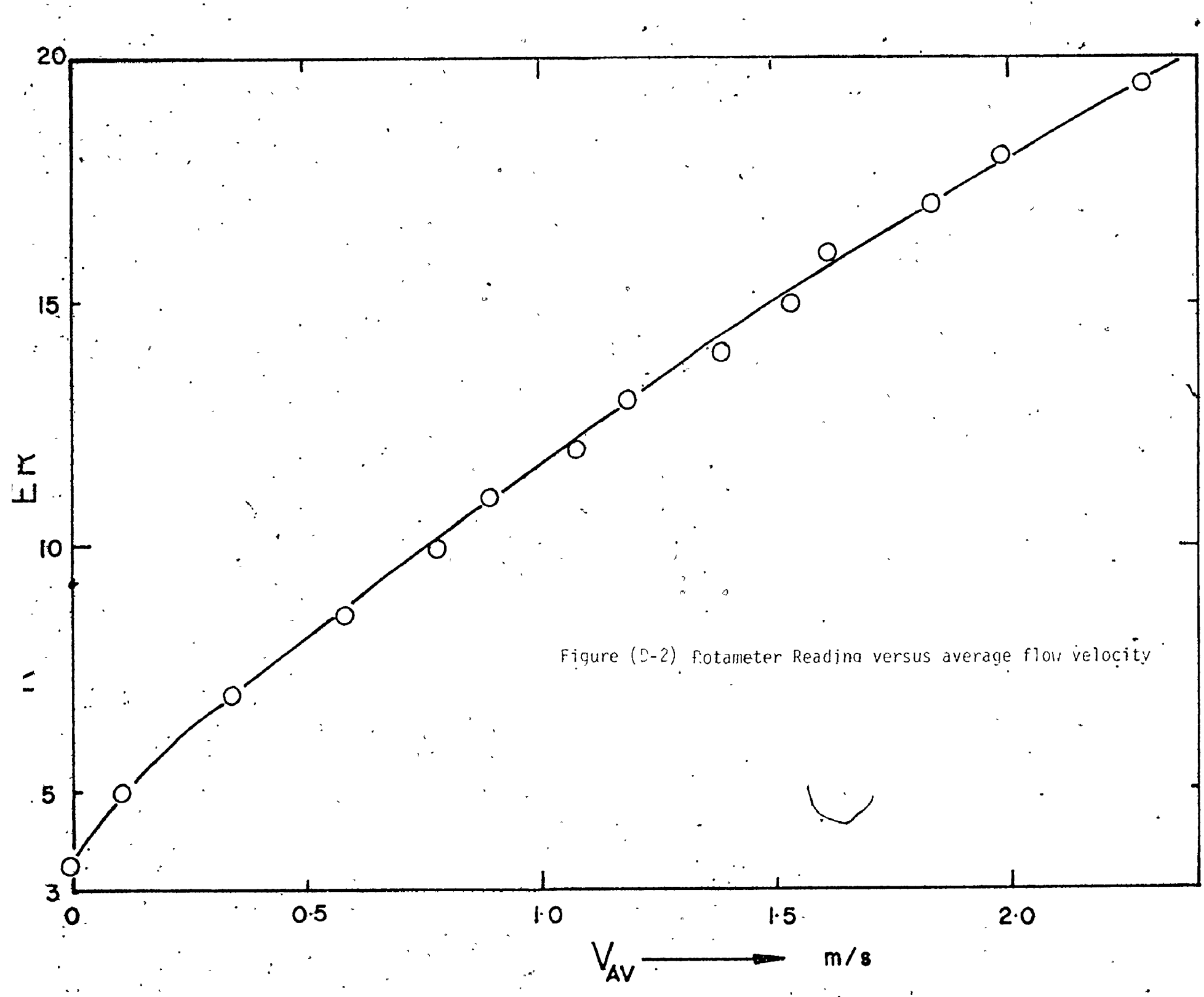

Figure (D-2) Rotameter Reading versus average flow velocity

APPENDIX E

CALIBRATION OF SIMPLE GRAVITY TYPE RHEOMETER

The simple gravity rheometer was described in Chapter 3. Basically, it employs a constant hydrostatic suction-head provided by a long vertical hose that is connected to the exit end of a capillary tube as shown in Figure (E-1). The pressure differential across the capillary was virtually constant and therefore, the discharge rate of a given viscosity fluid was constant.

The volume of the fluid being tested was the same for each run (250 c.c.), while the capillary has a cross section and length of 1.5 mm and 30 cm respectively. The theory of the rheometer for turbulent flow in the fluid is as follows:

$$c_f = \tau_o / (\gamma \frac{U^2}{2g}) \qquad (E-1)$$

$$\text{but } \tau_o = \Delta P(1/4\ \pi d^2)/\pi dL$$

$$= \Delta P\ d/4L \qquad (E-2)$$

$$\text{and since } U_o = L/t \qquad (E-3)$$

$$\text{then, } c_f = (\frac{g}{2} \Delta p \frac{d^2}{L^3}) \frac{t^2}{\gamma} = \text{constant} \times \frac{t^2}{\gamma} \qquad (E-4)$$

Equation (E-4) is useful since Δp, g, d and L are constants and t^2 and γ are characteristics dependent on the

fluid. Note that the specific weight γ of the test fluid depends on the concentration of the final polymer solution, but since this is a minute quantity (of order of 10-60 wppm), the change in the specific weight is small and that γ may be taken as a constant. Hence we may write Equation (E-4) as:

$$C_f = \text{constant} \times (t^2) \qquad \text{(E-5)}$$

So by measuring the time required to discharge a certain volume of the fluid, and the time required to discharge the same volume of water, the percentage drag reduction can be established as follows:

$$\frac{\Delta C_f}{C_{f_w}} = (C_f)_w - (C_f)_p / (C_f)_w = \text{reduction in skin friction}$$

$$= \frac{Kt_w^2 - Kt_p^2}{Kt_w^2}$$

$$= 1 - \left(\frac{t_p}{t_w}\right)^2 \qquad \text{(E-6)}$$

where subscripts w and p stand for water and polymer solutions respectively. The parameter $\Delta C_f / C_{f_w}$ is plotted against concentration as shown in Figure (E-2). The importance of such a plot is that it shows a maximum reduction in skin friction of about 50% around a concentration of 7 wppm.

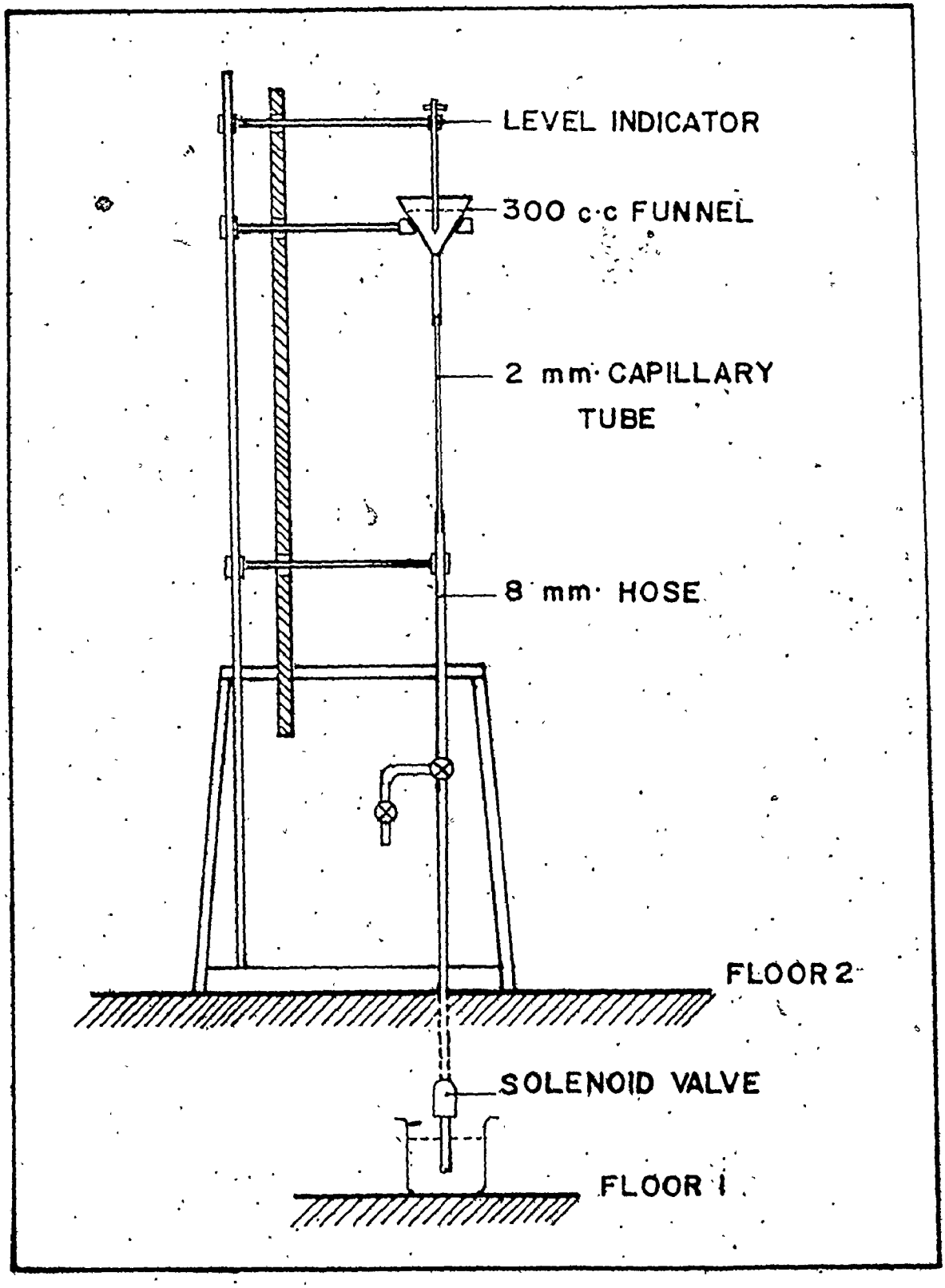

Figure (E-1) : Simple GRAVITY RHEOMETER.

TABLE (E-1): CALIBRATION OF SIMPLE GRAVITY RHEOMETER

Concentration (wppm)	First time reading t_1 (sec.)	Second time reading t_2	$[1-(\frac{t_1}{t_o})^2]\%$	$[1-(\frac{t_2}{t_o})^2]\%$
0	33.6	33.6	0	0
1500	46.85	49.9	-94.42	-120.56
750	35.6	37.9	-12.26	- 27.23
345	30.45	31.1	17.87	14.33
150	26	27.2	40.12	34.46
75	25.6	26.25	41.95	38.95
37.5	24.4	25.2	47.26	43.75
18.75	24.1	24.15	48.55	48.34
9.38	24.5	24.4	49.86	50.27
4.69	24.9	25.25	48.21	46.74
1.99	28.65	28.65	31.43	31.43
0.891	31.8	31.4	15.53	17.64

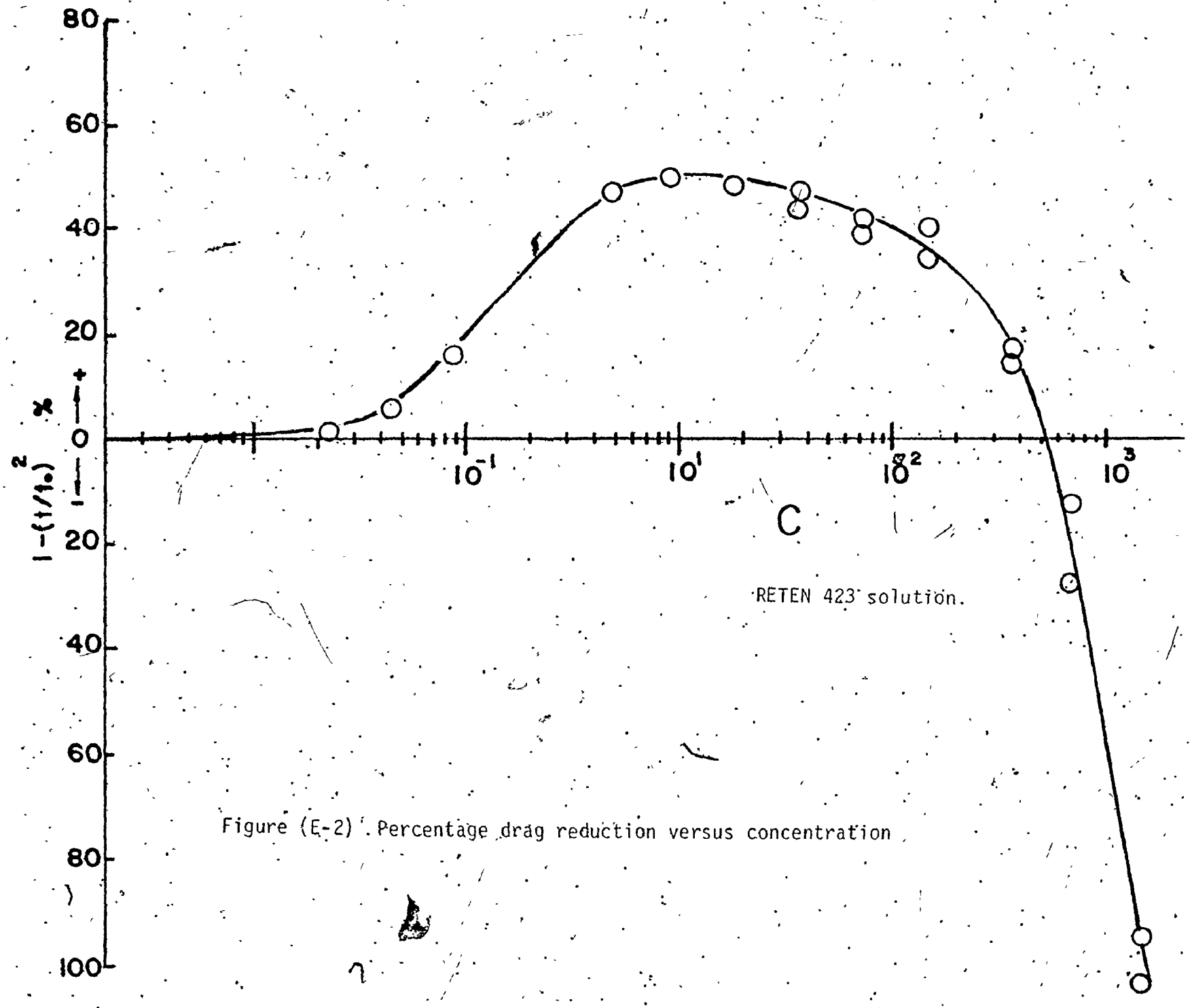

Figure (E-2) : Percentage drag reduction versus concentration

APPENDIX (F)

PHOTOGRAPHIC STUDY

The object of the photographic study was an attempt to define the flow phenomena involved around the body when drag reduction additives are introduced to the fluid. It had been previously proposed by Latto that the polymer affects the separation angle and therefore, the form drag. This to some extent was confirmed in a rather limited study on hydrodynamic suspension of spheres reported in Reference [24]. However it was felt that there was a need to obtain more comprehensive data on the subject. In order to do this, a special plexiglass test section was produced, see Figure (F-1), which was composed of a tube having the same I.D. as the original test section but with a reduced wall thickness. The tube was surrounded with a box made of plexiglass which was filled with an aqueous glycerine solution which had a composition such that minimum distorsion of the picture would occur. In order to minimize the refraction, the distance between the front viewing wall of the box and the tube was made as small as possible. Flow visualization was achieved by the use of a fine Aluminum powder suspension (Sheffield Company, A-9432) which highlighted the flow patterns. The streamlines were

illuminated using two 100 watts movie lights located on both sides of the box. Side covers with 2 mm vertical slits were fitted to the box to produce a thin longitudinal transverse beam of light.

A series of photographs were taken for each of the sphere sizes over the range of flow velocities tested, with at least three photographs per flow condition. Typical pictures with and without polymer (for $R_D = 1.3 \times 10^4$) are shown in Figure (F-2). Unfortunately it was found that there was a large deviation of the separation angle for each group of pictures taken under the same conditions. This was due, in part, to local periodic instabilities and it was found that the results are scattered. This phenomena was not observed with the previous work with untethered spheres and therefore, can be attributed to the support system or the act of tethering the body. The instabilities were not pronounced in the drag measurements, but nonetheless, would be a reason for some of the differences observed between the untethered and tethered data. Under the circumstances it is therefore, recommended that a technique which could time-average the results be used. Such a method would be to obtain surface pressure profile around the body and hence define the pressure discontinuity and therefore, the separation point.

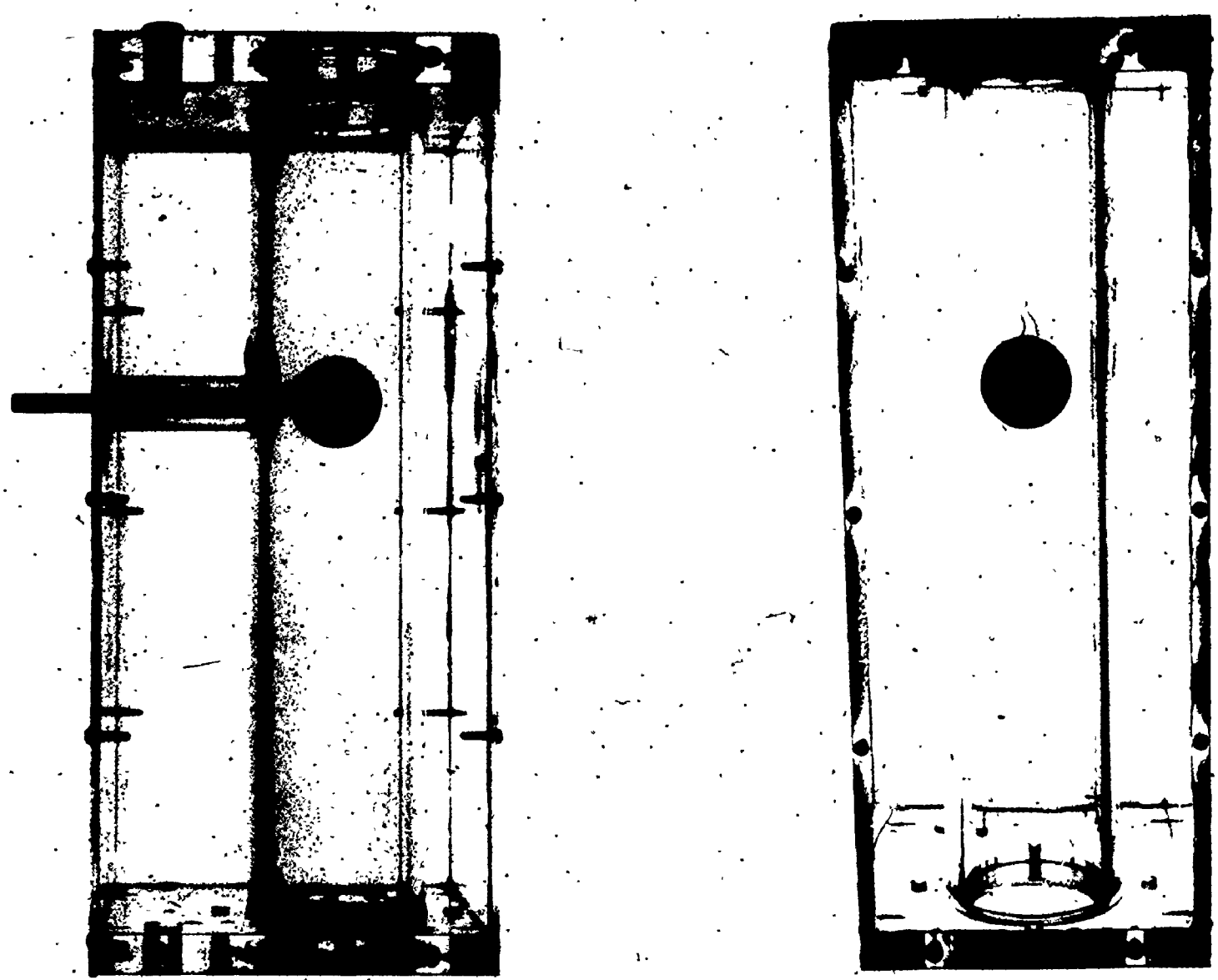

Figure (E-1), photograph of the photographic cell

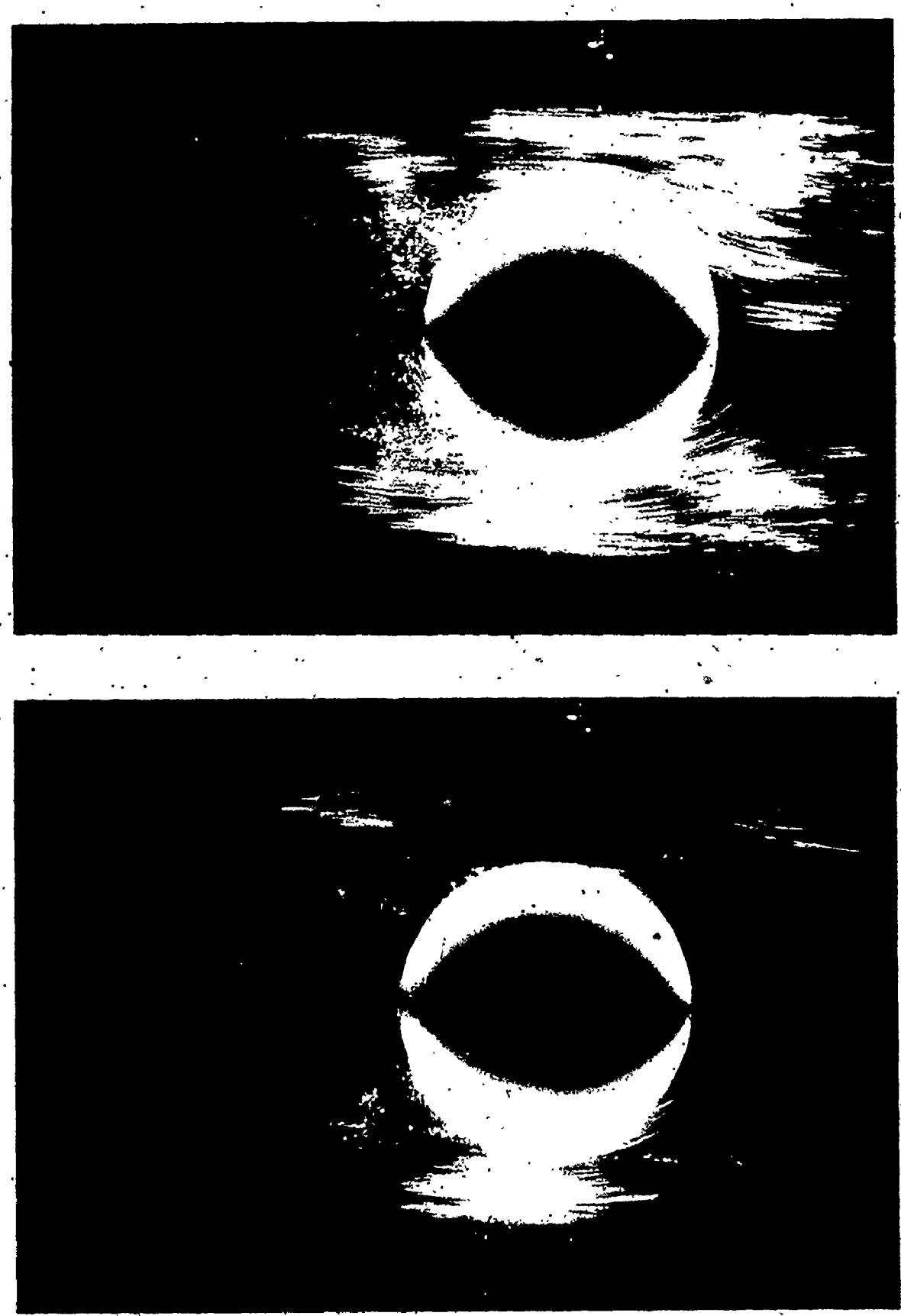

Figure (E-2) Upper: photograph of sphere of d/D = 0.6181 in water at $R_D = 1.3 \times 10^4$

Lower: photograph of same sphere under same R_D in a of 60 wppm

APPENDIX (G)

COMPUTER PROGRAM, DATA AND RESULTS

```
      READ(5,*)(OR(I),I=1,N)
      READ(5,*)(P(I),I=1,N)
60    AA=PI*(AO**2)/4
      DIR=AO/5.08
      WRITE(6,100)J
      WRITE(6,220)CON,DIR
      WRITE(6,230)
65    100 FORMAT(1H1,2X,*TEST NO.*,I3,/)
      220 FORMAT(2X,*POLY. CON.=*,F10.4,2X,*D/O =*,F10.4,/)
      230 FORMAT(1X,*VELOCITY*,3X,*ST. GAGE READING OR*,5X,*PRESS. DROP*,3X
     *,*DRAG COEF. CD*,5X,*DE. NO. RN*,3X,*PERCENTAGE DRAG RED.*,3X,
     *,*DRAG FORCE*,3X,*PRESS.FUNC.*,/)
70    DO 200 I=1,N
      P(I)=P(I)*GR*(DENW-DEN)+AL*GR*DEN
      IF(DIR.LE.0.5)OR(I)=OR(I)-ORR(I)
      D(I,J)=C*OR(I)
      PRF(I,J)=(P(I)-PL(I))/(DEN*5.08*GR)
75    CO(I,J)=GR*D(I,J)/(0.5*DEN*AA*(U(I)**2))
      IF(CON.EQ.0.0)CDO(I)=CO(I,J)
      CDO(I,J)=(CDO(I)-CO(I,J))*100./CDO(I)
      SUMDR=SUMDR+CDO(I,J)
      RN(I,J)=(U(I)*AO*DEN)/VIS
80    WRITE(6,300)U(I),OR(I),P(I),CO(I,J),RN(I,J),CDO(I,J),D(I,J)
     *,PRF(I,J)
      300 FORMAT (1X,F10.4,6X,F10.4,3X,E10.4,4X,F13.4,4X,F13.4,4X,F13.4,
     *4X,F15.4,4X,F10.4,/)
      CALL PLOTPT(ALOG(RN(I,J)),ALOG(CO(I,J)),H(J))
85    200 CONTINUE
      SUMAV=SUMDR/N
      WRITE(6,250)SUMAV
      250 FORMAT(/,4X,*AVERAGE DRAG RED. =*,F10.4,/)
      400 CONTINUE
90    CALL OUTPLT
      DO 600 J=1,K
      DO 500 I=1,N
      CALL PLOTPT(RN(I,J),PRF(I,J),H(J))
      500 CONTINUE
95    600 CONTINUE
      CALL OUTPLT
      DO 650 J=1,K
      DO 550 I=4,N
      CALL PLOTPT(ALOG(RN(I,J)),ALOG(PRF(I,J)),H(J))
100   550 CONTINUE
      650 CONTINUE
      CALL OUTPLT
      DO 700 J=1,K
      DO 675 I=1,N
105   CALL PLOTPT(RN(I,J),CDO(I,J),H(J))
      675 CONTINUE
      700 CONTINUE
      CALL OUTPLT
      DO 720 J=1,K
110   DO 710 I=1,N
      CALL PLOTPT(RN(I,J),D(I,J),H(J))
      710 CONTINUE
      720 CONTINUE
      CALL OUTPLT
```

```
      PROGRAM TST (INPUT,OUTPUT,TAPE5=INPUT,TAPE6=OUTPUT)
      DIMENSION U(25),DR(25),P(25),CD(25,10),RN(25,10),PL(25),PRF(25,10)
     *,F(25),RNT(25),D(25,10),FT(25),DRR(25),CDO(25),CDO(25,10)
      INTEGER H(10)
C     U=VELOCITY OF APPROACH
C     DR=STRAIN GAGE INDICATOR READING
C     P=PRESSURE DIFFERENCE ACROSS TEST SECTION
C     CD=DRAG COEFF.
C     RN=REYNOLDS NUMBER
C     D=DRAG FORCE IN GMS.
C     DT=TUBE DIAMETER
C     AD=SPHERE DIAMETER
C     AL=LENGTH OF TEST SECTION
C     RNT(I)=REYNOLDS NUMBER BASED ON TUBE DIAMETER
C     ALL DIMENSIONS IN GM,CM,SEC.SYSTEM
      N=16
      DENM=1.583
      DEN=1.0
      VIS=.013
      GR=980.0
      PI=3.14
      READ(5,*)AL,DT
      READ(5,*)(U(I),I=1,N)
      READ(5,*)(PL(I),I=1,N)
      READ(5,*)(DRR(I),I=1,N)
      WRITE(6,30)
30    FORMAT (1H1,4X,*COEF. OF FRICTION F*,5X,*THEO. COEF.(FT)*,5X,
     **RENOLDS NO.(TUBE)*,/)
      DO 10 I=1,N
      RNT(I)=(U(I)*DT*DEN)/VIS
      Y=RNT(I)
      X=0.316/(Y**0.25)
40    Z=1/(SQRT(X))+0.86*ALOG(2.51/(Y*SQRT(X)))
      DZ=-(1/(2*(X**1.5))+0.43*Y/X)
      XN=X-(Z/DZ)
      IF(ABS(XN-X).LE.1E-6)GO TO 45
      X=XN
      GO TO 40
45    FT(I)=XN
      PL(I)=PL(I)*GR*(DENM-DEN)
      F(I)=2.0*PL(I)*DT/(AL*DEN*(U(I)**2))
      PL(I)=(0.5*FT(I)*AL*DEN*(U(I)**2)/DT)+AL*GR*DEN
      WRITE(6,35)F(I),FT(I),RNT(I)
35    FORMAT(9X,F10.4,4X,F14.4,8X,F14.4,/)
      CALL PLOTPT(ALOG(RNT(I)),ALOG(F(I)),2)
      CALL PLOTPT(ALOG(RNT(I)),ALOG(FT(I)),9)
10    CONTINUE
      CALL OUTPLT
      DO 25 I=1,N
      CALL PLOTPT(U(I),PL(I),9)
25    CONTINUE
      CALL OUTPLT
      K=5
      READ(5,*)(H(L),L=1,K)
      DO 400 J=1,K
      SUMDR=0.0
      READ(5,*)AD,C,CON
```

TEST NO. 1

POLY. CON.= 0.0000 D/D = .8681

VELOCITY	ST. GAGE READING DR	PRESS. DROP	DRAG COEF. CD	RE. NO. PN	PERCENTAGE DRAG RED.	DRAG FORCE	PRESS.FUNC.
10.0000	1.0500	.1515E+06	26.9605	3392.3077	0.0000	21.0000	.4286
22.0000	3.4000	.1541E+06	16.0374	7463.0769	0.0000	68.0000	.8978
35.0000	7.9000	.1572E+06	16.5589	11873.0769	0.0000	158.0000	1.4644
48.0000	11.8000	.1666E+06	13.1504	16283.0769	0.0000	236.0000	3.2784
62.0000	19.3000	.1744E+06	12.8918	21032.3077	0.0000	386.0000	4.7448
76.0000	27.9000	.1854E+06	12.4027	25781.5385	0.0000	558.0000	6.8227
90.0000	36.8000	.1964E+06	11.6655	30530.7692	0.0000	736.0000	8.8519
105.0000	48.0000	.2089E+06	11.1790	35619.2308	0.0000	960.0000	11.2323
119.0000	60.0000	.2262E+06	10.8792	40368.4615	0.0000	1200.0000	14.5176
134.0000	70.5000	.2403E+06	10.0814	45456.9231	0.0000	1410.0000	17.1402
150.0000	83.0000	.2576E+06	9.4719	50884.6154	0.0000	1660.0000	20.3595
166.0000	98.0000	.2732E+06	9.1316	56312.3077	0.0000	1960.0000	23.2368
184.0000	108.0000	.2873E+06	8.1908	62418.4615	0.0000	2160.0000	25.7469
201.0000	119.0000	.3046E+06	7.5630	68185.3846	0.0000	2380.0000	28.8836
219.0000	132.0000	.3219E+06	7.0663	74291.5385	0.0000	2640.0000	31.9831
237.0000	150.0000	.3454E+06	6.8570	80397.6923	0.0000	3000.0000	36.3133

TEST NO. 2

POLY. CON.= 10.0000 D/D = .8681

VELOCITY	ST. GAGE READING DR	PRESS. DROP	DRAG COEF. CD	RE. NO. RA	PERCENTAGE DRAG RED.	DRAG FORCE	PRESS.FUNC.
10.0000	.3500	.1509E+06	8.9865	3392.3077	66.6667	7.0000	.3023
22.0000	3.2000	.1540E+06	16.9763	7463.0769	5.8824	64.0000	.8932
35.0000	6.7000	.1582E+06	14.0436	11873.0769	15.1899	134.0000	1.6595
48.0000	11.9000	.1650E+06	13.2618	16283.0769	-.8475	238.0000	2.9571
62.0000	19.0000	.1744E+06	12.6914	21032.3077	1.5544	380.0000	4.7448
76.0000	27.9000	.1839E+06	12.4027	25781.5385	0.0000	558.0000	6.5128
90.0000	37.5000	.1948E+06	11.8874	30530.7692	-1.9022	750.0000	8.5720
105.0000	47.0000	.2152E+06	10.9461	35619.2308	2.0833	940.0000	12.4947
119.0000	53.0000	.2199E+06	9.6100	40368.4615	11.6667	1060.0000	13.2552
134.0000	65.0000	.2325E+06	9.2949	45456.9231	7.8014	1300.0000	15.5620
150.0000	76.0000	.2450E+06	8.6730	50884.6154	8.4337	1520.0000	17.8347
166.0000	87.8000	.2576E+06	8.1812	56312.3077	10.4182	1756.0000	20.0923
184.0000	95.8000	.2716E+06	7.2049	62418.4615	12.0370	1900.0000	22.5909
201.0000	108.7000	.2858E+06	6.9084	68185.3846	8.6556	2174.0000	25.1078
219.0000	126.8000	.3062E+06	6.7884	74291.5385	3.9394	2536.0000	28.5328
237.0000	139.0000	.3218E+06	6.3541	80397.6923	7.3333	2780.0000	31.5816

TEST NO. 3

POLY. CON.= 20.0000 D/D = .8681

VELOCITY	ST. GAGE READING	PRESS. DROP	DRAG COEF. CD	RE. NO. RN	PERCENTAGE DRAG RED.	DRAG FORCE	PRESS.FUNC.
10.0000	.3500	.1572E+06	8.9868	3392.3077	66.6667	7.0000	1.5631
22.0000	2.8000	.1588E+06	14.8543	7463.0769	17.6471	56.0000	1.8457
35.0000	6.2000	.1619E+06	11.9956	11873.0769	21.5190	124.0000	2.4170
48.0000	11.2000	.1681E+06	12.4817	16283.0769	9.0847	224.0000	3.5893
62.0000	18.5000	.1776E+06	12.3574	21032.3077	4.1451	370.0000	5.3750
76.0000	25.5000	.1869E+06	11.3358	25781.5385	8.6022	510.0000	7.1325
90.0000	32.8000	.1964E+06	10.3975	30530.7692	10.8696	656.0000	8.8819
105.0000	39.0000	.2027E+06	9.0829	35619.2308	18.7500	780.0000	9.9639
119.0000	46.0000	.2121E+06	8.3407	40368.4615	23.3333	920.0000	11.6829
134.0000	53.0000	.2246E+06	7.5789	45456.9231	24.8227	1060.0000	13.9842
150.0000	63.8000	.2340E+06	7.2803	50884.6154	23.1325	1276.0000	15.6312
166.0000	74.0000	.2497E+06	6.8953	56312.3077	24.4898	1480.0000	18.5210
184.0000	88.4000	.2654E+06	6.7043	62419.4615	18.1481	1768.0000	21.3400
201.0000	101.0000	.2842E+06	6.4193	68185.3846	15.1261	2020.0000	24.7869
219.0000	116.0000	.3030E+06	6.2102	74291.5385	12.1212	2320.0000	28.2016
237.0000	132.0000	.3234E+06	6.0342	80397.6923	12.0000	2640.0000	31.9029

TEST NO. 4

POLY. CON.= 30.0000 D/D = .9681

VELOCITY	ST. GAGE READING OR	PRESS. DROP	DRAG COEF. CD	RE. NO. RN	PERCENTAGE DRAG RED.	DRAG FORCE	PRESS.FUNC.
10.0000	1.5000	.1525E+06	38.5151	3392.3077	-42.8571	30.0000	.6191
22.0000	3.4000	.1550E+06	18.037	7463.0769	0.0000	68.0000	1.0883
35.0000	7.0000	.1586E+06	14.6724	11873.0769	11.3924	140.0000	1.7858
48.0000	13.0000	.1681E+06	14.4877	16283.0769	-10.1695	260.0000	3.5883
62.0000	19.3000	.1744E+06	12.8918	21032.3077	0.0000	386.0000	4.7448
76.0000	28.1000	.1823E+06	12.4916	25781.5385	-.7168	562.0000	6.1915
90.0000	35.6000	.1948E+06	11.2851	30530.7692	3.2609	712.0000	8.5720
105.0000	42.7000	.2027E+06	9.9446	35519.2308	11.0417	854.0000	9.9699
119.0000	51.0000	.2152E+06	9.2473	40368.4615	15.0000	1020.0000	12.3141
134.0000	59.0000	.2246E+06	8.4369	45456.9231	16.3121	1180.0000	13.9842
150.0000	65.0000	.2340E+06	7.4177	50884.6154	21.6867	1300.0000	15.6312
166.0000	74.0000	.2450E+06	6.8953	56312.3077	24.4898	1480.0000	17.5675
184.0000	86.5000	.2622E+06	6.5602	62418.4615	19.9074	1730.0000	20.7038
201.0000	102.0000	.2795E+06	6.4826	68185.3846	14.2857	2040.0000	23.9454
219.0000	118.0000	.2999E+06	6.3173	74291.5385	10.6061	2360.0000	27.5734
237.0000	134.5000	.3187E+06	6.1484	80397.6923	10.3333	2690.0000	30.9504

TEST NO. 5

POLY. CON.= 40.0000 D/D = .8681

VELOCITY	ST. GAGE READING	DR PRESS. DROP	DRAG COEF. CD	RE. NO. RN	PERCENTAGE DRAG RED.	DRAG FORCE	PRESS.FUNC.
10.0000	.8500	.1556E+06	21.8252	3392.3077	19.0476	17.0000	1.2480
22.0000	3.2000	.1572E+06	16.9763	7463.0769	5.8824	64.0000	1.5278
35.0000	6.9000	.1619E+06	14.4628	11873.0769	12.6582	138.0000	2.4055
48.0000	12.3000	.1697E+06	13.7078	16283.0769	-4.2373	246.0000	3.9096
62.0000	17.6000	.1760E+06	11.7562	21032.3077	8.8083	352.0000	5.0546
76.0000	25.8000	.1839E+06	11.4692	25781.5385	7.5269	516.0000	6.5128
90.0000	32.0000	.1932E+06	10.1439	30530.7692	13.0435	640.0000	8.2507
105.0000	42.0000	.2058E+06	9.7816	35619.2308	12.5000	840.0000	10.6011
119.0000	52.4000	.2184E+06	9.5012	40368.4615	12.6667	1048.0000	12.9453
134.0000	65.0000	.2325E+06	9.2949	45456.9231	7.8014	1300.0000	15.5630
150.0000	74.0000	.2466E+06	8.4449	50884.6154	10.8434	1480.0000	18.1560
166.0000	89.8000	.2653E+06	8.3676	56312.3077	8.3673	1796.0000	21.6531
184.0000	104.0000	.2811E+06	7.8875	62418.4615	3.7037	2080.0000	24.4950
201.0000	119.0000	.3030E+06	7.5630	68185.3846	0.0000	2380.0000	28.5737
219.0000	138.0000	.3281E+06	7.3881	74291.5385	-4.5455	2760.0000	33.2397
237.0000	155.0000	.3485E+06	7.0856	80397.6923	-3.3333	3100.0000	36.9410

TEST NO. 6

POLY. CON.= 60.0000 D/D = .3681

VELOCITY	ST. GAGE READING	DR PRESS. DROP	DRAG COEF. CD	RE. NO.	PERCENTAGE DRAG RED.	DRAG FORCE	PRESS. FUNC.
10.0000	.9000	.1541E+06	23.1090	3392.3077	14.2857	10.0000	.9335
22.0000	3.1000	.1572E+06	15.4459	7463.0769	8.6236	62.0000	1.5244
35.0000	6.7000	.1619E+06	14.0430	11873.0769	15.1899	134.0000	2.4035
48.0000	11.9000	.1681E+06	13.2618	16283.0769	-.8475	238.0000	3.5883
62.0000	16.9000	.1760E+06	11.2887	21032.3077	12.4352	338.0000	5.0661
76.0000	24.7000	.1901E+06	10.9802	25781.5385	11.4695	494.0000	7.7752
90.0000	35.8000	.1948E+06	11.0949	30530.7692	4.8913	700.0000	8.5720
105.0000	43.0000	.2058E+06	10.0145	35619.2308	10.4167	860.0000	10.6011
119.0000	53.0000	.2184E+06	9.6100	40368.4615	11.6667	1060.0000	12.9453
134.0000	64.0000	.2340E+06	9.1519	45456.9231	9.2199	1280.0000	15.8778
150.0000	76.0000	.2481E+06	8.6730	50884.6154	8.4337	1520.0000	18.4659
166.0000	93.0000	.2685E+06	8.6657	56312.3077	5.1020	1860.0000	22.2957
184.0000	108.0000	.2873E+06	8.1908	62418.4615	0.0000	2160.0000	25.7469
201.0000	126.0000	.3093E+06	8.0079	68185.3846	-5.8824	2520.0000	29.8361
219.0000	145.0000	.3328E+06	7.7628	74291.5385	-9.8485	2900.0000	34.1838
237.0000	165.0000	.3564E+06	7.5427	80397.6923	-10.0000	3300.0000	38.5179

TEST NO. 7

POLY. CON.= 0.0000 D/D = .7402

VELOCITY	ST. GAGE READING QR	PRESS. DROP	DRAG COEF. CD	RE. NO. PN	PERCENTAGE DRAG RED.	DRAG FORCE	PRESS.FUNC.
10.0000	1.0000	.1498E+06	5.1040	2892.3077	0.0000	2.8900	.0642
22.0000	4.2000	.1505E+06	4.4291	6363.0769	0.0000	12.1380	.1817
35.0000	10.1000	.1519E+06	4.2082	10123.0769	0.0000	29.1890	.4096
48.0000	20.0000	.1539E+06	4.4305	13883.0769	0.0000	57.8000	.7307
62.0000	28.6000	.1559E+06	3.7974	17932.3077	0.0000	82.6540	1.0264
76.0000	43.0000	.1588E+06	3.7997	21981.5385	0.0000	124.2700	1.4852
90.0000	63.0000	.1622E+06	3.9698	26030.7692	0.0000	182.0700	2.0190
105.0000	82.0000	.1662E+06	3.7962	30369.2308	0.0000	236.9800	2.6480
119.0000	104.0000	.1710E+06	3.7484	34418.4615	0.0000	300.5600	3.4314
134.0000	133.0000	.1771E+06	3.7405	38756.9231	0.0000	384.3700	4.4359
150.0000	158.0000	.1828E+06	3.5841	43384.6154	0.0000	456.6200	5.3369
166.0000	190.0000	.1873E+06	3.5192	48012.3077	0.0000	549.1000	5.9878
184.0000	227.0000	.1961E+06	3.4221	53218.4615	0.0000	656.0300	7.4132
201.0000	270.0000	.2074E+06	3.4110	58135.3846	0.0000	780.3000	9.3577
219.0000	310.0000	.2152E+06	3.2990	63341.5385	0.0000	895.9000	10.5539
237.0000	348.0000	.2262E+06	3.0895	68547.6923	0.0000	982.6000	12.3731

TEST NO. 8

POLY. CON.= 20.0100 D/D = .7402

VELOCITY	STA GAGE READING OR	PRESS. DROP	DRAG COEF. CD	RE. NO. RN	PERCENTAGE DRAG RED.	DRAG FORCE	PRESS.FUNC.
10.0000	5.9000	.1502E+06	30.1135	2892.3077	-490.0000	17.0510	.1600
22.0000	8.3000	.1508E+06	8.7527	6363.0769	-97.6190	23.9870	.2391
35.0000	12.0000	.1520E+06	4.9999	10123.0769	-18.8119	34.6800	.4315
48.0000	18.2000	.1536E+06	4.0318	13883.0769	9.0000	52.5980	.6962
62.0000	27.5000	.1564E+06	3.6514	17932.3077	3.8462	79.4750	1.1132
76.0000	34.0000	.1590E+06	3.0044	21981.5385	20.9302	98.2600	1.5091
90.0000	47.9000	.1624E+06	3.0183	26030.7692	23.9683	138.4310	2.0535
105.0000	57.8000	.1651E+06	2.6758	31369.2308	29.5122	167.0420	2.4185
119.0000	80.0000	.1711E+06	2.8834	34418.4615	23.0769	231.2000	3.4429
134.0000	102.0000	.1771E+06	2.8993	38756.9231	23.3083	294.7800	4.4474
150.0000	122.8000	.1826E+06	2.7855	43384.6154	22.2785	354.8920	5.3025
166.0000	140.0000	.1868E+06	2.5931	48012.3077	26.3159	404.6000	5.8845
184.0000	160.0000	.1917E+06	2.4121	53218.4615	29.5154	462.4000	6.5469
201.0000	180.0000	.2017E+06	2.2740	59135.3846	33.3333	520.2000	8.2261
219.0000	210.0000	.2089E+06	2.2343	63341.5385	32.2581	606.9000	9.3000
237.0000	240.0000	.2184E+06	2.1808	68547.6923	29.4118	693.6000	10.7978

TEST NO.9

POLY. CON.= 40.0100 O/D = .7402

VELOCITY	ST. GAGE READING	DR	PRESS. DROP	DRAG COEF. CD	RE. NO. RN	PERCENTAGE DRAG REC.	DRAG FORCE	PRESS.FUNC.
10.0000	1.8000	.1502E+06	9.1872	2992.3077	-80.0000	5.2020	.1630	
22.0000	5.2000	.1511E+06	5.4836	6363.0769	-23.8095	15.0280	.2954	
35.0000	8.2000	.1520E+06	3.4165	10123.0769	18.8119	23.6980	.4201	
48.0000	13.0000	.1538E+06	2.8799	13883.0769	35.0000	37.5700	.7077	
62.0000	21.0000	.1565E+06	2.7883	17932.3077	26.5734	60.6900	1.1412	
76.0000	30.4000	.1594E+06	2.6863	21981.5385	29.3023	87.8560	1.5894	
90.0000	44.9000	.1633E+06	2.8292	26030.7692	28.7302	129.7610	2.2436	
105.0000	58.0000	.1669E+06	2.6851	30369.2308	29.2693	167.6200	2.7972	
119.0000	76.0000	.1716E+06	2.7392	34418.4615	26.9231	219.6400	3.5576	
134.0000	100.0000	.1772E+06	2.8425	38756.9231	24.8120	289.0000	4.4533	
150.0000	124.4000	.1835E+06	2.8219	43384.6154	21.2658	359.5160	5.4746	
166.0000	145.0000	.1893E+06	2.6857	48012.3077	23.6842	419.0500	6.3895	
184.0000	173.8000	.1959E+06	2.6081	53219.4615	23.7885	499.9700	7.3847	
201.0000	195.0000	.2042E+06	2.4635	58135.3846	27.7778	563.5500	8.7195	
219.0000	227.0000	.2121E+06	2.4157	63341.5385	26.7742	656.0300	9.9312	
237.0000	256.0000	.2184E+06	2.3262	68547.6923	24.7059	739.8400	10.7978	

TEST NO.10

POLY. CON.= 60.0100 D/D = .7402

VELOCITY	ST. GAGE READING	DR	PRESS. DROP	DRAG COEF. CD	RE NO. RN	PERCENTAGE DRAG RED.	DRAG FORCE	PRESS.FUNC.
10.0000	1.8000	.1502E+06		9.1972	2892.3077	-80.0000	5.2020	.1495
22.0000	4.2000	.1503E+06		4.4291	6363.0769	0.0000	12.1380	.1472
35.0000	9.0000	.1523E+06		3.7499	10123.0769	10.8941	26.0100	.4859
48.0000	14.0000	.1542E+06		3.1014	13883.0769	30.0000	40.4600	.7786
62.0000	21.0000	.1562E+06		2.7883	17932.3077	26.5734	60.6900	1.0838
76.0000	31.8000	.1594E+06		2.8100	21981.5385	26.0465	91.9020	1.5894
90.0000	44.0000	.1622E+06		2.7725	26030.7692	30.1587	127.1600	2.0190
105.0000	59.0000	.1661E+06		2.7314	30369.2308	28.0446	170.5100	2.6250
119.0000	76.0000	.1718E+06		2.7392	34418.4615	26.9231	219.6400	3.5921
134.0000	99.6000	.1773E+06		2.8311	38756.9231	25.1128	287.8440	4.4933
150.0000	121.0000	.1829E+06		2.7449	43384.6154	23.4177	349.6900	5.3713
166.0000	140.0000	.1885E+06		2.5931	48012.3077	26.3158	404.6000	6.2288
184.0000	160.0000	.1940E+06		2.4121	53218.4615	29.5154	462.4000	6.9945
201.0000	182.5000	.1999E+06		2.3056	58135.3846	32.4074	527.4260	7.8474
219.0000	212.2000	.2089E+06		2.2582	63341.5385	31.5484	613.2580	9.3000
237.0000	238.0000	.2136E+06		2.1445	68547.6923	30.5682	682.0400	9.8453

TEST NO.11

POLY. CON.= 0.0000 D/D = .6181

VELOCITY	ST. GAGE READING	OR PRESS. DROP	DRAG COEF. CD	RE. NO. RN	PERCENTAGE DRAG RED.	DRAG FORCE	PRESS.FUNC.
10.0000	.5000	.1498E+06	5.3636	2415.3846	0.0000	2.1180	.0682
22.0000	1.4000	.1501E+06	3.1029	5313.8462	0.0000	5.9304	.1013
35.0000	3.4000	.1508E+06	2.9773	8453.8462	0.0000	14.4024	.1791
48.0000	5.6000	.1516E+06	2.6073	11593.8462	0.0000	23.7216	.2716
62.0000	8.6000	.1531E+06	2.3999	14975.3846	0.0000	36.4296	.4526
76.0000	12.2000	.1546E+06	2.2659	18356.9231	0.0000	51.6792	.6369
90.0000	16.2000	.1563E+06	2.1454	21738.4615	0.0000	68.6232	.8370
105.0000	21.5000	.1588E+06	2.0919	25361.5385	0.0000	91.0740	1.1561
119.0000	29.0000	.1610E+06	2.1968	28743.0769	0.0000	122.8440	1.4230
134.0000	36.5000	.1642E+06	2.1806	32366.1538	0.0000	154.6140	1.8537
150.0000	43.5000	.1673E+06	2.0739	36230.7692	0.0000	184.2660	2.2383
166.0000	54.0000	.1716E+06	2.1021	40095.3846	0.0000	228.7440	2.8318
184.0000	65.8000	.1744E+06	2.0848	44443.0769	0.0000	278.7288	3.0591
201.0000	78.0000	.1795E+06	2.0710	48549.2308	0.0000	330.4080	3.7903
219.0000	89.8000	.1836E+06	1.9906	52896.9231	0.0000	377.0040	4.2045
237.0000	108.0000	.1882E+06	2.0626	57244.6154	0.0000	457.4880	4.7383

TEST NO.12

POLY. CON.= 20.0100 D/D = .6181

VELOCITY	ST. GAGE READING	DR	PRESS. DROP	DRAG COEF. CD	RE. NO. RN	PERCENTAGE DRAG REC.	DRAG FORCE	PRESS.FUNC.
10.0000	.2000		.1498E+06	1.5940	2415.3846	70.2814	.6294	.0797
22.0000	1.1000		.1502E+06	1.8113	5313.8462	41.6242	3.4619	.1243
35.0000	2.6500		.1510E+06	1.7241	8453.8462	42.0924	8.3401	.2250
48.0000	5.0000		.1521E+06	1.7296	11593.8462	33.6638	15.7368	.3634
62.0000	7.8000		.1533E+06	1.6172	14975.3846	32.6148	24.5482	.4928
76.0000	11.3000		.1551E+06	1.5592	18356.9231	31.1844	35.5634	.7287
90.0000	17.0000		.1571E+06	1.6727	21738.4615	22.0345	53.5024	.9976
105.0000	21.5000		.1592E+06	1.5542	25361.5385	25.7035	67.6648	1.2364
119.0000	26.5000		.1616E+06	1.4914	28743.0769	32.1034	83.4008	1.5493
134.0000	32.8000		.1639E+06	1.4559	32356.1538	33.2349	103.2282	1.7953
150.0000	41.4000		.1675E+06	1.4665	36230.7692	29.2902	130.2941	2.2727
166.0000	50.0000		.1712E+06	1.4461	40095.3846	31.2059	157.3600	2.7400
184.0000	59.5000		.1749E+06	1.4007	44443.0769	32.8170	187.2584	3.1729
201.0000	72.5000		.1788E+06	1.4302	48549.2308	30.9424	228.1720	3.6126
219.0000	83.0000		.1832E+06	1.3792	52896.9231	30.7122	261.2176	4.1242
237.0000	91.5000		.1873E+06	1.2985	57244.6154	37.0543	287.9688	4.5662

TEST NO.13

POLY. CON.= 40.0100 D/D = .6181

VELOCITY	ST. GAGE READING DR	PRESS. DROP	DRAG COEF. CD	RE. NO. RN	PERCENTAGE DRAG RED.	DRAG FORCE	PRESS.FUNC.
10.0000	.1000	.1499E+06	.7970	2415.3846	85.1407	.3147	.1026
22.0000	.7500	.1504E+06	1.2350	5313.8462	60.1993	2.3604	.1587
35.0000	2.4000	.1508E+06	1.5614	8453.9462	47.5554	7.5533	.1905
48.0000	4.5000	.1522E+06	1.5866	11593.8462	40.2975	14.1624	.3864
62.0000	7.2000	.1532E+06	1.4928	14975.3846	37.7943	22.6598	.4756
76.0000	11.0000	.1549E+06	1.5178	18356.9231	33.0113	34.6192	.6943
90.0000	17.0000	.1571E+06	1.6727	21738.4615	22.0345	53.5024	.9851
105.0000	21.8000	.1591E+06	1.5181	25361.5385	27.4313	66.0912	1.2134
119.0000	27.8000	.1618E+06	1.5646	28743.0769	28.7778	87.4922	1.5837
134.0000	34.0000	.1651E+06	1.5091	32366.1538	30.7923	107.0048	2.0373
150.0000	42.8000	.1677E+06	1.5160	36230.7692	26.8991	134.7002	2.3186
166.0000	51.8000	.1712E+06	1.4982	40095.3846	28.7304	163.0250	2.7400
184.0000	60.5000	.1746E+06	1.4242	44443.0769	31.6879	190.4056	3.1040
201.0000	69.3000	.1778E+06	1.3671	48549.2308	33.9904	218.1010	3.4175
219.0000	81.8000	.1824E+06	1.3460	52896.9231	32.3818	254.9232	3.9750
237.0000	92.5000	.1866E+06	1.3125	57244.6154	36.3684	291.1160	4.4170

TEST NO. 14

POLY. CON.= 60.0100 D/D = .6181

VELOCITY	ST. GAGE READING DR	PRESS. DROP	DRAG COEF. CD	RE. NO. RN	PERCENTAGE DRAG RED.	DRAG FORCE	PRESS.FUNC.
10.0000	.1000	.1499E+06	.7970	2415.3846	85.1407	.3147	.1026
22.0000	.9000	.1504E+06	1.4820	5313.9462	52.2380	2.8325	.1587
35.0000	2.4000	.1508E+06	1.5614	8453.8462	47.5554	7.5533	.1905
48.0000	4.7500	.1522E+06	1.6431	11593.8462	36.9806	14.9492	.3864
62.0000	7.9000	.1532E+06	1.6379	14975.3846	31.7509	24.8629	.4756
76.0000	11.2000	.1547E+06	1.5454	18356.9231	31.7934	35.2486	.6599
90.0000	14.9000	.1562E+06	1.4661	21738.4615	31.6656	46.8933	.8025
105.0000	21.8000	.1588E+06	1.5181	25361.5385	27.4313	66.0912	1.1675
119.0000	27.0000	.1611E+06	1.5196	28743.0769	30.8274	84.9744	1.4345
134.0000	34.2000	.1640E+06	1.5180	32366.1538	30.3852	107.8342	1.8193
150.0000	42.2000	.1669E+06	1.4948	36230.7692	27.9238	132.8118	2.1579
166.0000	50.0000	.1699E+06	1.4461	40095.3846	31.2069	157.3603	2.4875
184.0000	60.8000	.1743E+06	1.4313	44443.0769	31.3491	191.3498	3.0407
201.0000	69.5000	.1779E+06	1.3710	48549.2308	33.7999	218.7304	3.4404
219.0000	79.0000	.1819E+06	1.3128	52896.9231	34.0514	248.6288	3.8717
237.0000	96.0000	.1872E+06	1.3622	57244.6154	33.9597	302.1312	4.5432

TEST NO. 15

POLY. CON.= 0.0000 D/D = .4390

VELOCITY	ST. GAGE READING DR	PRESS. DROP	DRAG COEF. CD	RE. NO. RN	PERCENTAGE DRAG RED.	DRAG FORCE	PRESS.FUNC.
10.0000	.0500	.1495E+06	.9999	2230.0000	0.0000	.1992	.0232
22.0000	.4500	.1499E+06	1.8593	4906.0000	0.0000	1.7924	.0585
35.0000	.6000	.1504E+06	.9795	7805.0000	0.0000	2.3898	.1056
48.0000	1.0000	.1511E+06	.8680	10704.0000	0.0000	3.9830	.1687
62.0000	1.7000	.1519E+06	.8844	13826.0000	0.0000	6.7711	.2417
76.0000	2.8000	.1527E+06	.9694	16948.0000	0.0000	11.1524	.2733
90.0000	4.3000	.1539E+06	1.0616	20070.0000	0.0000	17.1269	.3907
105.0000	5.4000	.1554E+06	.9795	23415.0000	0.0000	21.5082	.5258
119.0000	7.3000	.1574E+06	1.0309	26537.0000	0.0000	29.0759	.7468
134.0000	9.4000	.1594E+06	1.0469	29882.0000	0.0000	37.4402	.9614
150.0000	11.4000	.1612E+06	1.0132	33450.0000	0.0000	45.4062	1.0977
166.0000	14.2000	.1638E+06	1.0305	37018.0000	0.0000	56.5586	1.3639
184.0000	17.3000	.1663E+06	1.0219	41032.0000	0.0000	68.9059	1.5535
201.0000	21.0000	.1699E+06	1.0395	44823.0000	0.0000	83.6430	1.9796
219.0000	24.1000	.1730E+06	1.0049	48837.0000	0.0000	95.9903	2.2509
237.0000	27.8000	.1760E+06	.9898	52851.0000	0.0000	110.7274	2.4770

TEST NO. 16

POLY. COV.= 20.0100 D/D = .4390

VELOCITY	ST. GAGE READING DR	PRESS. DROP	DRAG COEF. CD	RE. NO. RN	PERCENTAGE DRAG RED.	DRAG FORCE	PRESS.FUNC.
10.0000	.1000	.1499E+06	1.3991	2230.0000	-39.9247	.2787	.1035
22.0000	.2000	.1503E+06	.5781	4906.0000	68.9056	.5573	.1503
35.0000	.7000	.1508E+06	.7995	7805.0000	18.3773	1.9506	.1974
48.0000	1.0000	.1515E+06	.6073	10704.0000	30.0377	2.7866	.2491
62.0000	1.8000	.1524E+06	.6551	13826.0000	25.9222	5.0159	.3335
76.0000	2.4000	.1535E+06	.5813	16948.0000	40.0323	6.6878	.4340
90.0000	4.2000	.1547E+06	.7255	20070.0000	31.6647	11.7037	.5514
105.0000	5.6000	.1562E+06	.7107	23415.0000	27.4465	15.6050	.6864
119.0000	7.7000	.1579E+06	.7608	26537.0000	26.2041	21.4568	.8616
134.0000	9.2000	.1600E+06	.7169	29882.0000	31.5262	25.6367	1.0877
150.0000	10.9000	.1619E+06	.6778	33450.0000	33.1062	30.3739	1.2354
166.0000	13.4000	.1646E+06	.6804	37018.0000	33.9792	37.3404	1.5246
184.0000	15.5000	.1668E+06	.6405	41032.0000	37.3170	43.1923	1.6682
201.0000	19.1000	.1699E+06	.6614	44823.0000	36.3676	53.2241	1.9796
219.0000	21.7000	.1725E+06	.6330	48837.0000	37.0049	60.4692	2.1591
237.0000	25.3000	.1760E+06	.6302	52851.0000	36.3292	70.5010	2.4885

TEST NO. 17

POLY. CON.= 40.0100 D/D = .4390

VELOCITY	ST. GAGE READING CR	PRESS. DROP	DRAG COEF. CD	RE. NO. RN	PERCENTAGE DRAG RED.	DRAG FORCE	PRESS.FUNC.
10.0000	.1000	.1499E+06	1.3991	2230.0000	-39.9247	.2787	.1035
22.0300	.2000	.1503E+06	.5781	4906.0000	68.9056	.5573	.1388
35.0000	.3000	.1508E+06	.3426	7805.0000	65.0188	.8360	.1859
48.0000	.9000	.1514E+06	.5465	10704.0000	37.0339	2.5079	.2376
62.0000	1.7000	.1523E+06	.6188	13826.0000	30.0377	4.7372	.3220
76.0000	2.7500	.1534E+06	.6661	16948.0000	31.2870	7.6632	.4225
90.0000	4.8000	.1548E+06	.8291	20070.0000	21.9025	13.3757	.5628
105.0000	6.2000	.1561E+06	.7868	23415.0000	19.6729	17.2769	.6635
119.0000	8.3000	.1579E+06	.8200	26537.0000	20.4538	23.1288	.8616
134.0000	10.0000	.1597E+06	.7792	29882.0000	25.5720	27.8660	1.0188
150.0000	11.6000	.1615E+06	.7213	33450.0000	28.8103	32.3246	1.1551
166.0000	14.2000	.1640E+06	.7210	37018.0000	30.0377	39.5697	1.3983
184.0000	16.1000	.1661E+06	.6653	41032.0000	34.8905	44.8643	1.5305
201.0000	20.0000	.1693E+06	.6926	44823.0000	33.3692	55.7320	1.8649
219.0000	22.9000	.1720E+06	.6680	48837.0000	33.5213	63.8131	2.0443
237.0000	26.4000	.1756E+06	.6576	52851.0000	33.5609	73.5662	2.3967

TEST NO. 18

POLY. CONST = 60.0100 D/D = .4390

VELOCITY	ST. GAGE READING DR	PRESS. DROP	DRAG COEF. CD	RE. NO. RN	PERCENTAGE DRAG RED.	DRAG FORCE	PRESS.FUNC.
10.0000	.1000	.1498E+06	1.3991	2230.0000	-39.9247	.2787	.0805
22.0000	.4000	.1500E+06	1.1563	4906.0000	37.8113	1.1146	.0929
35.0000	.3000	.1506E+06	.3426	7805.0000	65.0188	.8360	.1515
48.0000	1.7000	.1513E+06	1.0323	10704.0000	-18.9360	4.7372	.2146
62.0000	2.0000	.1520E+06	.7279	13826.0000	17.6914	5.5732	.2647
76.0000	3.3000	.1529E+06	.7994	16948.0000	17.5444	9.1958	.3192
90.0000	4.7000	.1548E+06	.8118	20070.0000	23.5295	13.0970	.3743
105.0000	6.5000	.1557E+06	.8249	23415.0000	15.7861	18.1129	.3832
119.0000	7.9000	.1574E+06	.7805	26537.0000	24.2873	22.0141	.4468
134.0000	10.2000	.1590E+06	.7948	29882.0000	24.0834	28.4233	.5696
150.0000	11.9000	.1608E+06	.7400	33450.0000	26.9691	33.1605	1.0059
166.0000	14.6000	.1629E+06	.7413	37018.0000	28.0669	40.6844	1.1803
184.0000	18.3000	.1656E+06	.7563	41032.0000	25.8936	50.9948	1.4272
201.0000	20.9000	.1680E+06	.7238	44823.0000	30.3708	58.2399	1.6009
219.0000	24.2000	.1708E+06	.7060	48837.0000	29.7474	67.4357	1.8033
237.0000	27.5000	.1739E+06	.6850	52851.0000	30.7926	76.6315	2.0524